Summer 6-27-2013

Probe Ca2+/Camodulin reguation of membrane proteins engineering

Xueyun Liu
xliu23@student.gsu.edu

Xueyun Liu
Georgia College and State University, xliu23@student.gsu.edu

PROBE Ca^{2+}/CAMODULIN REGULATION OF MEMBRANE PROTEINS BY PROTEIN ENGINEERING

by

XUEYUN LIU

Under the Direction of Jenny J. Yang

ABSTRACT

Calmodulin (CaM) is a eukaryotic Ca^{2+} signaling protein which can interact with more than 300 enzymes in the cell including membrane proteins Ryanodine receptor1 (RyR1) and gap junction protein connexin 43 (Cx43). By binding to Ca^{2+}, CaM undergoes a conformational change which exposed the hydrophobic patch that access to the target protein. wt-CaM and three mutant CaM (isolate C and N domain of CaM, deletion of five residues from the central linker of CaM) are designed for studying the specific contributions to calcium binding affinity and calcium induced conformational change. wt-CaM exhibits metal binding affinity to calcium analog Tb^{3+} with a Kd of 3.97 nM using FRET assay and metal-buffer system and activates target protein phosphodiesterase assay. The K_d values of domain specific calcium binding affinity of CaM probed by intrinsic Phe or Tyr are 12.2 and 2.77 uM, respectively. In addition,

Ca^{2+} also induces helicity for both w.t. CaM and C-terminal domain variant. Further, conditions such as medium and Glucose amount for isotopic labeling of CaM by ^{15}N, ^{13}C and D_2O have been optimized with relatively high yield of hetero-isotopic labeled CaM. This prepared us to probe the detailed interaction of CaM and its target protein and calcium induced conformational change by high resolution NMR. Furthermore, RyR1 mini domain, which contains two CaM binding regions of RyR1 was designed to study the binding mode of the two regions with CaM. Obtaining bacterial expressed and purified RyR1 mini domain was achieved by engineered with a His-Tag which overcomes the insoluble issue that occurred in the initial study of expression and purification with a GST tag. Moreover, to probe the interaction of CaM to the cytosolic loop of Cx43 that contains two putative CaM binding sites as well as the role of transmembrane region of Cx43, we have successfully expressed and purified fragments $Cx43_{88-154}$ and $Cx43_{99-154}$ as a His-tag protein encompassing regions 88-154 and 99-154 of Cx43 with predicted CaM binding sites with and without additional transmembrane region from Cx43. Both fragments were obtained with high yield after expressed as inclusion body and His-tag purification. Fragment $Cx43_{88-154}$ was shown to bind dansylated CaM with a K_d of 0.107 μM using florescence spectroscopy.

INDEX WORDS: Calmodulin, Calcium, Ryanodine receptor 1, Connexin, gap junction,

PROBE Ca^{2+}/CAMODULIN REGULATION OF MEMBRANE PROTEINS BY PROTEIN ENGINEERING

by

XUEYUN LIU

A Thesis Submitted in Partial Fulfillment of the Requirements for the Degree of

Master of Science

in the College of Arts and Sciences

Georgia State University

2013

PROBE Ca^{2+}/CAMODULIN REGULATION OF MEMBRANE PROTEINS BY PROTEIN ENGINEERING

by

XUEYUN LIU

Committee Chair: Jenny Yang

Committee: Donald Hamelberg

Siming Wang

Gangli Wang

Robert Wohlhueter

Electronic Version Approved:

Office of Graduate Studies

College of Arts and Sciences

Georgia State University

June 2013

DEDICATION

I would like to take some moment to thanks my family, my parents, my grandparents, and other family's members, without their support I cannot finish my thesis study. I want to specially thank to my parents, Ruping and Christopher Smirl for their support throughout my studies. Thank you mother for the investment of my education during my undergraduate and graduate study without any compliant. Thank you father for believe me and push me for any challenge that I was facing during my graduate study, and for all the endless prove reading of my papers. I would also like to thank to my grandparents for their supports during my childhood. Thank you both for all the love and patients which provide to us during the special conditions. Without you two, I cannot stay here and finish my thesis research. At last, I want to thank all my aunts and my cousins for their support through the online conversations.

ACKNOWLEDGEMENTS

First of all, I want to give thanks to Dr. Jenny J. Yang. Thank you for giving me an opportunity to explore my journey in the science field. I really cherish Dr. Jenny J. Yang allow me to join her research team and be part of her research during my undergraduate year. I also appreciate her guide and help for my research project. I also like to give thanks to Dr. Jie Jasmine Jiang as a mentor during my undergraduate research study. I appreciate you to train me with a solid research base. Thank you Dr. Johnny Yanyi Chen to give me the guides for my thesis research, I cannot finish my thesis without your suggestions and detailed help. I also want to thank both Johnny Chen and Julia Juan Zou for all the support of the research challenges. I would want also to thanks other lab members, specially, Alice Chen, Joy Zhuo, Jina Qiao, Jason Jiang, and David Xue for all the help throughout my research project. Without all of you, I cannot achieve this far. I would like to thanks to Bob Wolhuster for taking his precious time to be my personal editor of my thesis and give me many valuable suggestions. At last, I want to thank to my committee members for their time to support my research.

TABLE OF CONTENTS

TABLE OF FIGURES

LIST OF TABLES

LIST OF ABBREVIATIONS

BI	Before induction
AI	After induction
SP	supernatant
DE	debris
CaM	Calmodulin
RyR	Ryanodine receptor
Cx	Connexin
BBB	Beads before binding
BAB	Beads after binding
BAC	Beads after cleave
CD	Circular dichroism
IPTG	Isopropyl β-D-1-thiogalactopyranoside
DDT	Dichlorodiphenyltrichloroethane
PMSF	Phenylmethanesulfonyl fluoride
EGTA	Ethylene glycol tetraacetic acid

1. Introduction

1.1. Important role of calcium and calcium binding proteins in the biological systems

Calcium (Ca^{2+}) is one of the most abundant elements on earth, and is essential for many living organisms. This bivalent is the basic component of bone, teeth, and exoskeleton of animal. Ca^{2+} plays a critical role in variety of biological phenomena, such as muscle contraction, fertilization, cell differentiation, proliferation, and finally, in cell death.[1] Since Ca^{2+} functions as cellular signaling, the Ca^{2+} concentration is tightly regulated. The versatile speed, amplitude and spatial-temporal patterning of Ca^{2+} in eukaryotic cells control vital biological processes by precisely modulating the activity of a repertoire of signaling components including cellular receptors, ion channels, pumps, exchangers, Ca^{2+} buffers, Ca^{2+} effectors, Ca^{2+}-sensitive enzymes and transcription factors in different cellular compartments.[2] At the cellular level, free Ca^{2+} can derive from both external and internal. Ca^{2+} can enter form external environment by passing through channels that span the plasma membrane. Ca^{2+} can also release from internal Ca^{2+} storages such as the sarcoplasmic reticulum/Endoplasmic reticulum (SR/ER).

In general, there is cellular ionized Ca^{2+} gradient that is important for the regulation of Ca^{2+} in the cellular level. The concentration of Ca^{2+} in the extracellular $[Ca^{2+}]_o$ and in the sarcoplasmic reticulum $[Ca^{2+}]_{ER}$ is 10^{-3} M; on the other hand, the Ca^{2+} concentration in the intracellular environment is ~10^{-8} – ~10^{-7} M.[3] When the cell is at the rest stage, the cytoplasmic Ca^{2+} concentration is maintained by the ATP dependent Ca^{2+} pump. Extracellular Ca^{2+} sensed by the extracellular Ca^{2+}-sensing receptor, is believed to maintain the long-term Ca^{2+} homeostasis by replenishing the internal calcium stores. In contrast, the internal calcium stores are directly responsible for the changes in cytosolic Ca^{2+} concentration through the activity of

two principal Ca^{2+} release channels, e.g., the ryanodine (RyR) receptor and the inositol 1,4,5-triphosphate (IP_3) receptor.[4] Stimulus such as hormone can increase the cytoplasmic Ca^{2+} concentration up to 10^{-6} M. Because the concentration of the Ca^{2+} is tightly regulated, Ca^{2+} becomes the appropriate second messenger molecule to respond to external stimuli by forming the tight complexes through interaction with specific Ca^{2+} receptor or Ca^{2+} binding proteins.

Those Ca^{2+} receptors or Ca^{2+} binding proteins can be defined into three group: Ca^{2+} sensor protein (e.g. calmodulin), buffer protein (e.g. parvalbumin), or Ca^{2+} stabilized protein (e.g., thermolysin).[5] The Ca^{2+} sensor protein increases the Ca^{2+} concentration and translates this information into many biological responses. On another hand, Ca^{2+} buffer proteins modulate the Ca^{2+} signal and remove any potential harmful ions from the cytoplasm. Once the Ca^{2+} enters the cytoplasm, it binds to numerous Ca^{2+} binding protein for farther regulation. Many of the Ca^{2+} binding proteins have a helix-loop-helix structure called EF-hand shows as **Figure 1. A**. The EF hand is one of the most common motifs in proteins of bacteria, archaea, and eukaryotes. In each EF hand motif, the two α helices are connected by a flexible loop that provide ligands for metal ions. By binding to Ca^{2+}, this motif may undergo conformational changes that enable them to modulate other proteins. The geometry of the Ca^{2+} coordination in the EF-hand motif is formed by a pentagonal bipyramidal with seven oxygen atoms from the carboxyl or hydroxyl group of the, carbonyls from the main chain, and a water bridge.

EF-hand motifs can divide into two groups, the canonical EF-hand and the pseudo EF hand. For the canonical EF-hand, resides at positions 1, 3, 5, 12 from the 12 residue of EF hand loop binds to Ca^{2+} through the side chain carboxylate or carbonyl group. (**Figure 1.2 A**) Where the pseudo EF hand loop shows in **Figure 1.2 B** bind to Ca^{2+} with the resides with positions 1, 4, 6, and 9 of the 14-residue EF hand loop through the carbonyls group of the main chain.[6] In

eukaryotic cells, the primary Ca^{2+} singling protein is calmodulin. Calmodulin, belong to canonical EF-hand family proteins that contain four EF-hand. CaM undergoes a conformation change once it binds to Ca^{2+}, the conformation change allows the active CaM interact with many target proteins.

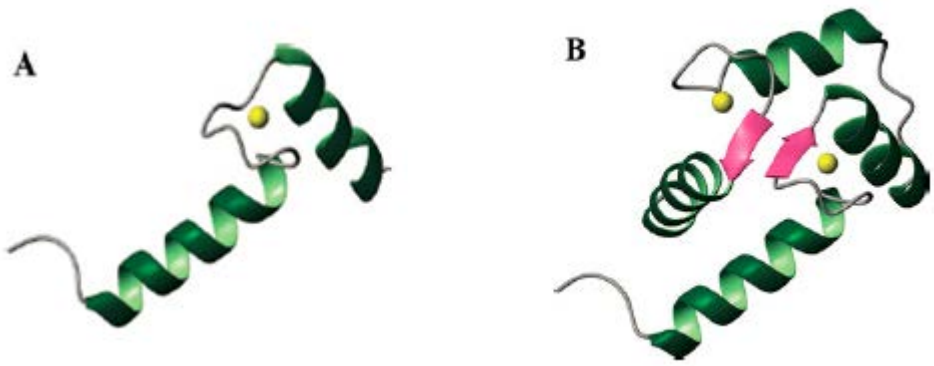

Figure 1.1. Structure of an EF-hand motif formed by an helix-loop-helix.
A. Ca^{2+} form of one EF-hand of N domain of CaM; B. Ca^{2+} form of pair of EF-hands of N domain of CaM (PDB code 1EXR). (The figure is adopted from Gifford *et al.*[7])

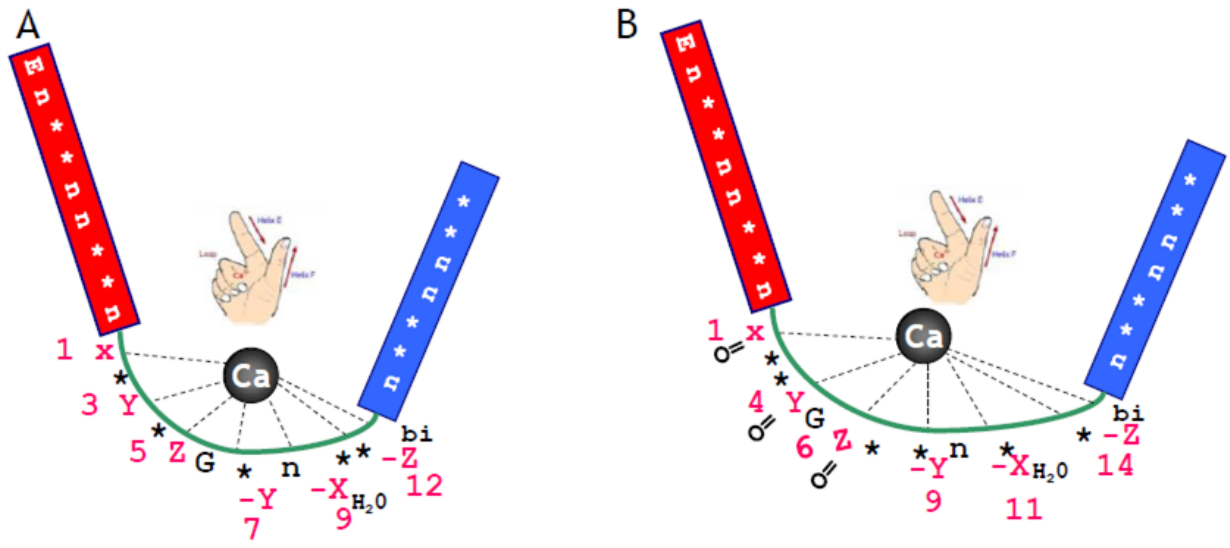

Figure 1.2. Geometry of typical helix-loop-helix EF-hand Ca^{2+} binding motif. A. Canonical EF-hand Ca^{2+} binding motif is formed by conserved hydrophobic residues (n) at both helices and loop position 8 and G at loop position 6. Calcium is coordinated by conserved residues at loop positions 1 (x), 3 (Y), 5 (Z), 7 (-Y), 9 (-X) and 12 (Z). B. Pseudo EF-hand Ca^{2+} binding motif is formed by 14-resdidue calcium binding loop and two flanking helices with conserved hydrophic residues (n). negatively charged residues Asp at loop position 1 and Glu at loop position 12 for a canonical and 14 for a pseudo EF-hand motifs contribute greatly for the calcium binding affinity of an EF-hand motif.

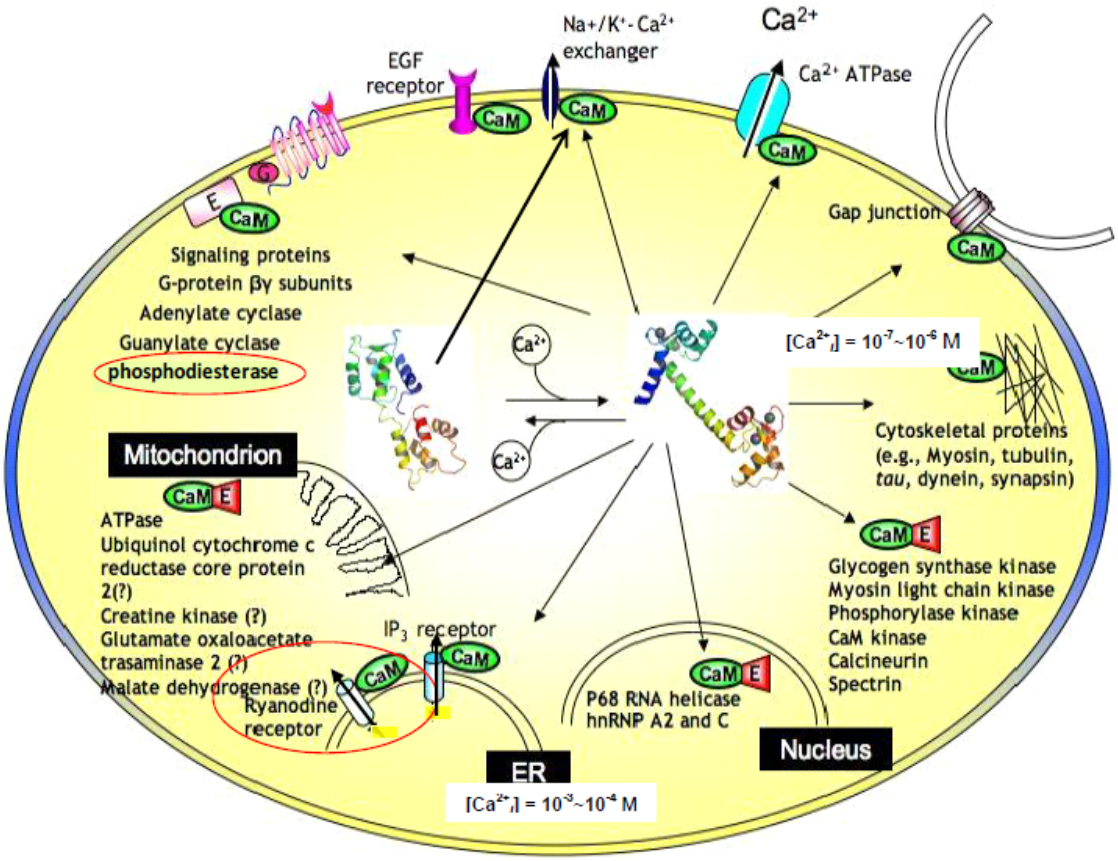

Figure 1.3. Cellular distribution of CaM, and its regulated proteins such as gap junction proteins for cellular communication and RyR for calcium homeostasis, as well as cytosolic proteins such as phosphodiesterase (PDE).

1.2. CaM, a Ca^{2+} binding protein

Calmodulin (CaM) is an acidic intracellular Ca^{2+} signaling protein that contains 148 amino acids with an atomic mass of 16.7kDa. CaM was first discovered as a cyclic nucleotide phosphodiesterase activator protein in the brain and heart.[8] Later on, it was rediscovered several times by other researchers and eventually shown to involve the same Ca^{2+} binding protein.

CaM is an ubiquitous intracellular calcium binding protein located in all mammalian cell including yeast and plants (**Fig. 1.3**). The primary sequences of CaM are highly conserved in all eukaryotic proteins. All known vertebrate CaM are identical. This high degree of conservation may be essential for the maintenance of interaction with a diverse family of CaM binding protein.[9]

CaM contains 148 amino acids that formed four EF-hands **(Figs. 1.1-1.2**). Every two EF hands form N-domain (residue 1-75) and a C-domain (76-148) that connected by a flexible linker. Through its reversible or irreversible binding to Ca^{2+}, the resultant conformational changes and the interaction with target proteins, CaM is capable of transducing the intracellular Ca^{2+} signal changes into a myriad of divergent cellular events. Among myriads of Ca^{2+} binding proteins which modulate cell signaling, CaM plays an essential role and it has been extensively studied due to its ubiquitous expression in eukaryotes in addition to its versatile ability to activate or inhibit more than 300 functional enzymes, cellular receptors and ion channels (**Fig. 1.3**).[10] In the apo-CaM (Ca^{2+} free form), shows in **Figure 1.4 A**, the two helices of EF hand are almost parallel to each other. However, when CaM binds to Ca^{2+} (Ca^{2+}-CaM form), showed in **Figure 1.4 B**, the two helices of the EF hand become perpendicular to each other. Ca^{2+} binds to CaM which causes a conformational change. The central region that connects the two helices becomes more helical and exposed more hydrophobic residues to the surrounding surface, which make CaM

easily to bind with specific proteins for specific response.[7] Ca^{2+} concentration of the cytosol changed from 10^{-7} to 10^{-5}, CaM undergoes a conformational change by binding with Ca^{2+} and interact with numerous target proteins, such as ryanodine receptor, IP3 receptor in the endoplasmic reticulum (ER), gap junction at the plasma membrane. (**Figure 1.3**)

The Ca^{2+} concentration range to which CaM responds increases as a result of the 10-fold higher Ca^{2+} affinity of the C-terminal domain (Ca^{2+}-binding sites III and IV) compared to the N-terminal domain (Ca^{2+}-binding sites I and II).[11] These different Ca^{2+} affinities contribute to CaM's functional bifurcation which allows the two domains of CaM to serve different functions. For example, Ca^{2+}-dependent facilitation of Cav2.1 voltage-gated Ca^{2+} channels requires Ca^{2+} binding to CaM's C-terminal while Ca^{2+}-dependent inhibition of these channels requires Ca^{2+} binding to CaM's N-terminal. Further, the two lobes of CaM may separately decode global and local Ca^{2+} signals. Therefore, one strategy to manipulate cellular responses to Ca^{2+} signals may be to modify the Ca^{2+} affinity of the protein which decodes the signal. Because of its functional bifurcation, CaM is an attractive target. By manipulating the affinity of one domain of CaM it may be possible to selectively enhance a specific CaM function. One of the most interesting characteristic features of CaM is the diversity in the target proteins that it regulates. Most of the CaM binding targets share very little sequence identity; however, many of them have a number of common characteristics. The majority of many CaM binding targets are around 16-30 amino acid long and have the intensity to form amphipathic α helices with both basic and hydrophobic faces.[12]

To date, it is not clear how CaM as a whole and each structural components of CaM, such as N, C, domain, and central helix of CaM are able to regulate various target proteins **(Fig. 1.4**). In Chapter 3 more detailed studies of wt-CaM and three different mutant CaM (C and N isolated

CaM, and central linker deleted CaM), in term of expression and purification study, secondary structural analysis, metal titration, and functional assay will be described in Chapter 3 in this thesis.

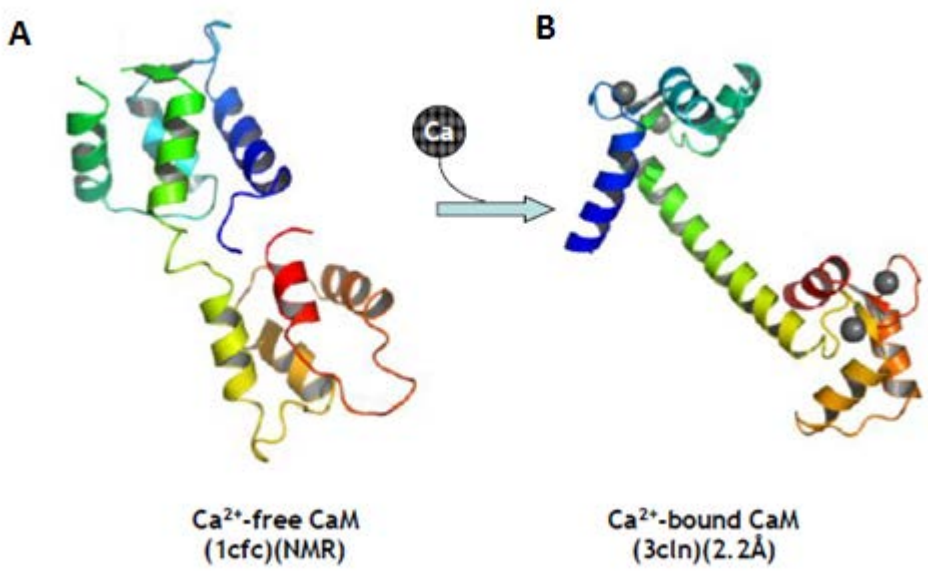

Figure 1.4. Conformational change of CaM upon binding to four calcium ions cooperatively.
A. Ca^{2+} free form of CaM (PDB code 1CFC); B. Ca^{2+} binding form of CaM(PDB code 3CLN).

1.3. Yeast Calmodulin

Like CaM in animals, CaM in yeast also performs many essential functions, and disruption of CaM gene is lethal. Yeast calmodulin (yCaM) from *Saccharomyces cerevisiae* is CaM isoform that share about 60% sequence identity with vertebrate CaM (vCaM) (**Fig. 3.2**). Like other CaM, yCaM have four EF hands, and it also performs a Ca^{2+} dependent enzymatic activity. Ca^{2+} binding sites II and IV of yCaM have several residues are different from the vCaM that need to be highly concerted because they are the Ca^{2+} ligands. For EF II of yCaM, glycine 61 is replaced by histidine. In EF hand IV of yCaM, not only glutamate 140 (Conserved bidentated chelating residue) is replaced by glutamine, also EF-hand loop residue 2 is deleted. (**Figure 3.2** Glutamate at position 12 in all vCaM EF hand is needed to provide two Ca^{2+} bind ligands. Therefore, mutations of EF IV of yCaM affect the Ca^{2+} binding ability.[13] yCaM is able to perform enzymatic activity to phosphodiesterase (PDE) and myosine light chain kinase (MLCK) of vertebrates; however, the activity is much lower than the vCaM.[14] Hidenori Yoshino and his group using solution X-ray scattering showed that yCaM showed an asymmetric globular like shape instead of the dumbbell shape of CaM that is essential to form open conformation for the target protein.[15] The Ca^{2+} binding to two domains of the yCaM show a cooperative manor of the target protein, whereas the two domains of CaM behave individually.

To understand whether such dramatic differences in calcium induced conformational change of yCaM compared with w.t CaM are due to their differences in calcium binding affinity with alteration in EF-hand calcium binding sites as well as the methylation process of yeast CaM, I will also report some initial effort in purification of yCaM from yeast in Chapter 3.

1.4. Ryanodine receptor

Ryanodine receptors (RyRs) are Ca^{2+} release channel that located in the sarcoplasmic/endoplasmic reticulum (SR/ER) membrane and release Ca^{2+} from the intracellular SR lumen during excitation-contraction coupling in both cardiac and skeletal muscle (**Fig. 1.3**). RyRs can bind to ryanodine with high affinity and specificity; therefore, RyRs named after the plant alkaloid ryanodine. RyRs are homotetramer with molecular weight that is greater and 2,009 kDa (~550 kDa each subunit), and are the largest know ion channels to date.[16] There are three mammalian isoforms (RyR1-3), these three mammalian isoforms RyRs shared 65% identity. RyR1 was first detected in the skeletal muscle, and it is highly expressioned from the skeletal muscle. RyR2 was first found in the cardiac muscle in 1990 by Nakai *et al.*[17] and Otsu *et al.*[18] RyR3 is disturbed everywhere, but many primary express in the brain. **Figure 1.5** shows the structure comparison of three mammalian RyR isoforms. For the nonmammalian vertebrate, such as fish and birds express isoform RyRα and RyRβ. RyRα show high expression level in the skeletal muscle; RyRβ is expressed in many tissue include skeletal muscle, cardiac muscles, and lung.[19] In this lab research, RyR1 is the main focus of this thesis.

RyR1 have a mushroom shape that composed of four identical subunits. Each subunit contains a transmembrane (TM) region and cytoplasmic (CY) region. (**Figure 1.6**) Recently, cryoelectron microscopy (cryo-EM) has improved the RyR1 structure with subnanometer resolution.[20] Ca^{2+} regulates RYR1 both in the cytoplasm and in the luman of SR. RyR1 activity shows a bell shaped dependence on the Ca^{2+} concentration, which means the low Ca^{2+} concentration (~1μM) active the channel, where high Ca^{2+} inhibit the channel at high concentration (~mM).

In addition to calcium, CaM can also regulate the RyR1 and it was reported to have one or several potential binding sites at each subunit. RyR1 can be regulated by both apo-CaM and Ca^{2+} form of CaM. At submicromolar Ca^{2+}, CaM (apoCaM) activates partially RyR1, whereas at millmolar Ca^{2+}, Ca^{2+}-CaM becomes a partial inhibitor. Resides 3614-3643 have been identified to be one of the CaM binding region by Susan Hamilton group.[21] Moreover, both apo-CaM and Ca^{2+} form CaM can bind to this region. Cryo-EM studies have been used to mapping the location of two forms of CaM binding toward this region of RyR1 in three-dimensional structure as shown in **Figure 1.6**. The CaM binding sites are located in the CY region, and the location between the apo and Ca^{2+} form of CaM are ~33 Å apart. The close location of apo- and loaded form of CaM binding sites could be due to the fast respond of switch from an activator to an inhibitor to the channel when the Ca^{2+} concentration increase. Beside region 3614-3643, region 1975-1999 is also a CaM binding site that was found by Susan Hamilton group.[22] Later on, same group of people found region 4064-4210 of RyR1 contains two putative EF hand motifs that can compete with CaM for RyR1 3614-3643.[23] Mutations in the RyR1 gene can debilitate many life-threat muscle diseases, such as malignant hyperthermia (MH), central core disease (CCD). Patients who have MH cause by the RyR1 channel to open more easily and close more slowly; as a result, large amount of Ca^{2+} release from SR within muscle cell. This results in skeletal muscle to contract abnormally and lead to rigid muscle. On the other hand, central core disease is muscle weakness which cause by the RyR1 less sensitive to open to release the Ca^{2+} that is essential for the skeletal muscle contraction.

Previous member Dr. Jie Jiang in Yang group has performed extensive studies for the CaM regulation of RyR1 using peptide models and NMR. In her Ph.D. dissertation studies, has shown that CaM is able to bind both regions of 3614-3643 and 1975-1999 of RyR1. To

understand the nature of CaM binding to these regions, she designed RyR1 mini domain which contain region 3614-3643 and 1975-1999 of RyR1 with GST tag to study how CaM interact with this two regions. I will report my effort in expression and purification of such Mini-domains in Chapter 6. More detailed information is discussed in chapter 6.

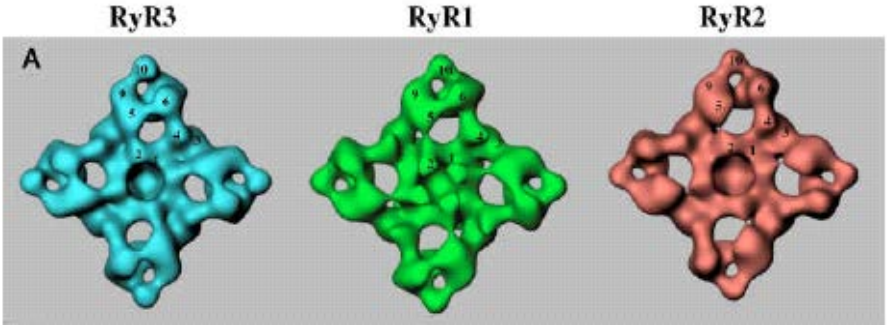

Figure 1.5. Structure comparison of RyRs isoforms. The figure is adopt from Wagenknecht *et al.*[24]

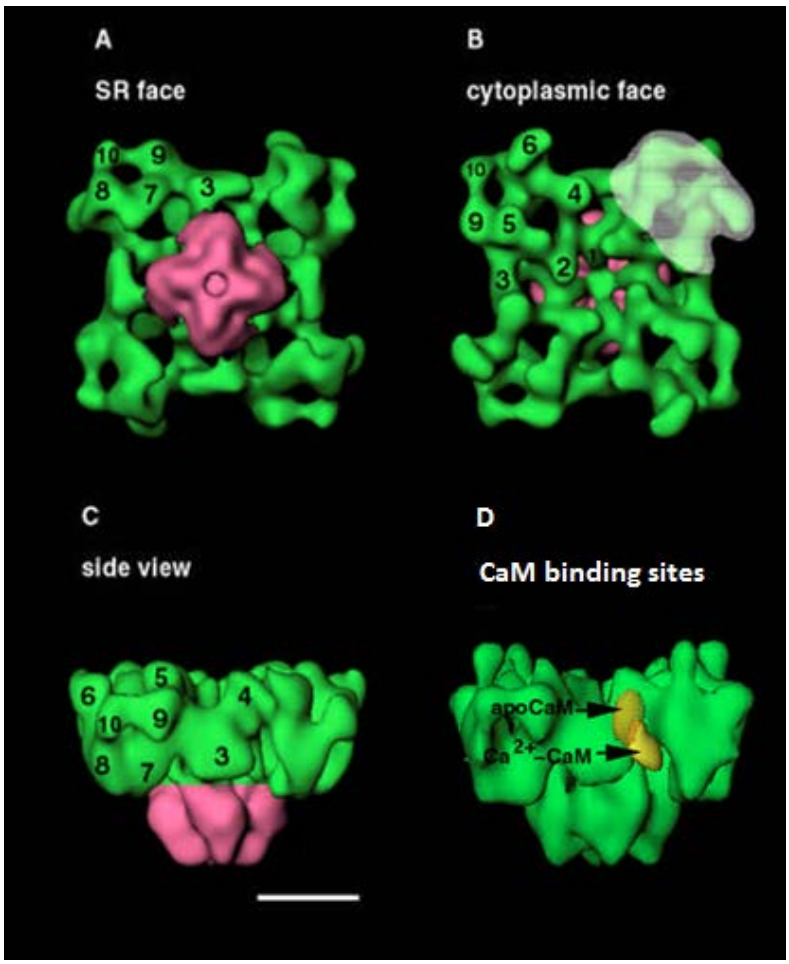

Figure 1.6. Different view of RyR1.
A. SR face of RyR1; B. Cytoplamic view of RyR1; C. side view of RyR1; D. different form of CaM binding region on RyR1. The figure is adopt from Wagenknecht et al.[24]

1.5. Gap Junction

As shown in **Fig. 1.3**, calmodulin also regulates gap junctions. Gap junction allows adjacent cell to communicate with each other by passive diffusion of many ions, second messengers, water, and electrical impulse through the channel. As shown in **Figure 1.7**, six connexin (Cx) subunits can form a hemi-channel (connexon) in the plasma membrane, which can dock with another hemi-channel in the plasma membrane of an adjacent cell to form a complete gap junctional channel. Each connexin subunit is formed by four transmembrane spanning proteins that contain two extracellular loops, a cytoplasmic loop and with C and N-terminal region at each side of the cytoplasmic loop region.[25] There are three cysteine residues within both extracellular loops that are highly conserved. The cysteines at opposite loop can form disulfide-bridge that can stabilize the loops during the docking process.[26] There is always more than one type of connexin expressed in the mammalian cell. The different compositions of connexin isoforms can contribute to form heterometric and heterotypic gap junction channels that can lead to variety of regulatory. Connexin are named according to the species from which they were derived and theoretical molecular masses. Furthermore, connexin can be divided into subgroups into α, β, and γ subgroup according to their sequence identity and the length of the cytoplasmic loop. To date, there are at least 20 connexin genes which have been identified in the human genome, among which connexin 43 is the most ubiquitous connexin.

Gap junctions have been shown to be regulated by $[Ca^{2+}]_i$ mediated by CaM interacting directly with the connexin proteins. CaM was proposed to have a role in the Ca^{2+} induced uncoupling of gap junction since CaM inhibitors was observed to prevent the response. Gap junction proteins expressed in different tissues are associated with a large number of

developmental disease, such as deafness (Cx26 and Cx30), oculodentodigital dysplasia (Cx43), and congenital cataracts (Cx43 and Cx50).[27]

Previous members Dr. Yubin Zhou and Yanyi Chen (Johnny) in our group have located two potential CaM binding sites on the cytoplasmic loop of Cx43 with one binding affinity is higher than the other.[28] Two peptides encompassing both CaM binding regions were designed, among which one peptide contains the entire cytoplasmic loop and another peptide contains the entire cytoplasmic loop and several residues embedded in the membrane region. The purpose is to compare the CaM function towards those two peptides and more detailed study is discussed in Chapter 6.

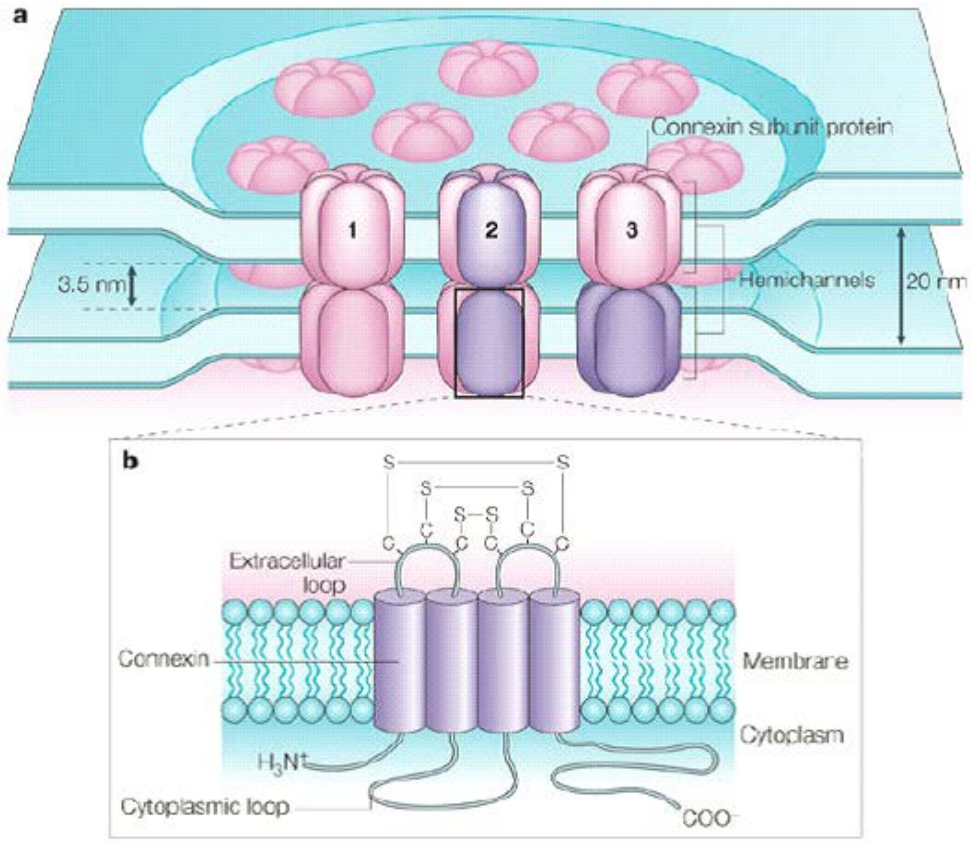

Figure 1.7. Anatomy of connexin protein family. The figure is adopt from Sohl *et al.*[26]

1.6. The Objective of this thesis

The first objective of this research is to study the expression and purification of wt-CaM and its variants, and then compare with the yCaM. Secondary structure analysis of the wt-CaM and its variants is study the secondary structure changes with additional of Ca^{2+}. Metal titration is also study by monitoring the intrinsic fluorescence intensity and the fluorescence resonance energy transfer to study the binding affinity of CaM towards metals (Chapter 3).

The second objective of this research is to optimize the expression condition of isotopic labeled CaM. Many of the protein studied in our lab is CaM binding protein. By monitoring the chemical shift of each residue of the isotopic labeled CaM from NMR, the interaction of CaM with many massive proteins the protein-protein can be solved.

The third objective of this research is to understand the role of the structural components of two domain of CaM interact with two CaM binding site of RyR1. RyR1 mini domain is designed that contain two of the CaM binding sites of RyR1. By using the RyR1 mini domain, we can testify the two models that we purposed in chapter 4.

The last objective of this research is to design CaM binding peptide of connexin family. Many regions on the cytoplasmic loop have been predicted to be CaM binding site. We designed two Cx43 peptides, one of the peptides is the entire cytoplasmic loop, and another peptide of Cx43 contains entire cytoplasmic loop and part of the trans-membrane domain. By compare the different interaction of CaM with those two peptides, we can understand the importance of the trans-membrane domain of this membrane protein (Chapter 6).

2. Material and Methods

2.1. Proteins expression and purification of CaM and its varies

2.1.1. Expression and purification of CaM and its mutants

CaM and its mutants from rat were transformed in E. coli cell strain BL21(DE3)pLysS competent cell that contain vector pET-7 by heat shock method. A health colony was selected and inoculated in the Luria Bertani (LB) medium with 100 mg/L ampicillin at 37 °C. Isopropyl β-D-1-thiogalactopyranoside (IPTG) with final concentration of 200 μM was added for protein induction when the optical density reached (OD600 reach 0.6-0.8). The protein was continuously expressed for 4-5 hours at 37 °C after the induction, and cell pellet was collected.

CaM cell pellet was re-suspended in 30 mL homogenization buffer (2 mM EGTA, 1 mM DDT, 1 mM PMSF, and 50 mM Tris with pH adjust to 7.5 by HCl). The resulting solution was subjected to sonication 3 time for 30 seconds with 5 minute interval between each sonications in order to avoid protein degradation due to heat produced by the sonicator's sound waves.The solution was subject to the French press at 1500 pis or cell disruptor. The solution was heated at 85°C for 5 min to denature any heat unstable unwanted protein. The solution then was centrifuge at 17000 rpm for 45 min. The supernatant was injected to pre-equilibrate Phenyl-sepharose columns in the presence of 5 mM $CaCl_2$ for overnight binding. The column was washed by buffer 1 (0.5 mM $CaCl_2$, 50 mM Tris, pH=7.5 adjust with HCl), the non-specific binding protein was washed away by buffer 2 (0.5 mM $CaCl_2$, 500 mM NaCl, 50 mM Tris, with pH 7.5 adjusted with HCl). Protein fragments were eluted from column by elution buffer (50 mM Tris, 5 mM EDTA at pH 7.5 adjusted with HCl).

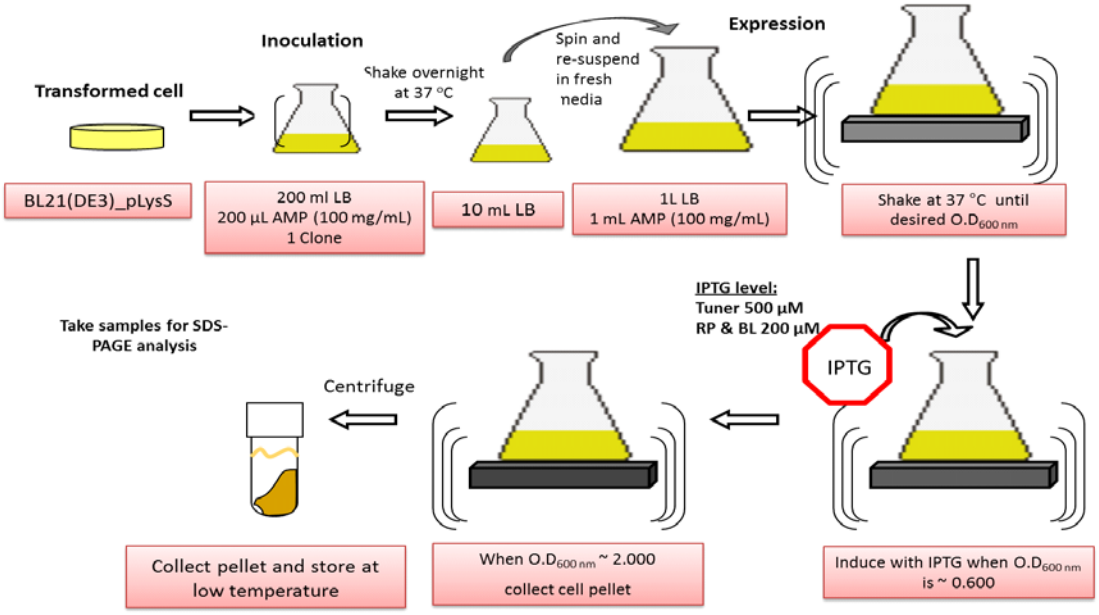

Figure 2.1. Summary of expression procedure.

2.1.2. Expression of ^{15}N labeled CaM by using SV medium

^{15}N labeled CaM were expressed in SV medium with contain 4.4 g/L KH_2PO_4, 7.94 g/L K_2HPO_4, 0.05g/L $MgSO_4$, 0.0079g/L $Fe(NH_4)_2(SO_4)_2$, and 5g of glucose. 0.5g/L of $^{15}NH_4Cl$ was the source for the isotopic nitrogen labeling protein. 200 µM of IPTG was added for the induction when OD_{600} reach to 0.6-0.8. The cell pellet then was collected after 4-5 hour after the induction. The collected cell pellet was purified by using the purify methods according as mentioned as 2.1.1.

2.1.3. Expression of ^{15}N and ^{13}C labeled protein

The double labeled CaM were expressed in M9 medium which contains 6 g Na_2HPO_4, 3g KH_2PO_4, 0.0015 g $FeSO_4$, 0.2407 g $MgSO_4$, 0.0011 g $CaCl_2$, 1.0 mL micronutrients, 0.5 g NaCl, 5 mg thiamine, and 1.0 mL of vitamin supplements. 0.5 g/L of $^{15}NH_4Cl$ and 2 g of ^{13}C glucose were added as the source for the isotopic nitrogen and carbon labeling protein. (detailed ingredients is in the appendix) 200 µM of IPTG was added for the induction and the cell pellet was collect after 4-5 hours after induction. The protein was purified by using the same purification method as mentioned at 2.1.1.

2.1.4. Expression of ^{2}H, ^{15}N, and ^{13}C labeled protein

One healthy colony was selected from the minimal plate and inoculated into 50 mL of 100% water based M9 medium and grew for overnight at 37 °C. 10 mL of overnight grew 100% water based M9 medium was centrifuged at 3000-4000 rpm at 20°C for 5-10 min. The cell

pellet was transfered into 50 mL 70% D_2O based M9 medium and grew for 24 hours at 37°C to reach optical density. 10 mL of overnight grew 70% D_2O based M9 medium was centrifuged at 3000-4000 rpm at 20°C for 5-10 min. The cell pellet was transfered into 50 mL 100% D_2O based M9 medium to grow for 24 hours at 37°C to reach optical density. The overgrew 50 mL 100% D_2O based M9 medium was transfered into 950 mL of freshly prepared 100% based M9 medium, and it was continuously grew at 37 °C. 200 μM of IPTG was added for the induction when OD_{600} around 1.0. The cell pellet then was collected 5 hours after the induction. The collected cell pellet was purified by suing the same purification method as mentioned as 2.1.1.

2.2. Purification of yeast CaM

The cell pellet of yCaM of Saccharomyces cerevisiae was a gift from UCLA. The pellet was lysised by using the same method as describe as 2.1.2, however, the protein was not heated for 5 min at 85°C to denature any unstable unwanted proteins. The supernatant was precipitated as Yoshikazu Ohya *et al*. described.[13]

2.3. Expression and purification of RyR1 mini domain

2.3.1. Expression and purification of GST tagged RyR1 mini domain

The GST fused RyR1 mini domain was transformed into plasmid vector pGEX-2T and expressed into E. coli cell strain BL21(DE3) with same method as mentioned in 2.1.1. The purification procedures followed the protocols for GST-fusion protein purification using

glutathione sepharose 4B beads (GE Healthcare). The GST-tag fused to proteins was cleaved on beads by thrombin.

2.3.2. Purification of GST tagged RyR1 mini domian by using Refolding Method

The cell pellet was dissolved into lysate buffer (30-50 mL PBS, 1 µL Benzonase Nucleas, 2 mM Mg^{2+}, 20 µL PMSF). The mixture was sonicated three times, followed by centrifuge at 17 krpm for 30 minutes at 4°C. The debris was washed 3-4 times with 2% Triton-x-100 until the debris turns white. The washed debris was dissolved in to 25 mL of 8 M Urea and 5 mM EDTA and stirred overnight at 60 rpm at 4°C. The solution was centrifuged again at 17,000 rpm for 20 minutes at 4°C. The supernatant was transferred to falcon tubes and PBS was added dropwise until the volume was doubled, and the solution was stirred for 2 hours. The dialysis was done in 2 M Urea for 4 hours, and transferred to 10mM Tris buffer for overnight dialysis. The further purification process was the same as the regular procedure.

2.4. Molecular cloning and plasmid reconstruction

The CaM binding regions of Cx43, Cx26, and RyR1 mini domain were amplified by using a polymerase chain reaction (PCR) and were inserted into a reconstructed vector that combined vector pET-32a and pET-15b. The sequence of the reconstructed peptides are conformed by GENEWiz. INC.

2.5. Expression and purification of reconstructed protein

The reconstruction plasmids were transformed into E. coli BL21(DE3) and expressed with thioredoxin protein fused at N-terminal with contain of his-tag in M9 medium with 100 mg/L carbenicillin at 37^0C. 200 uM of IPTG was added when the OD_{600} reached 0.8 to induced the protein expression. The temperature was reduced to 28 °C after the induction, and it was over expressed for overnight. The cell pellet was collected by centrifuge at 7,000 rpm for 15 minutes. Protein was purified by using His-tagged refolding method.

2.6. Concentration Determination

The concentration of the proteins was determined by measuring the absorbance of specific residue at certain wavelength. Beer's Law was used to calculate the concentration of each protein. **Equation (1)**

$$A = \varepsilon * c * l \quad \textbf{Equation (1)}$$

Where A is the absorbance, c is the concentration, ε is the molar absorptivity, and l is the pathway. For the C-CaM, the concentration was determine by monitoring the Tyrosine absorbance at excitation wavelength 277 nm with ε_{277}=3030 M^{-1} cm^{-1}; the concentration of the N-CaM was determine by monitoring the Phenylalanine absorbance at excitation wavelength 258 nm with ε_{258}=1073 M^{-1} cm^{-1}; the concentration of del-CaM and wt-CaM was determine by monitoring the excitation wavelength 277nm with ε_{277}=3030 M^{-1} cm^{-1}. The concentration of the RyR1 mini domain was determined by measuring the absorbance of Tyrosine at wavelength 280 nm with molar absorptivity ε_{280}=8250 M^{-1} cm^{-1}.

2.7. Western Blotting

The electrophoresed gel is placed in the Blot Module with the nitrocellulose membrane. The negative charged protein from the electrophoresed gel is transferred into the nitrocellulose membrane with 225 mA for 2 hours in transfer buffer (25 mM Tris HCl, 190 mM Glycine, and 10% Methanol). The nitrocellulose membrane is place into the blocking solution (5% BSA in TBS) for 40 minutes at room temperature. The membrane then is place into primary antibody (Monoclonal Anti-polyHistindine clone His-1. Anti-body is of the mouse IgG2a isotype) diluted in the fresh blocking buffer with ratio 1:1000. The second Anti-body is diluted with blocking buffer with ratio 1:3000 is apply to the membrane and incubate with room temperature for 1 hour. The location of the antibody is revealed by incubating it with a colorless substrate that the attached enzyme converts to a colored product that can be seen and photographed.

2.8. Circular Dichroism Spectroscopy

The secondary structures of proteins were determined at far UV region (190-280 nm) of circular dischrosim (CD) spectrometer (Jasco-810 spectropolarimeter) at room temperature in a 1 mm light pathway cuvette with Tris-KCl buffer (10 mM Tris at pH 7.4, 100 mM KCl) in a 1 cm light-path length quarta cuvette. All spectra are evaluated with the background subtracted and were comprised of an average of 10 scans with protein concentration of 5 μM. The spectrum CaM and it varies with Ca^{2+} and without Ca^{2+} were collected respectively to compare the conformational change due to the binding with Ca^{2+}.

2.9. Phosphodiesterase (PDE) Assay

A series of protein samples in 20µL were prepared by a continuous dilution with dilution of three times each, and the first diluted sample with 1.2 mM concentration. All the samples were analyzed in MOPS buffer (10 mM MOPS, 100 mM KCl at pH=7.2, 200 µM EGTA , and 10 mM $CaCl_2$) with total scan time as 200 seconds monitored by PTI fluoremeter at room temperature with excitation wavelength as 282 nm and emission wavelength as 442 nm. 4 µM of substrate mant-cGMP (a fluorescent derivative cGMP) itself in buffer was first scanned for 50 second, then addition 50 second scan was monitored by adding 0.5 µL of 10 mM PDE (3',5'-cyclic-nucleotide-specific from bovine brain); finally, the 1 µL of the first diluted protein was added and 100 seconds scan was monitored. The same procedure was repeated with the rest of the diluted proteins.

2.10. Equilibrium Calcium Titrations

The change caused by the Ca^{2+} binding to a specific domain were monitored by observed calcium dependent changes at the C terminal in intrinsic tyrosine fluorescence intensity (λ_{ex}=277 nm, λ_{em}=320 nm) and N terminal in phenylalanine (λ_{ex}=253 nm, λ_{em}=280 nm). 5 µM wt-CaM in buffer A (50 mM HEPES, 100 mM KCl, 5 mM NTA, 0.5 mM EGTA at pH7.4) was monitored for the tyrosine signal in 1 cm pathway fluore-cuvette, Ca^{2+} stock (50 mM HEPES + 100 Mm KCl + 5mM NTA, 15mM $CaCl_2$, pH=7.4) was titrated into 5 µM wt-CaM solution to monitor the tyrosine intensity increase. The decreased signal of phenylalanine was monitored by titrating Ca^{2+} stock (50 mM HEPES, 100 mM KCl, 5 mM NTA, 50 mM $CaCl_2$ at pH 7.4) into 10 µM wt-CaM in buffer A. The free Ca^{2+} concentration was determined by monitored the signal of 450

μM of Oregon Green 488 BAPTA [1,2,-bis-(o-aminophenoxy)ethane-*N, N, N', N'* –tetraacetic acid]-5N in buffer A and fitting to **Equation (2)**

$$[Ca^{2+}]_{free} = K_d \frac{f_{[X]} - f_{[min]}}{f_{[max]} - f_{[min]}}$$ **Equation (2)**

Where $f_{[X]}$ is the fluorescence at each titration point, and f_{min} and f_{max} are the fluorescence intensities at zero Ca^{2+} and saturating Ca^{2+} respectively. K_d is the Oregon Green dissociation constant for Ca^{2+}, which is 21.7 μM at λ_{ex}=495 nm and λ_{em}=520 nm. The titration data were fitted to a non-linear Hill Equation (3)

$$f = \frac{[Ca^{2+}]^n}{K_d{}^n + [Ca^{2+}]^n}$$ **Equation (3)**

Where *f* is the relative fluorescence change, K_d is the dissociation constant of Ca^{2+} to CaM, *n* is the Hill coefficient and $[Ca^{2+}]$ is the free Ca^{2+} concentration that is calculated from Equation (2)

2.11. Tb^{3+} Titration in Buffer System

2 μM of wt-CaM was prepared to a buffer system A (50 mM HEPES, 100 mM KCl, 200 mM NTA, and 2 μM protein at pH 7.2) and monitored with PTI fluoremeter at λ_{ex}=280 and λ_{em}=500-600 nm. Tb^{3+} from the stock (50 mM HEPES, 100 mM KCl, 200 mM NTA, 2 μM protein, and 200 μM Tb^{3+} at pH 7.2) was titrated into buffer A to monitored the signal change. Tb^{3+} itself were used as control and subtract from the protein signal, because Tb^{3+} itself also has fluoresce signal. The free Tb^{3+} concentration were determined by using Hill equation (**Equation 3 and 4**).

$$K_d = \frac{[M][L]}{[ML]} = \frac{[Tb]_{free} * [NTA]_{free}}{[Tb]_{total} - [Tb]_{free}}$$ **Equation (4)**

$$[Tb]_{free} = \frac{-(K_d + [NTA]_{total} - [Tb]_{total}) + \sqrt{(K_d + [NTA]_{total} - [Tb]_{total})^2 - 4 * K_d * [Tb]_{total}}}{2}$$

Equation (5)

K_d of the Tb^{3+} is 3.15 nM at λ_{ex}=280. The titration data were fitted to a non-linear Hill **Equation (6)**

$$f = \frac{[Tb^{3+}]^n}{K_d{}^n + [Tb^{3+}]^n}$$ **Equation (6)**

Where *f* is the relative fluorescence change, K_d is the dissociation constant of Tb^{3+} to CaM, *n* is the Hill coefficient and [Tb^{3+}] is the free Tb^{3+} concentration that is calculated from Equation (5)

2.12. One dimension NMR study

The 1 D experiment was applied on Varian Inova 600 MHz spectrometer. Apo-CaM was prepared in 100 mM KCl, 5 mM MES, 100 µM NaN_3, pH = 6.5, with 10 mM EGTA and 10% D_2O at 21°C with a final concentration of 100 μM.

2.13. Dansylation of CaM

300 µM Dansyl Chloride was dissolved in acetonitrile and it was added to 100 µM wt-CaM in buffer (10 mM Mops, 100 mM KCl, 3 mM EGTA, 1 mM $CaCl_2$, pH=7.0). Three

conditions were tried out for the danyslation. There are 1) heat the reaction for 45 min at 75°C, 2) heat in a water bath for 5 min in a microwave at power of 700 W, and 3) react at 4°C for 2 hours.

2.14. Study of binding affinity of Danysl-CaM with CaM binding proteins

The binding affinity $Cx43_{88-164}$, $Cx43_{99-154}$, $Cx26_{99-154}$, $Cx26_{206-226}$, and RyR1 mini domain with Dyanysl labeled CaM was monitored the emission signal of danysl-CaM with present of CaM binding peptides. The Emission fluorescence spectra were collected with 5 μM dansyl-CaM in the presence of 50 mM Tirs, 100 mM KCl, 1 mM $CaCl_2$ with increase concentration of peptides with λ_{ex}=335 nm and λ_{em}=400-600 nm. A negative control of peptide with no CaM binding prediction site was also performed with same condition.

3. CaM mutants design to study the function of CaM towards CaM binding proteins

3.1. Introduction of CaM

CaM, Ca^{2+} binding protein (CaBPs) that function by undergoing conformational changes on binding of Ca^{2+}. This superfamily of CaBPs is characterized by common helix-loop-helix structure, also call EF hand for their Ca^{2+} binding sites. CaM contains four EF hands motif. For each EF hand, there is a Ca^{2+} binding loop that is formed by seven oxygen ligands in pentagonal bipyramidal geometry. The Ca^{2+} binding loop can be noted on their linear position and their location in the co-ordination of tertiary geometry: 1 (+X), 3 (+Y), 5 (+Z), 7 (-Y), 9 (-Z), and 12 (-Z)[7] as shown in **Figure 1. 2** and **Figure 3.1 B**. Five of the seven Ca^{2+} binding ligands are provided by the nine residue loop. The other two remaining ligand coming from a bidentate carboxylate ligand which provide by the side chain of residue at position 12 (-Z). Although this residue is not structurally part of the loop, it is normally referred as the twelfth residue of the EF loop and it is conserved with glutamate acid. Acids from position 1(+X), 3(+Y), and 5(+Z) provide monodentate ligands via side chain carboxylate, where amino acid at position 7 provides a ligand via main chain oxygen. Residue at position 9 (-X) form coordination with Ca^{2+} through a water molecule. All the oxygen ligands are provided by the negatively charged amino acids, glutamic acid and aspartic acid. Residues at position 1 and 3 are conserved with aspartate acid; position 5 is conserved with either aspartate acid or asparagine as shown in **Figure 3.1 A**. The residue at position 8 are highly conserved with hydrophobic residue Valine or Isoleucine, with main chain NH and CO group are facing away from the Ca^{2+} binding site. This residue is very important for a small antiparallel β sheet formation of two coupled EF hand within each domain.[7]

The 148 residue CaM contain 4 EF hands, two EF hand pair up by a short antiparallel β sheet to form a globular domain. Pair EF hand is the basic structural/functional unit instead of a single binding site. Such a paired property is presumed to stabilize the protein conformation and increase the Ca^{2+} affinity of each site over that of isolated metal binding sites.[29] Two domains, N and C are connected by a flexible linker. The secondary structure of the two domains itself does not have significant changed after the Ca^{2+} binding; however, the two globular domain increase solvent exposure of the hydrophobic core to adopted and the central linker adapted to more extended helical structure, which give the Ca^{2+} CaM a dumbbell shape appearance (**Fig. 1.2**). NOE data indicate that residues 78-81 are so flexible that behave as 'tether' which allow the two domains tumble independently of each other.[30] The linker is very functional importance for two domain come together and clamp around the target peptide. The flexible linker clearly server a key function that permit the two domain interaction with target binding site.

Ca^{2+} binding to CaM occur in two distinct stages by monitoring the NMR spectra of the hetero-labeled protein (ref). Stage I has high Ca^{2+} binding affinity, which is characterized by slow exchange behavior and occurs during the first two Ca^{2+} ions which indicate high Ca^{2+} binding affinity. Stage II has lower Ca^{2+} binding affinity and it is characterized by fast exchange behavior and it is occurs during the second two Ca^{2+} ions. The first Ca^{2+} ions bind to Ca^{2+} binding site III and IV that are located in the C domain of CaM. The second two Ca^{2+} ion bind to Ca^{2+} binding site I and II that is locate at the N domain of CaM. The binding of two Ca^{2+} ions to each globular domain is positively cooperative; however, there is not interdomain cooperativity.[31] Increasing the number of negatively charged residues from three to four within the Ca^{2+} binding loop stabilized the Ca^{2+} with protein complex. Introduce more than four negatively charged residues within the Ca^{2+} binding loop decrease the stability of the Ca^{2+}-

protein complex due to the electrostatic repulsion between the nearby negative charged residues.[32] Several mutations within the Ca^{2+} binding loop have designed and studied in our lab, and Table 1 summary the changing of the properties of each mutant.

CaM contains 9 methionine (Met) residues (6.1% Met), which has the higher percentage than the average percentage of Met residues in other proteins, 1.5% in standard protein data base.[33] The reason for large number of Met group in CaM is because the unique chemical properties of this amino acid, which is also critical for its biochemical function of CaM. Met is normally classified as a hydrophobic amino acid; however, the side chain is also very flexible due to the combination of unbranched chain and the C-S bond. Moreover, sulfur is more polarizable than carbon, which it lead to stronger van der Waals contacts and also give Met a more plastic nature, which allow it adapt to both secluded and solvent accessible environments.[34] Many studies have shown that the oxidation of Met residues decrease the binding ability and the activation ability of CaM to its target proteins.[35, 36, 37, 38] Mutation studies (Met→Leu, Met→Gln) have also prove that Met is also important for CaM to interact with target protein.[39]

In this chapter, isolated of C (1-75) and N (76-148) domain CaM and CaM with deleted linker (76-81 residues of the central linker region is deleted) were designed to examine the structure difference and for further function analysis toward CaM target protein/peptides. The CaM mutants are expressed and purified compared with the wt-CaM. The secondary structure analysis is done for wt-CaM and its variants by using the circular dischromism. Different metal binding is studied with wt-CaM, via Ca^{2+} and Tb^{3+} titration. PDE assay is used to exam the biological function of wt-CaM.

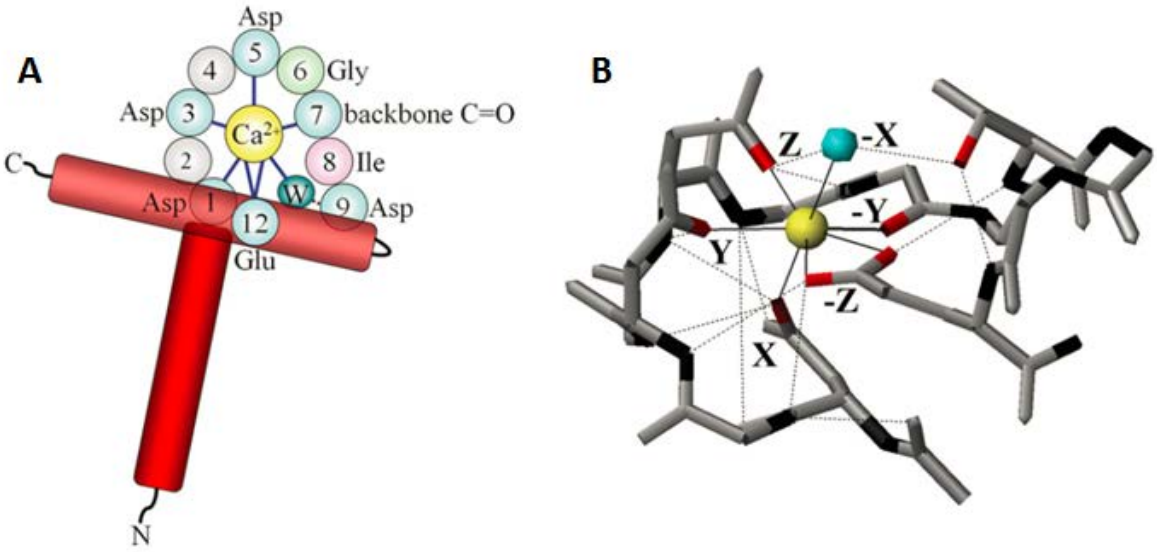

Figure 3.1. The coordination sphere of EF hand. The Figure is adopted from Gifford *et al.*[7] A) A schematic diagram of EF hand. B) A geometry coordinating of Ca^{2+} binding packet within the EF hand.

Table 3.1. Summary of CaM variants and property change.

CaM mutants	Change in Properties
T26D	Increase one negative charge in loop I; 30-34% decrease in ellipticity in the EGTA form, and 30-40% decrease in ellipticity. Increase Ca^{2+} binding affinity significantly for both C and N domain of CaM.
N60D	Increase one negative charge in loop II; 30-34% decrease in ellipticity in the EGTA form, and 2-8% decrease in ellipticity. No significate effect for Ca^{2+} binding affinity either C or N domain of CaM.
N97D	Increase one negative charge in loop III, 30-34% decrease in ellipticity in the EGTA form, and 30-40% decrease in ellipticity. Increase Ca^{2+} biding affinity of C domain and decrease the Ca^{2+} binding affinity of N domain of CaM.
Q135D	Increase one negative charge in loop IV; 9% decrease in ellipticity in the EGTA form, and 2-8% decrease in ellipticity. Decrease the Ca^{2+} binding affinity of C domain but increase Ca^{2+} binding affinity of N domain of CaM.

3.2. Introduction of yeast calmodulin

As discussed in Chapter 1.3, CaM from *Saccharomyces cerevisiae* is yCaM isoform that shares 60% identity with CaM. yCaM share lots of structural similarities with vertebrate CaM (vCaM). Like vCaM, yCaM is also a heat stable, acidic protein that binds Ca^{2+}, with a Ca^{2+} dependent mobility shift on polyacrylamide gel. This protein also be purified with a hydrophobic resin due to its Ca^{2+} dependent manner.[40] yCaM also exhibited a rich α helical secondary structure characteristic on the far UV spectrum,[41] and the tertiary structure of yCaM was also suggested to fold similar as the CaM.[42] Moreover, the C domain has a lower melting point than the N domain of the protein, indicating that C domain of yCaM is also less stable, a property that is similar to the C domain of CaM.[13] Furthermore, vCaM can replace yCaM to perform the essential function, such as PDE assay.

There are many structural similarities of yCaM with CaM; however, yCaM is also very different from CaM. Although yCaM contain four EF hand, the fourth EF hand cannot bind to Ca^{2+}, but retain the helix-loop-helix structure retains as the vCaM.[14] One of the amino acid from the 12 residues EF loop is deleted, and Glu at the position 12 that provides two binding ligands for the Ca^{2+} binding pocket is replaced with Gln. (**Figure 3.2**) This suggested that unable to bind Ca^{2+} is only due to the replacement of residues that are important to involved Ca^{2+} binding packet.[13] Because the defects in the Ca^{2+} binding at site IV, the N domain of yCaM have higher binding affinity towards to Ca^{2+} than the C domain. Starovasnik M. A. *et al.* used NMR to monitor the chemical shift of individual domains of yCaM during the Ca^{2+} titration. They found that during the Ca^{2+} titration, several peaks from the N domain of yCaM show slow exchange (peaks disappearing and then reappearing at new chemical shift) towards the first two Ca^{2+}

equivalents, and a fast exchange (peaks migrate toward their new chemical shift) from the C domain yCaM during the third Ca^{2+} equivalent.

yCaM do bind and active many CaM active enzyme, such as PDE and CaN, but with lower affinity. Moreover, yCaM does not active myosin light chain kinase (MLCK).[15] By using the solution X-ray scattering, the solution structure of yCaM show that the Ca^{2+} free form of yCaM has a dumbbell shape structure that is similar to the apo form of brain CaM (**Fig. 1.4**). However, the Ca^{2+} form of yCaM adopted an asymmetrical globular like structure that is very different from vCaM. Such calcium loaded structure of yCaM may be correlated to its lower affinity toward the CaM target protein.[15] Moreover, Ca^{2+} binding to CaM exposed Met rich hydrophobic surfaces that are responsible for the activation by recognizing the diverse sequences of CaM binding domain of targets. However, the Met rich hydrophobic surface is replaced by Leu in the yCaM, and its rigid and larger side chain exposed to solvent on Ca^{2+} binding.[43] As result, yCaM has less flexible and smaller hydrophobic surface compared to the N domain of CaM, which would be the factor for the limited level of activation of target enzymes.

To further understand of how CaM regulates other proteins, there are some questions that we need to be addressed. 1) How do we obtain large amount of CaM and its variants for understanding key determinants for calcium binding and recognition of target proteins ? 2) Are bacterial expressed and purified CaM and variants are well folded with its native function? 3) What are the domain-specific metal binding affinities of CaM? 4) Are there any calcium-induced conformational change for each domains of CaM? 5) Can we isolate sufficient vCaM for biochemical studies?

In this chapter, I will first report to achieve the objective is to study the expression and purification of wt-CaM and its variants, and then compare with the yCaM. Secondary structure analysis of the wt-CaM and its variants is study the secondary structure changes with additional of Ca^{2+}. Metal titration is also study by monitoring the intrinsic fluorescence intensity and the fluorescence resonance energy transfer to study the binding affinity of CaM towards metals Ca^{2+} and Tb^{3+}. In addition, PDE assay was used to test the native function of CaM.

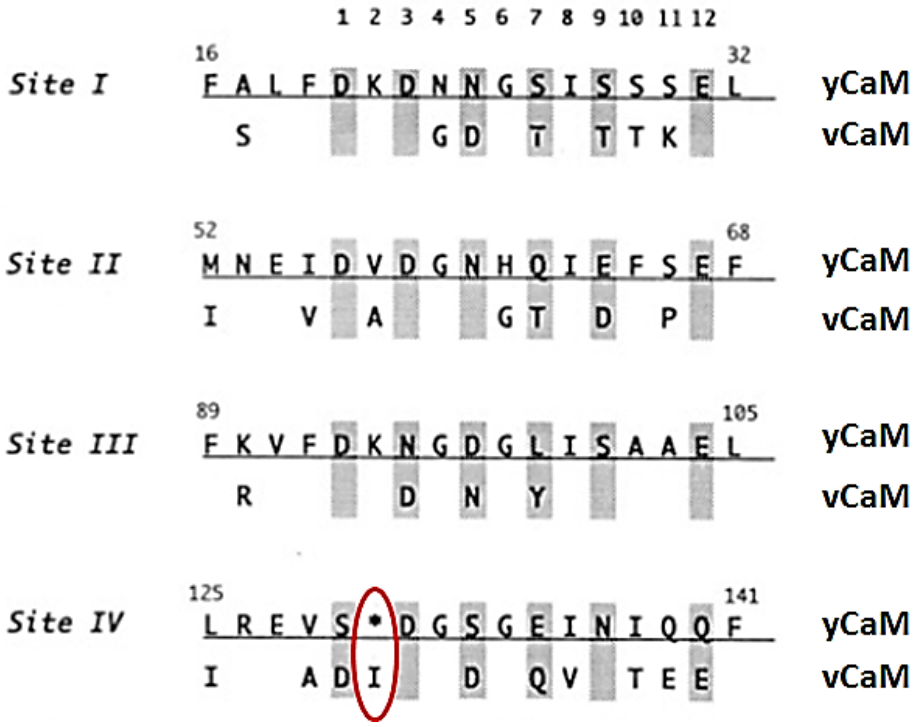

Figure 3.2. Comparison of primary sequence of four EF hands. The figure is adopt from Starovasnik et al.[13] (Top: yCaM; Bottom: vCaM).

3.2. Result

3.2.1. Expression and purification of CaM and variants

The C domain of CaM has approximate 10 fold higher Ca^{2+} affinity than the N domain of CaM. The big difference between the two domains makes CaM serve bifurcate function by allowing the two domain function independently.[17, 18] To study the specific function of individual domain of CaM, isolated C domain (C-CaM) and N domain of CaM (N-CaM) were designed to study their function toward the CaM binding protein. A mutant with 5 residue deleted from the helical linker region (del-CaM) was also designed to study the inter domain cooperativity and impact on CaM regulatory function.

The expression of CaM and variants were performed with tag less vector pET-7 at 37 °C for 4-5 hours in LB medium with E. coli cell strain BL21(DE3)pLysS after the induction. **Figure 3.3 A** shows the bacterial cell growth depend with time. The cell density was growing exponentially before the induction point, and the growth rate slow down after the addition of IPTG. SDS-PAGE shows low basal expression of other proteins before induction, and additional IPTG give a darker and thinker band indicate the protein was well expressed. (**Figure 3.3 B-E**)

Hydrophobic patch exposed to the environment with additional of Ca^{2+}, CaM and variants can use hydrophobic column for the purification process. SDS-PAGE shows the protein stay in soluble form at the supernatant after cell lysis as it should be. The elution of the protein also shows a single band indicate that the protein during the purification process was relatively pure. (**Figure 3.4 A-D**) **Figure 3.4 E** shows the UV spectrum of the wt-CaM and variant elution during the purification process. wt-CaM, del-CaM, and C-CaM shows very sharp peak at 278 nm by monitoring aromatic residue tyrosine. The N-CaM shows a sharp peak at 258 nm for

aromatic residue phenylalanine. The SDS-PAGE and the UV spectrum demonstrate that CaM and variants was relatively pure by using the hydrophobic method.

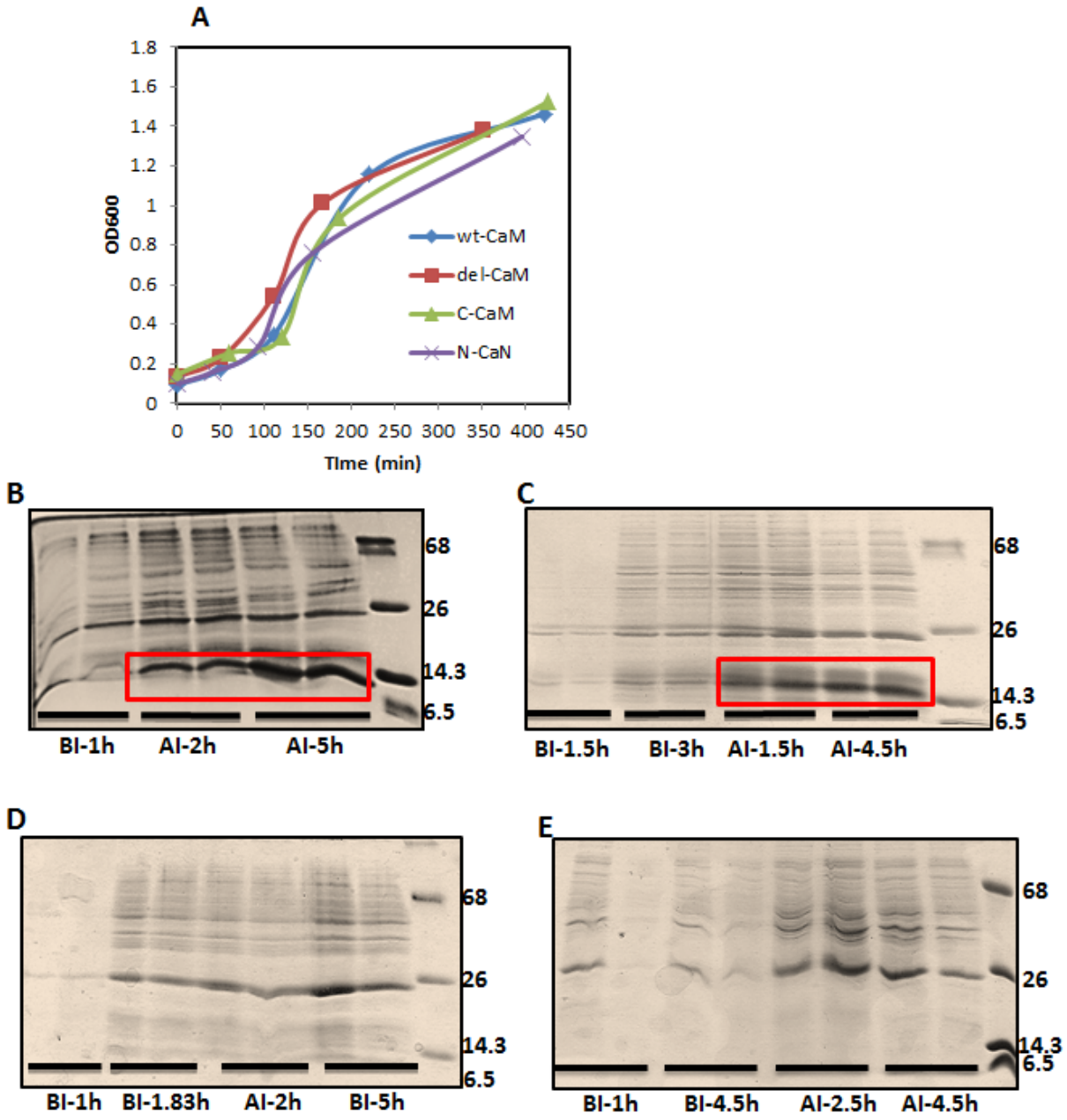

Figure 3.3. Expression of CaM and its variants.
A.Growth curve indicative of exponential increase in optical density of BL21(DE3)pLysS with CaM and its variants; B. 15% SDS-PAGE showing gradual production of protein with the passage of time of wt-CaM; C. SDS-PAGE of Del-CaM; D. SDS-PAGE of C-CaM; E. SDS-PAGE of N-CaM

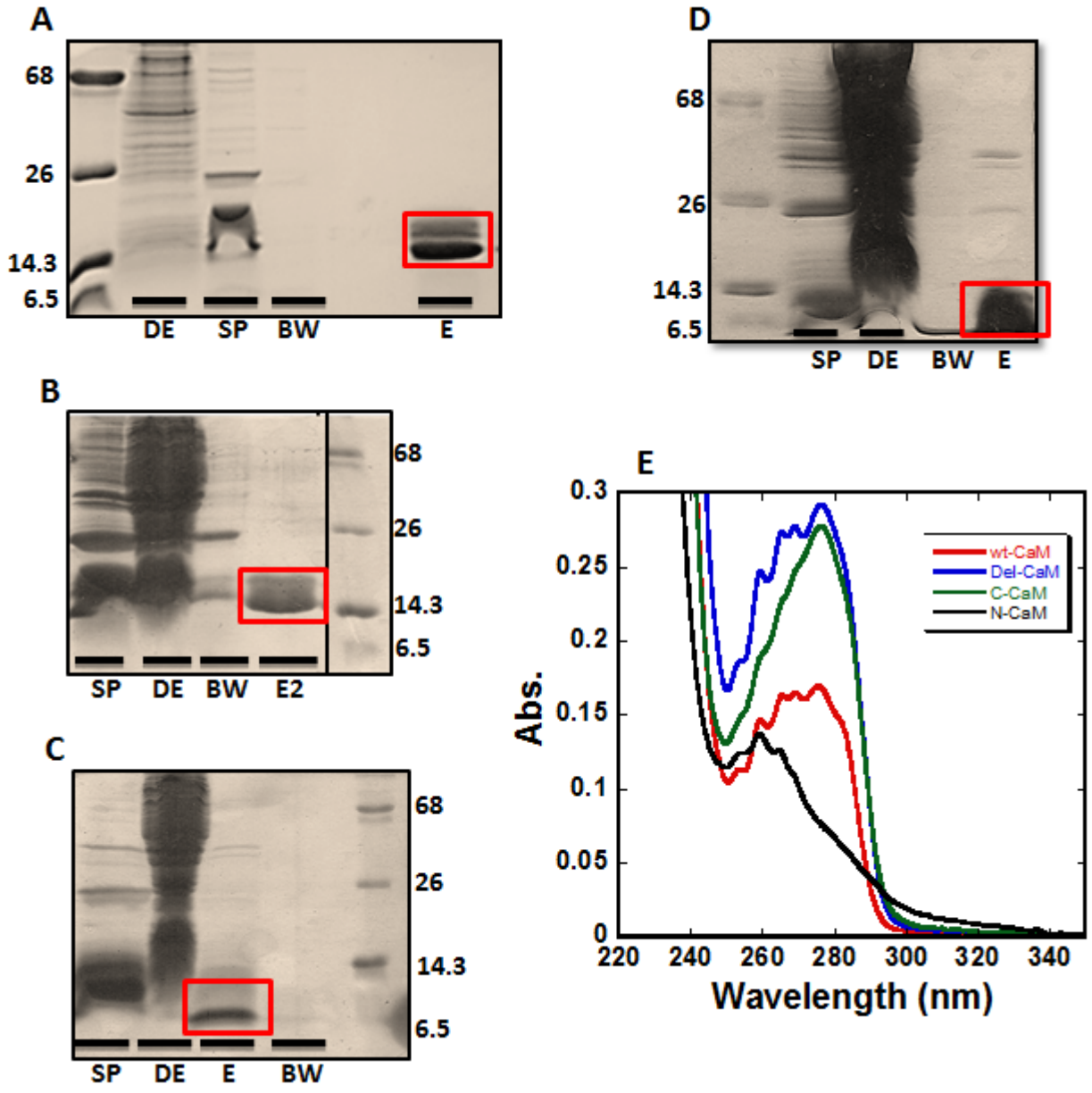

Figure 3.4. Purification of wt-CaM and its variants.
A). wt-CaM; B) del-CaM; C) C-CaM; D) N-CaM; E) UV spectra of wt-CaM and its variants elution. (DE: debris after cell lysis, SP: supernatant after cell lysis, BW: binding waste, E: elution)

Table 3.2. Summary of actual yield of wt-CaM and its variants.

Varies of CaM	Yield (mg/L)
wt-CaM	74
Del-CaM	78.5
N-CaM	54.6
C-CaM	36.4

3.2.2. Conformational analysis of wt-CaM and variants

CaM has two conformation, Ca^{2+} binding form of CaM (holo-CaM) and Ca^{2+} free form of CaM (apo-CaM). In the apo form, the two EF hands at each domain of CaM show an antiparallel fashion, which give domains a relatively compact structure. Once the Ca^{2+} binds to CaM, the two EF hands of the two domains adapt to perpendicular orientation by alter the interhelical angel of Ca^{2+} binding loop. Furthermore, the center linker connects the two domains become more extended and helical.

The secondary structure of the protein can be studied by monitor the far UV spectra of wt-CaM and its variant by using circular dichroism spectrometer. **Figure 3.5 A** showed both Ca^{2+} form (solid line) and EGTA form (dash line) of wt-CaM. Consistent with the substantial α helical content of both apo and Ca^{2+} loaded CaM and variants have large negative troughs at 208 and 222 nm in buffer contain 1 mM EGTA or 1 mM Ca^{2+}, and the ellipticity increase significantly in the present of Ca^{2+}. Del-CaM also shown similar spectra as wt-CaM as shown in **Figure 3.5 B**. **Figure 3.5 C** showed the Far UV spectrum of isolate N domain of CaM. In the EGTA form of N-CaM, the signal from the spectrum is very intense as the wt-CaM. However,

in the present of Ca^{2+}, there is no significant ellipticity change. On the other hand, the EGTA form of isolated C domain of CaM shows much less intense compare to other three form of CaM. Furthermore, there is dramatically increase in ellipticity in the Ca^{2+} form of C-CaM (**Figure 3.5 D**). This piece of data agree with the observation from Martin *et al.*, 1986, that they also observed that the conformational changes induced by Ca^{2+} is substantially greater in C-CaM than it is in N-CaM.[44] ^{1}H NMR data also suggest the spectral changes for first two Ca^{2+} ions bind to Ca^{2+} binding sites III and IV is dramatically bigger than the second two Ca^{2+} ions bind to Ca^{2+} binding site I and II at the N domain of CaM.[11] The observation that from the CD spectra agrees with the previous lab work and with other lectures evidence. The CD spectra also provide the information that wt-CaM and its variants have α helical characteristic as secondary structure, which also indicate that proteins are well folded.

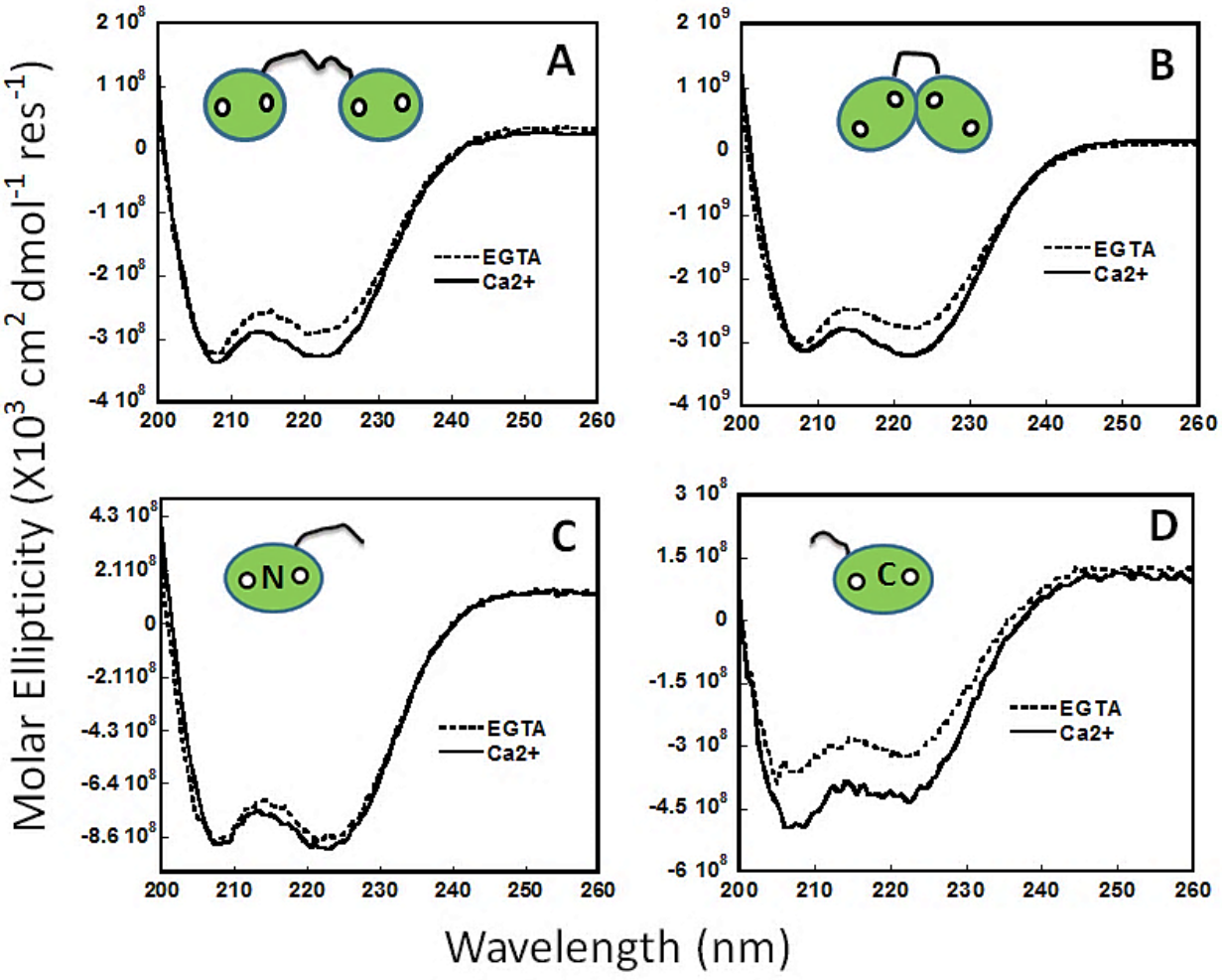

Figure 3.5. Far UV spectra of wt-CaM and CaM mutants.
The experiment was performed by 10 µM protein in 10 mM Tris, 100 mM KCl, at pH=7.4. of 1 mM EGTA form or 1 mM Ca^{2+} form of CaM and its variants. (A. wt-CM; B. del-CaM; C. N-CaM; D. C-CaM. - - - : Ca^{2+} form, ― : EGTA form)

3.2.3. Determining domain specific Ca^{2+} binding affinity of CaM

CaM contains two domains, N domain which composed of residues 1-75 (with Ca^{2+} binding site I and II), and C domain that composed residues 76-148 (with Ca^{2+} binding site of III and IV). Although the structure of two domains is very similar, the calcium binding affinity is 10 folders different between the two domains. There are two tyrosine (Tyr) residues at the EF hand binding pocket of the C domain of CaM which allow us to study the Ca^{2+} binding to the C domain of CaM (show in **Figure 3.6** green). However, the Ca^{2+} binding to N domain is hard to monitor since neither tryptophan nor tyrosine residues appear at the N domain. Wendy S. VanScyoc *et al.*[45] found that there are five phenylalanine (Phe) residue in the N domain of CaM (as shown in **Figure 3.6** red), and using this calcium dependent change in the phenylalanine fluorescence intensity can allow us to study the Ca^{2+} binding to the N domain of CaM. By comparing the calcium dependent change in phenylalanine fluorescence intensity of isolated N domain of CaM (CaM_{1-75}) and calcium dependent change in tyrosine fluorescence intensity of isolated C domain of CaM (CaM_{76-148}) with calcium dependent change phenylalanine and tyrosine fluorescence intensity of wt-CaM (CaM_{1-148}), they concluded that the Phe residue in the C domain of CaM are not emissive and then fluorescence intensity of Tyr in the C does not interfering the emission spectrum of Phe of N domain CaM.[45] Thus, intrinsic fluorescence from the excitation and emission wavelength of Phe and Tyr can be used to monitor equilibrium calcium titration of individual domains in full length CaM.

Domain specific Ca^{2+} binding affinities of CaM were determined by monitoring intrinsic phenyalanine and tyrosine fluorescence change during equilibrium Ca^{2+} titration. The fluorescence intensity of tyrosine increase as the Ca^{2+} concentration increase indicate the conformational change of C domain of CaM as Ca^{2+} binds to site III and IV as shows in **Figure**

3.7 A. The fluorescence intensity of phenylalanine decrease as the Ca^{2+} concentration increase indicate the conformational change of N domain of CaM as Ca^{2+} binding to sites I and II as shown in Figure 3.5. B. The Ca^{2+} dependence of phenylalanine and tyrosine fluorescence of wt CaM were fit with Hill equation and shows in **Equation (2)** at Chapter 2.9. **Figure 3.7 B and D**. illustrate the curve fitting of each titration point with Hill equation. The K_d of the C domain CaM is 2.7 μM, and it is significantly higher than the the K_d of the N domain CaM, 12.2 μM. This result agrees with our previous study result, which indicate that the binding ability of wt-CaM is consistent with the literature reported data.[46]

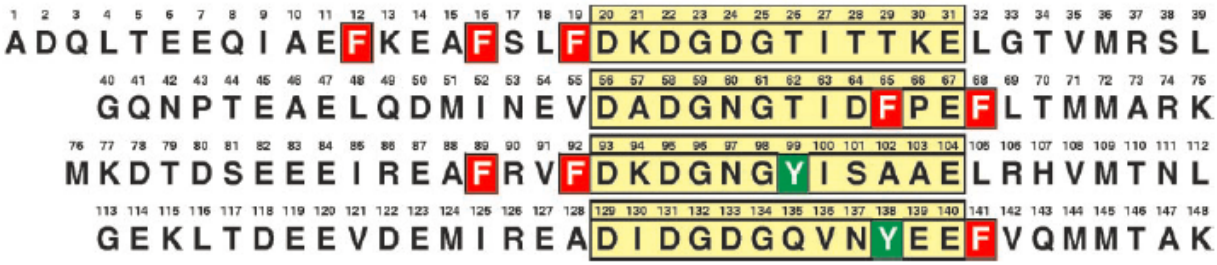

Figure 3.6. Primary sequence of rat CaM.
Residues in the yellow boxes are the residues involved in the EF hand binding packet with phenylalanine in red and tyrosine in green.

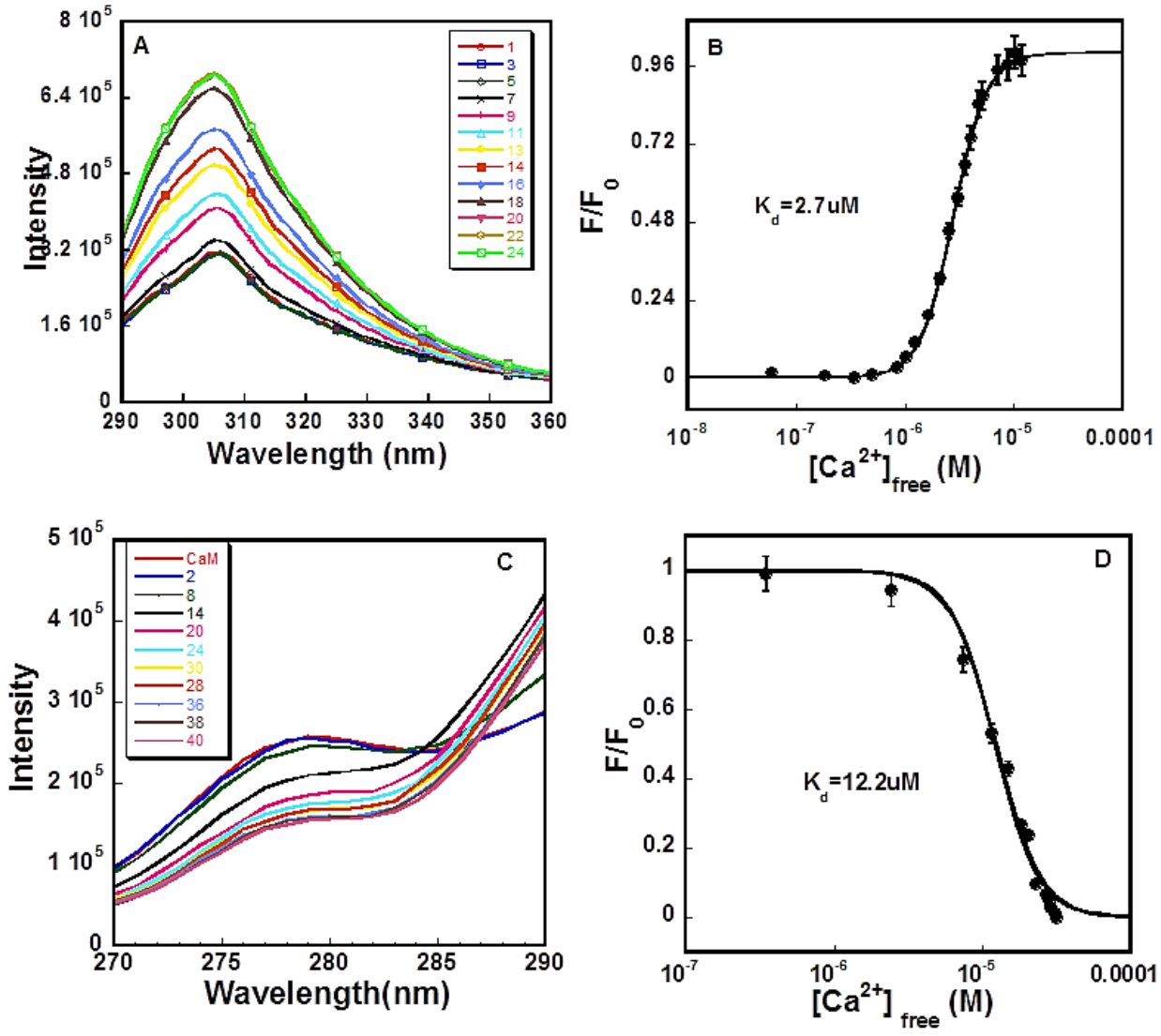

Figure 3.7. Determination of domain specific Ca2+ affinity of CaM by monitoring intrinsic CaM fluorescence of Phe and Tyr for N and C domain respectively.
Equilibrium $^{Ca2+}$ titration was perform in 10 µM CaM in buffer contain 50 mM HEPES, 100 mM KCl, 5 mM NTA, and 0.05 mM EGTA, pH=7.4. A. Mission scan of C domain of CaM by monitor the fluorescence intensity change of Tyr at λ_{ex}=277 nm and λ_{em}=320; B. Curve fit of C domain CaM; C. Mission scan of N domain of CaM by monitor the fluorescence intensity change of Phe at λ_{ex}=253 nm and λ_{em}=280 nm; D. Curve fit of N domain CaM.

3.2.4. Tb^{3+} titration

Terbium (Tb^{3+}), is a trivalent lanthanide process similar ionic radii and coordination number as Ca^{2+}. Tb^{3+} has unique fluorescence properties, and is greatly enhanced upon binding to a protein, a property highly useful for probe protein structure. It prefers binding to the charged or uncharged oxygen group, which make Tb^{3+} a good probe to study the interaction of Ca^{2+} with its receptor protein. Many biological system reactions can be performed efficiently with replacement of Tb^{3+} to the Ca^{2+} binding protein, such as activation of α-amylase[47], hemocyanines[48], and conversion of prothrombin to thrombin[49]. The ability of Tb^{3+} substitute for Ca^{2+} in CaM have been confirmed by monitored the mobility in polyacrylamide gel electrophoresis, intrinsic fluorescence spectra, binding to troponin I or calcineurin, and the activation of phophoidesterase.[50] Tb^{3+} indeed can replace Ca^{2+} without any contrary effect on physical and biological attribution of CaM. It can also act as an acceptor of fluorescence energy if it binds to fluorescence energy donor at appropriative distance. Therefore, Tb^{3+} can be used as probe of metal binding sites in CaM since Tb^{3+} and Ca^{2+} have similarity in their ionic radii and coordination chemistries.[51]

Monitoring Tb^{3+} binding to CaM can either be directly by exciting Tb^{3+} at 222 nm or indirectly by exciting tyrosine at 280 nm to generate resonance energy transfer. By directly exciting Tb^{3+} at 222 nm detect Tb^{3+} bound to any of the Ca^{2+} binding domain. Whereas, indirect excitation at 280 nm detect the Tb^{3+} fluorescence enhancement from resonance energy transfer (FRET) from tyrosine which is located at C domain of CaM.[50] By indirect excitation at 280 nm, we can also detect the conformational change of CaM through the enhancement of Tb^{3+} fluorescence intensity. Therefore, indirectly exciting Tyrosine at 280 nm and we can detect the

Tb^{3+} fluorescence intensity enhance through FRET cause by the conformational change of CaM binding with Tb^{3+}.

Tb^{3+} titration has to perform in the buffer system since the binding affinity is too high to be detected through direct titration method. **Figure 3.8 A** shows the Tb^{3+} fluorescence intensity by indirect excitation at 280 nm before the baseline. **Figure 3.8 B** shows the Tb^{3+} fluorescence intensity after the baseline. The free Tb^{3+} concentration is calculated by using Hill equation as show in **Equation (4)** and **(5)**. The disassociation constant (K_d) of Tb^{3+} with CaM is 3.97 nM by fitting non-linear Hill equation, and it is consistence with the primary lab data result (K_d=3.15 nM) value of of Tb^{3+} (More information can find from Jie Jiang's dissertation). **Figure 3.8 C** is the curve fit for the Tb^{3+} titration. The binding affinity of $Tb3^{+}$ of CaM is 1000 fold higher than the Ca^{2+} due to the higher electron charge, which can binds to negatively charged EF binding packet tighter than Ca^{2+}.

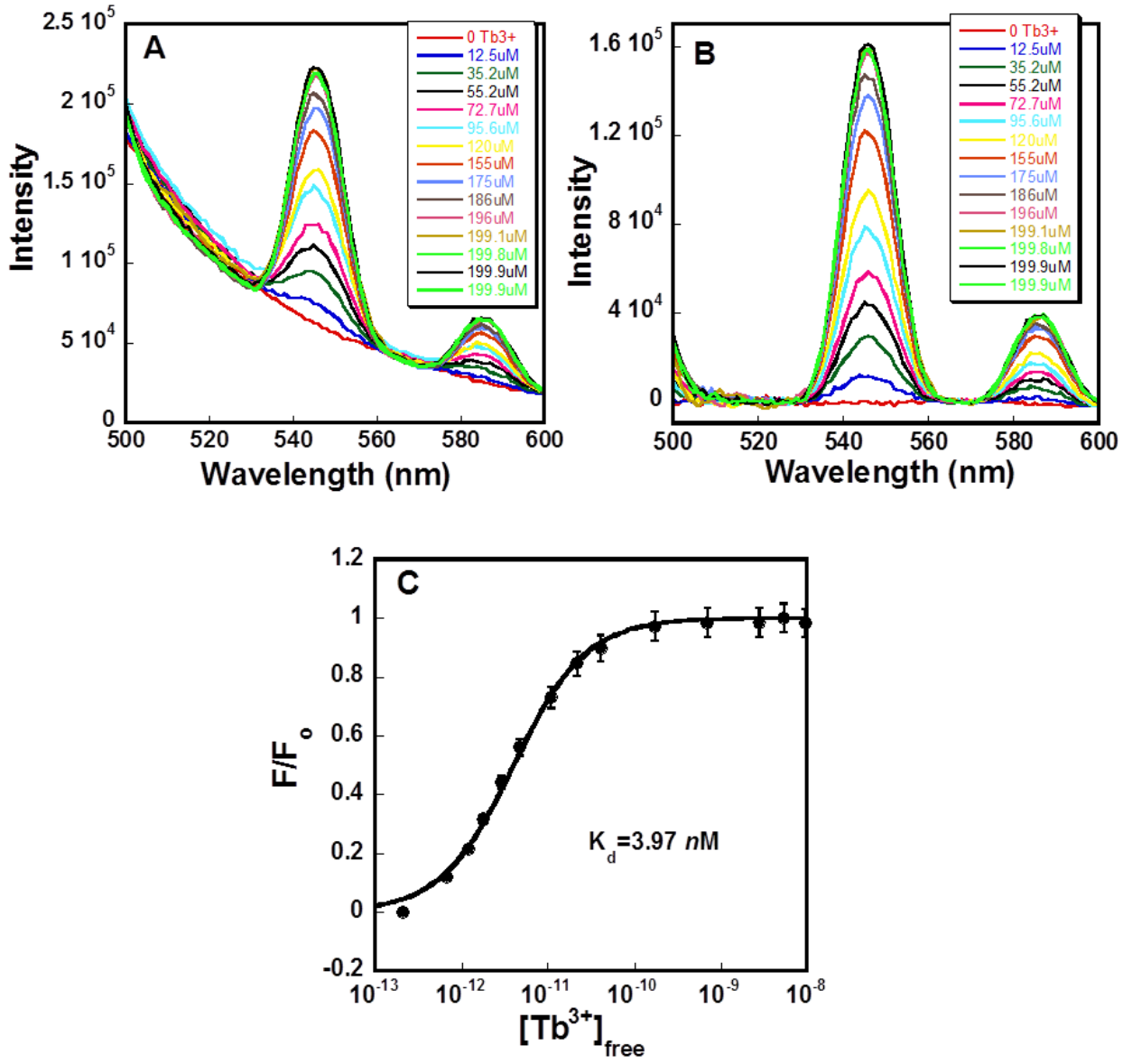

Figure 3.8. Titration of wt-CaM with Tb^{3+} by aromatic residue sensitized energy transfer florescence enhancement.

The experiment is performed on the PTI spectrometer by titrating Tb3+ buffer stock that contains 200µM Tb^{3+} with 50mM HEPES, 100mM KCl, 200mM NTA into and 2µM wt-CaM that is in 50mM HEPES, 100mM KCl, and 200mM NTA at pH 7.2. The emission spectra is monitor with λ_{ex}=280 nm and λ_{em}=500-600 nm. A. The fluorescence spectrum of wt-CaM with Tb^{3+} before baseline. B. The fluorescence spectrum after baseline. C. Curve fit data.

3.2.5. PDE Assay to monitor the biological function of CaM

Cyclic nucleotides, such cyclic adenosine monophosphate (cAMP) and cyclic guanosine monophosphate (cGMP) are intracellular second messengers, which have rapid concentration changes in response to different cell specific stimuli. The concentration of these second messengers is regulated by the cyclic nucleotide phosphodiesterase (PDE) to the steady-state level. Hydrolysis of the cyclic nucleotides by PDE is a unique mechanism for degradation. Kahiuchi and Yamazaki first show that Ca^{2+} can stimulate the PDE activity in the brain of rat, later on they found a protein which from that organ can enhance the enzyme sensitivity.[52] This endogenous protein was later known as CaM, an activator of PDE. In another word, the activity of PDE is Ca^{2+}/CaM dependent. PDE family proteins contain ~270 amino acids that is highly conserved and they can classify based on their primary sequence and its regulation. PDE1 belong to CaM stimulated PDE family, and it have been demonstrated that it has a higher affinity towards cGMP than cAMP.[53] In this experiment, the functional effect of PDE on the substrate of mant-cGMP resulting from interactions with Ca^{2+}-CaM of various concentrations was studied through a time based fluorescence titration method. The EC50 obtained through fitting the fluorescence data demonstrated the activation capabilities of wt-CaM.

Mant-cGMP is the fluorescence derivate cGMP, which allow us to monitor the fluorescence change during the hydrolysis process. **Figure 3.9 A** shows the constant fluorescence intensity of substrate mant-cGMP itself during the first 80 seconds. The fluorescence intensity decrease once the PDE is added in the present of Ca^{2+} (**Figure 3.9 A** from 80s-200s), which indicate that mant-cGMP is degraded by PDE with time. Additional of CaM further speed the hydrolysis process and the hydrolysis rate increase with increase of CaM concentration. The half maximal effective concentration (EC_{50}) is the concentration of a

compound where 50% of its maximal effect is observed. The EC_{50} of this PDE assay is 0.58 ± 0.03 nM.

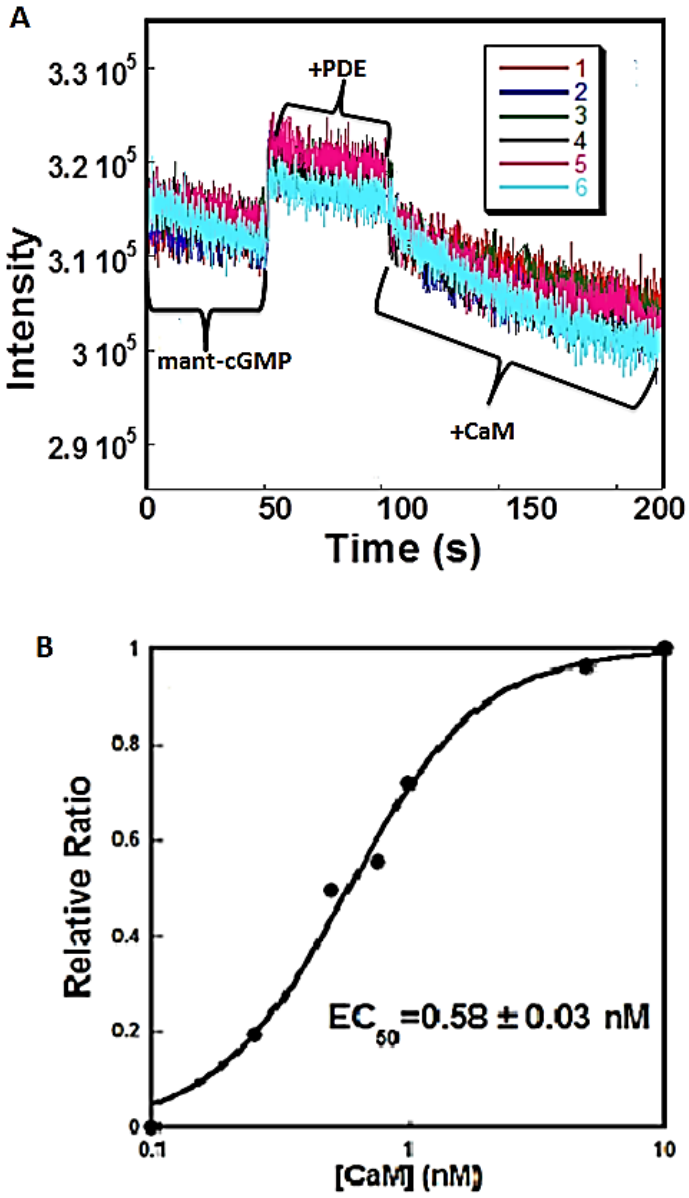

Figure 3.9. PDE function assay of wt-CaM through time based fluorescence spectroscopy on the PTI fluoremeter.
A) Raw data of fluorescence intensity change via time; B) Intensity change as function of protein concentration. (The assay is perform in 10 mM MOPS, 100 mM KCl at pH=7.2, 200 µM EGTA, and 10 mM $CaCl_2$ at room temperature.)

3.2.6. Purification of yeast calmodulin

6 g of yCaM cell pellet was gift from Dr. Steven Clarke at the UCLA. Trichloroacetic acid is used to precipitate protein follow by neutralization to re-dissolve the acidic protein. The Ca^{2+} form of soluble yCaM is binding to the phenyl-Sepharose column in the present of ammonium sulfate. (More detail protocol for yCaM purification is describe in Chapter 2.2) **Figure 3.10** shows the SDS-PAGE of sample from each step during the purification procedure. Line 7 is the ssupernatant of yCaM before bind to the hydrophobic column. Suppostly, most of the yCaM should retain in this stage; however, there is visible band either in Line 7 nor Line 8 (debris of yCaM after the neutralization) around 17.8 kDa. This might due to the limited protein that is present in the cell pellet. Ohya Y. *et al*[41] have reported that there is limited amount of yCaM is extracted from the 8 kg of baker's yeast. Thus, it is reasonable that small amount of the yCaM can extract from the 6 g of yCaM cell pellet.

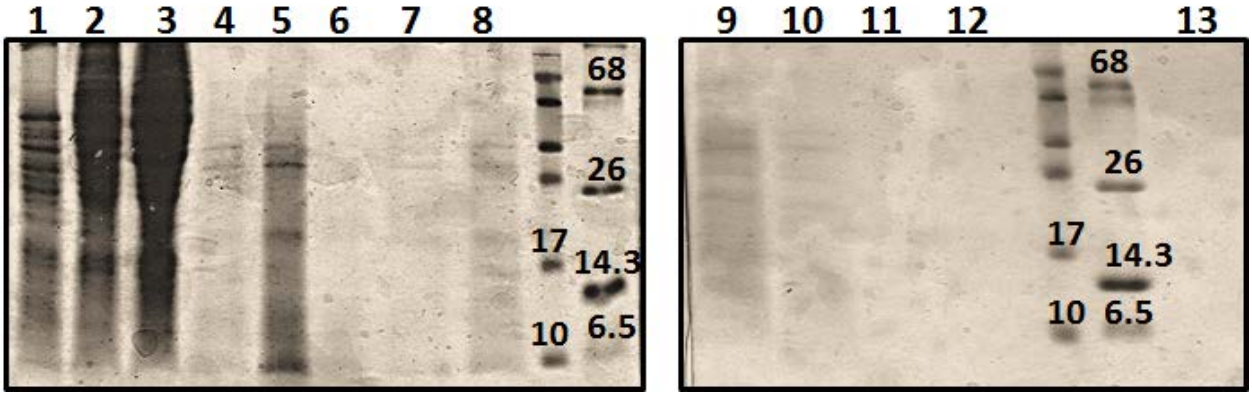

Figure 3.10. SDS-PAGe of purification process of yCaM.
1. Supernatant after lysis; 2. Debris after lysis; 3. Debris after treated with 50% Trichloroacetic acid; 4. Supernatant after treated with 50% Trichloroacetic acid; 5. Debris after treated with 50% Trichloroacetic acid 2nd time; 6. Supernatnat after treated with 50% Trichloroacetic acid 2nd time; 7. Supernatant before binds to the beads; 8. Debris before binds to beads; 9. Beads after binds before wash with washing buffer; 10. Binding waste; 11. Elution fragment 1; 12. Elution fragment 2; 13. Elution after concentrated.

3.2. Conclusion

Wt-CaM and its varies were well expressed as soluble protein at 37°C by using cell strain BL21(DE3)pLysS. By using hydrophobic interaction of CaM once it bind to Ca^{2+} during the purification process, wt-CaM and its varies can be purified with relatively high yield. The yield for the isolated C domain CaM (C-CaM) is relatively low compared to the other three type protein listed in **Table 3.2**. The relative low yield might be due to the weak stability of C-CaM compare to wt-CaM and N-CaM. The SDS-PAGE confirms that the purified wt-CaM and its variants show correct molecular weight. By monitoring the secondary structure of wt-CaM and its variants on the far UV spectra, wt-CaM and its variants show the helical structure contain of these protein. Also, addition of Ca^{2+} increase the ellipticity intensity on the spectra. All observed secondary structure characteristic of these proteins are consistent with reported studies, which indicate that the wt-CaM and its variants are correctly folded.

The Ca^{2+} titration of specific domain of CaM was performed by monitoring the fluorescence intensity change of Try and Phe of the C and N domain of CaM specifically. The K_d of the C and N domain of CaM are 2.7 and 12.2 μM, which is very consistent with data results as previous established (K_d=2.04 μM for C domain, K_d=11.5 μM for N domain). This indicates that both domain of wt-CaM contain the correct binding affinity towards Ca^{2+} ion.

In summary, we have shown that expression and purification of wt-CaM and its variants are successful. The secondary structure analysis proves that all the proteins folded as their native structure. The binding affinities of both Ca^{2+} and Tb^{3+} towards to wt-CaM are consistent with lecture value and data of pervious study by monitoring the intrinsic fluorescence intensity change and FRET. The PDE assay might be repeated by using a modified protocol; however, the wt-

CaM did show some degree activation on the PDE. On the other hand, the purification of yCaM is hard to determine whether is successful or not since the yield of the protein is very limited to detect. More protein is need to able to perform any type of study.

4. Heteronuclear labeling and fluorescence labeling of CaM

4.1. Introduction

Nuclear magnetic resonance (NMR) spectroscopy is a powerful tool for study the structure and function of biological macromolecules. The NMR allow the detail analysis of macromolecular structure, dynamics, and interaction of smaller macromolecules (< ~ 25 kDa). ^{14}N is the NMR silent isotope of nitrogen, but using ^{13}C-glucose and ^{15}N-ammonium serves as carbon and nitrogen source the protein signal can be improved. However, as the macromolecular complex of biochemical interest get larger than 25 kDa, the analysis of complete get limited.[54] The large molecules and complexes are complicated by increased line widths associated with slower tumbling and spectral overlap from the larger number of unique signals. The slow tumbling rate of larger macromolecules in solution leads to faster relaxation of transverse magnetization due to enhance spin-spin interaction. Both the enhance spin-spin interaction and overlap of larger number of unique signals decrease the resolution of the spectrum.[55]

To minimize the spin-spin interaction that lead to fast relaxation of transverse magnetization is to dilute the proton spins through uniform deuteration by express protein in deuterium water (D_2O) instead of H_2O. **Figure 4.1** showed the protein before labeled and protein after labeled. During the purification process, the protein is purified at the protonated solvents, the exchangeable N-H group of the main chain will change from N-^{2}H to N-^{1}H in the aqueous solution. Thus, the main chain signal is improved by "silent" the signal of the side-chains.[55]

As discussed in Chapter 1, several proteins studied in our lab are CaM binding protein. By monitoring the chemical shift of each residue of the isotopic labeled CaM from NMR, the

interaction of CaM with many massive proteins the protein-protein can be solved. There is a need to uniformly isotopic labeled CaM to increase the resolution of the NMR spectra. Thus, chemical shift of each residue due to binding of target binding can be assign. The objective of this part of work is to optimize the expression condition of isotopic labeled CaM, so that the yield of the isotopic labeled protein can be improve for the future NMR experiment.

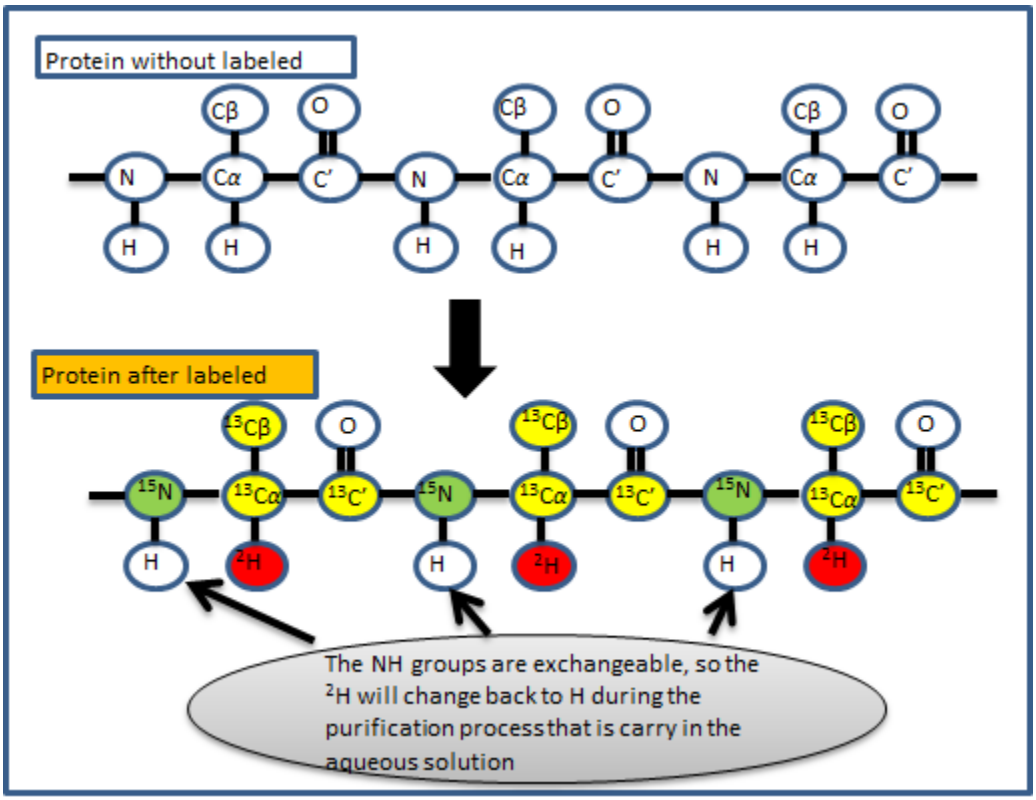

Figure 4.1. Comparison of protein before labeled and protein after labeled.

4.2. Result

4.2.1. Expression and purification of ^{15}N wt-CaM

The ^{15}N labeled wt-CaM is expressed in SV medium that contains KH_2PO_4, K_2HPO_4, $MgSO_4$, $Fe(NH_4)_2(SO_4)_2$, and of glucose using BL21(DE3)pLysS E. coli cell strain and tag-less vector pET-7. $^{15}NH_4Cl$ is the source for the nitrogen. The growth curve of the bacteria shows much slower growth rate compare with the growth rate in the LB medium due to the minimum nutrient in the SV medium. (**Figure 4.2 A**) The protein is expressed at 28 °C overnight after the addition of IPTG once the optical density of the bacteria reach to 0.8 at 600 nm. The bacteria were growing in the SV medium at 37 °C, and temperature is reduced to 28 °C after addition of IPTG. The SDS-PAGE shows the expression level of the protein, the bands become thinker with the passage of time that indicate the protein was formed during expression and specifically after induction with IPTG. (**Figure 4.2 B**)

^{15}N wt-CaM was expressed as soluble tag-less protein. SDS-PAGE shows ^{15}N wt-CaM is in the soluble supernatant form. The elution eluted from the hydrophobic chromatography shows a clear band, which indicated the protein is relative pure. (**Figure 4.2 C**) The UV spectra of ^{15}N wt-CaM elution from the hydrophobic column shows a similar peak at 280 nm as the non-labeled wt-CaM indicated that the protein was expressed well in the SV medium. (**Figure 4.2 D**)

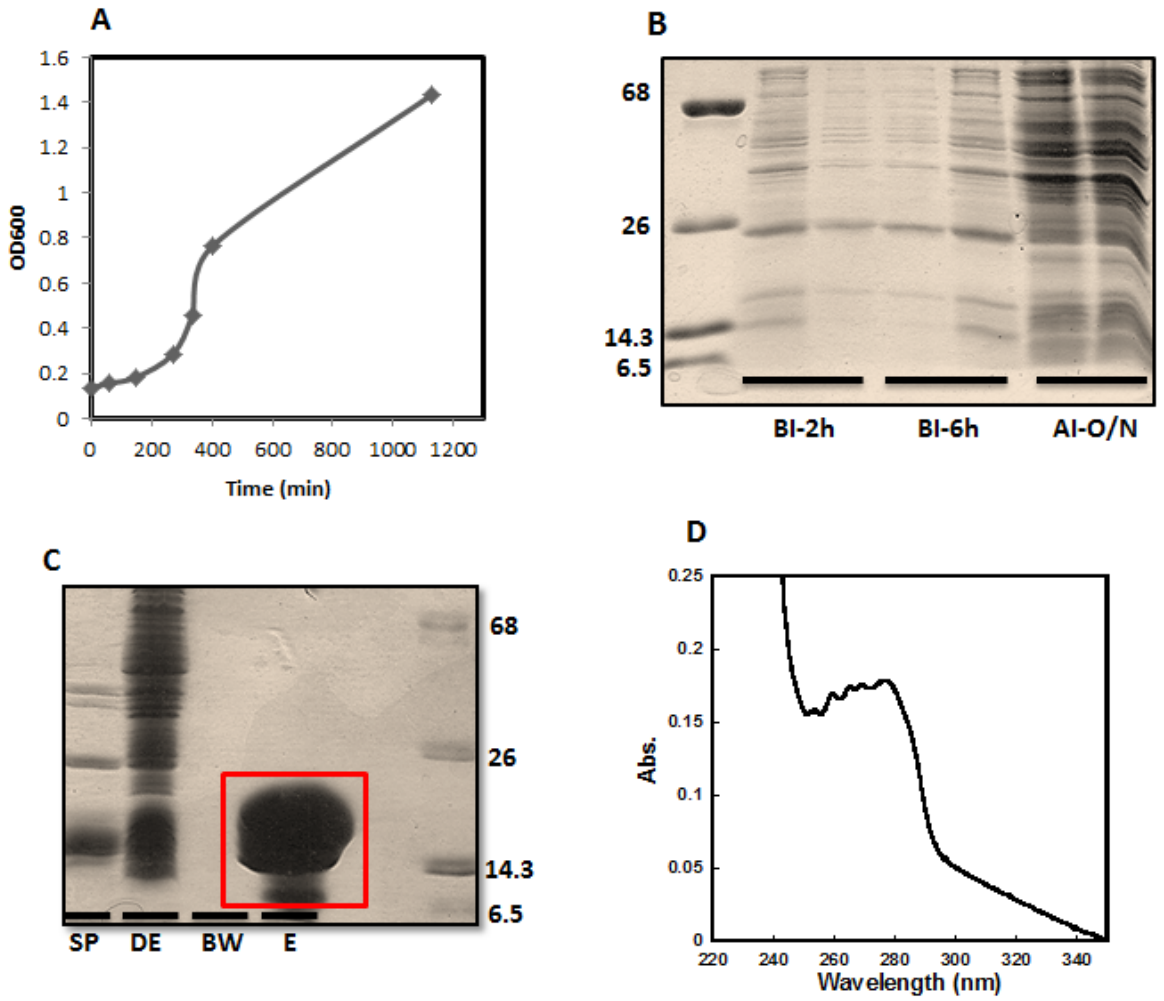

Figure 4.2. Growing condiction of ^{15}N labeled wt-CaM in SV medium.
A. Growth curve of bacteria density with dependent of time; B. SDS-PAGE of expression of ^{15}N wt-CaM; C. SDS-PAGE of purification of ^{15}N wt-CaM; D. UV spectra of ^{15}N wt-CaM elution. (BI: before induction, AI: after induction, SP: supernatant after cell lysis, DE: debris after cell lysis, E: elution)

4.2.2. Expression and purification of ^{15}N and ^{13}C wt-CaM

The M9 medium contain Na_2HPO_4, KH_2PO_4, $FeSO_4$, $MgSO_4$, $CaCl_2$, micronutrients, NaCl, thiamine, and of vitamin supplements. M9 medium has more nutrients than the SV medium. Therefore, M9 medium is used to express the isotopic labeled protein to improve the quantity yield of the protein. ^{15}N NH_4Cl and ^{13}C glucose are the source for nitrogen and carbon. (Detail ingredient of the M9 medium can be found in appendix) ^{13}C glucose can be very costly; therefore, amount of glucose is tested to determine the minimum amount of glucose that is required to efficiently to express protein. Hans Vogan's lab had reported 2 g of the glucose can be used to express protein efficiently. Thus, 5 g and 2 g of glucose were used to test the expression level of protein. ^{15}N and ^{13}C labeled wt-CaM was expressed in M9 medium using BL21(DE3)pLysS E. coli cell strain and tag-less vector pET-7 at 37 °C for 4-5 hours after additional IPTG once the optical density reached 0.8 at 600 nm. **Figure 4.3 A** shown the bacteria growth rate in M9 medium contain 2 g and 5 g of glucose, and both conditions shows very similar growth rate. SDS-PAGE also shows the comparison of protein expression in both conditions, and there is no different of both conditions. (**Figure 4.3 B**) The SDS-PAGE and UV spectrum also provide protein purified from both SV condition has no signification different**.** **Table 4.1** shown the yield of protein produced from 2 g glucose and 5 g glucose are 56 and 62 mg/mL, which indicate no significant protein yield difference between 2 g and 5 g glucose as nutrient supply. All the data results indicate that the 2 g of glucose give almost equal amount of protein yield as the 5 g of glucose; thus, 2 g of ^{13}C glucose is used to express the isotope label CaM.

The double labeled ^{15}N and ^{13}C wt-CaM is expressed in SV medium that contain 2 g of ^{13}C glucose. **Figure 4.4 A** shown the growth rate of double label wt-CaM, the optical density

(O.D.) graph is slow at the beginning but it soon recovered when the O.D. reach to 0.5 at 600 nm. The SDS-PAGE shows the expression condition of protein along with time, the basal expression of other protein was before induction. After the addition of IPTG, the engineered protein was produced as O.D. increased, which demonstrating a successful expression outcome. (**Figure 4.4 B**) The double labeled protein is purified by using the hydrophobic choreography. The SDS-PAGE shows the purification condition of each step. Most of the protein remains in the supernatant as soluble condition after the cell lysis around 18 kDa, which is the correct protein molecular weight. The elution that come out the hydrophobic column showed two bands at ~18 and ~14 kDa, the migration of the two bands due to the both present of EGTA and Ca^{2+} form of CaM.[56] (**Figure 4.4 C**) The UV spectra show the elution of ^{15}N and ^{13}C labeled wt-CaM, the spectra show a very sharp peak at 280 nm and the shape of the peak are the typical CaM elution spectra. All the data shows demonstrating ^{15}N and ^{13}C wt-CaM was well expressed and purified.

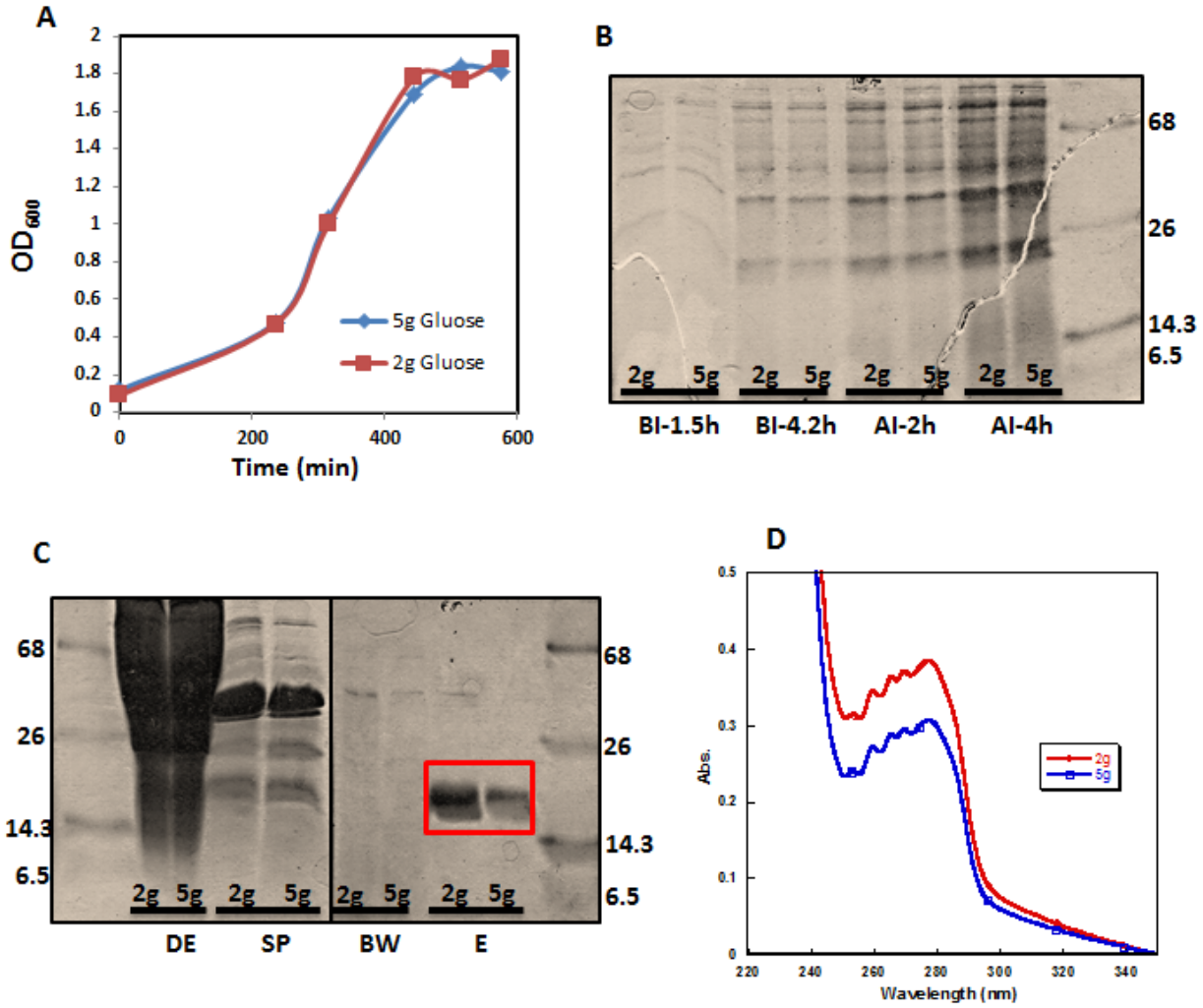

Figure 4.3. Comparison of wt-CaM expression in 2 g and 5 g of glucose in M9 medium. A.Comparison of growth curve of wt-CaM in M9 medium contain 2 g glucose and 5 g of glucose; B. SDS-PAGE of comparison of expression of wt-CaM in M9 medium contain 2 g glucose and 5 g of glucose (BI-before induction; AI-after induction); C. SDS-PAGE of comparison of purification of wt-CaM in M9 medium contain 2 g glucose and 5 g of glucose (P-cell pellet; SP-supernatant; BW-binding waste; E-elution); D. Comparison of UV spectrum of wt-CaM elution in M9 medium contain 2 g glucose and 5 g of glucose.

Table 4.1. Comparison of yield of wt-CaM in M9 medium contains 2 g and 5 g of glucose.

Amount glucose used	Yield (mg/L)
2g	56
5g	62

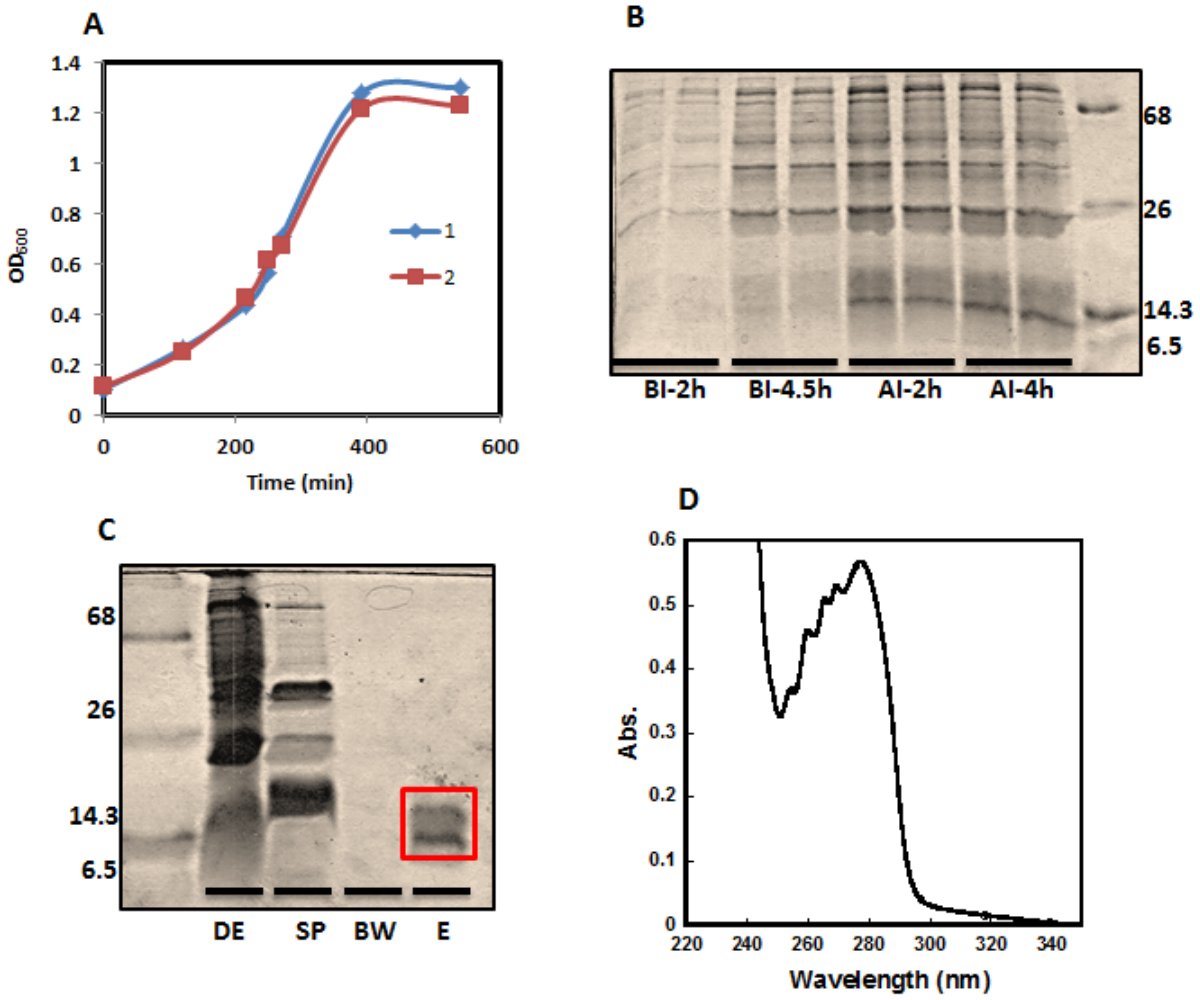

Figure 4.4. Expression and purification of ^{15}N and ^{13}C wt-CaM.
A. Growth curve of ^{15}N and ^{13}C wt-CaM with dependent of time; B. SDS-PAGE of expression of ^{15}N and ^{13}C wt-CaM (BI:before induction, AI: after induction); C. SDS-PAGE of purification of ^{15}N and ^{13}C wt-CaM (DE: debris after cell lysis, SP-supernatant after cell lysis, BW: binding waste, E: elution); D. UV spectra of ^{15}N and ^{13}C wt-CaM elution.

4.2.3. Expression and purification of ^{2}H, ^{15}N, and ^{13}C wt-CaM

^{2}H, ^{15}N, and ^{13}C wt-CaM is expressed in M9 medium with deuterium water (D_2O). The D_2O has amount of toxicity on the bacteria growth, bacteria need to adopt the harsh growing condition. After the transformation, colonies are growing at the SV medium instead of nutrient enrich LB medium. A health colony is selected and inoculated into 50 mL M9 medium with 0% D_2O and grow at 37 °C overnight. The cell pellet is collected from overnight grew 0% D_2O medium by centrifuge and transfer into a fresh 50 mL M9 medium that contain 70% D_2O. The bacteria is grow for 24 hours in the 70% D_2O M9 medium to recover the bacteria density. The cell pellet is collected from overnight grew 70% D_2O medium by centrifuge and transfer into a fresh 50 mL M9 medium 100% D_2O for 24 hours at 37 °C to recovered the cell density. Small amount of the over expressed bacteria that in 50 mL 100% M9 medium is transferred into 1 L of 100% M9 medium that contain ^{15}N NH_4Cl and 2 g of ^{13}C glucose for nitrogen and carbon sources for large scale expression. The bacteria were growing at 28 °C for 24 hours to let the bacteria to recover the optical density to 0.6 at 600 nm. The protein is expressed for 5 hours at 37 °C after the addition of IPTG.

SDS-PAGE show the protein expressed condition is very similar from 0% D_2O to 100% D_2O in the small scale expression. For the large scale expression, the SDS-PAGE shows the basal expression of other protein was low before the induction. After the addition of IPTG, the engineered protein was produced as optical density increase demonstrates a successful expression outcome. (**Figure 4.5 A**) Since the protein is triplet isotopic labeled, the molecular weight should be higher than the wt-CaM expressed in the LB medium. The CaM expressed after the induction is indeed shows a higher molecular weight than 17 kDa on the SDS-PAGE. The elution protein shows a clear band indicate that the purity of the protein is relatively high.

The UV spectra of the eluted protein shows very similar peak as the wt-CaM, ^{15}N wt-CaM, and double labeled wt-CaM, which indicate the protein was well expressed.

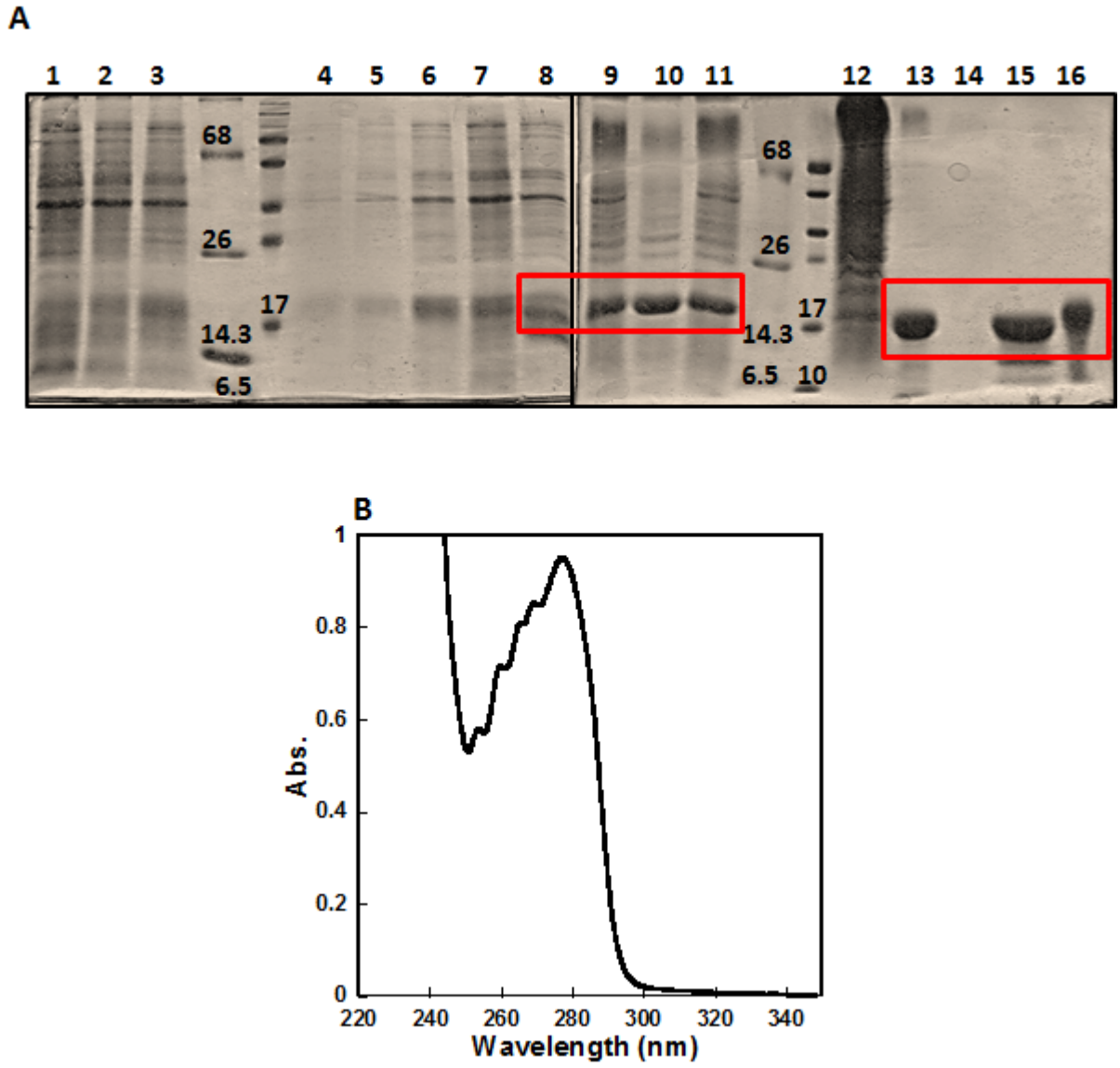

Figure 4.5. Expression and Purification of ^{2}H, ^{15}N, and ^{13}C wt-CaM.
A. SDS-PAGE of expression and purification of ^{2}H, ^{15}N, and ^{13}C wt-CaM (1. Small scale of bacteria growth in 0% D_2O at 37 °C overnight; 2. Small scale of bacteria growth in 70% D_2O at 37 °C overnight; 3. Small scale bacteria growth in 100% D_2O at 37 °C overnight; 4&5. Large scale bacteria growth in 100% D_2O at 37 °C for 6 hours before induction; 6&7. Large scale bacteria growth in 100% D_2O at 30 °C for overnight; 8&9. Large scale bacteria growth in 100% D_2O at 37 °C for 4 hours after induction; 10&11. Large scale bacteria growth in 100% D_2O at 37 °C for 5 hours after induction; 12. Debris cell lysis; 13. Supernatant after cell lysis; 14. Binding waste; 15&16 elution.) B. UV spectra of ^{2}H, ^{15}N, and ^{13}C wt-CaM elution.

Table 3. Summary theoretical yield of isotopic labeled wt-CaM.

Labeled CaM	Yield (mg/L)
^{15}N	42
^{15}N and ^{13}C	69
^{2}H, ^{15}N, and ^{13}C	40

4.2.4. Danyslation of wt-CaM

Dansylated CaM (Dy-CaM) is used to study the interaction of CaM with its binding protein by monitor the hydrophobic patch expose of the CaM. The dansylated CaM is used because the approximate 80% fluorescence increase when Dy-CaM interact with ligands. The fluorescence intensity change is much higher than any aromatic residue in the CaM itself. Another reason to use Dy-CaM for the protein-protein interaction study is because many CaM binding protein contain some aromatic residue, to differentiate the fluoresce intensity change cause by the conformational change of CaM by interact with its CaM binding protein with the fluoresce intensity change cause by the aromatic residue form the CaM binding protein, the change of fluoresce emission intensity from the Dy-CaM cam be used to monitor conformational change of CaM by interaction with it binding protein or peptides by using 335 nm was excitation wavelength.

The reaction rate between dansyl chloride and protein or peptide has been studied as function of pH and temperature by many researchers. **Figure 4.6** shown the reaction of dansylation of a peptide. N-terminal of the amino acid or side chain of amino acid, such as lysine

can be labeled by dansyl chloride depend on the pH value. In our study, the N-terminal of CaM is the desire position for the dansylation. Therefore, all the dansylation reaction is hold at pH=7.0 to insure that the side chain of lysine (pKa = 10.53) is in the protonated form, so that only N terminal of the protein is dansylated. Many temperatures have been studied to use for the dansylation of protein. To speed up the reaction, several conditions were used to test the optical temperature for single dansylation of CaM. The reaction was heated at 75°C for 45 min was mention by Park et al to dansyl labeled protein.[57] Chiapppetta *et al.* also mention the dansyl labeled protein by heating the reaction for 5 min in a microwave oven at a power of 700 W. Our previous study have used to dansyl labeled protein by carried the reaction at 4°C for overnight. Three of the conditions are tired to compare the reaction condition. **Figure 4.7** shown the UV spectrum of Dy-CaM by using three different conditions. Three of the condition show peaks around 320 nm and the CaM peck shift from 277 to 240 nm, which is the UV absorbance wavelength of dansyl group

Figure 4.8 shows the mass spectrum of dansylated CaM for all three conditions. Weight gain from one dansylated site is 233.29, thus the molecular weight from one dansylated site is ~16940 Da. **Figure 4.8 A** is the mass spectra of dansylated CaM from condition of dansylation at 75°C for 45 min. The highest peak shows the molecular weight of 16706.8 Da indicate most of the protein are in the unlabeled form. The second highest peak shows the molecular weight of 16942.4 Da that is half the intensity of the highest peak, which indicates that ~30% of the CaM gained one dansyl group. **Figure 4.8 B** shows the mass spectra of dansylated CaM from condition of dansylation at 4°C for 2 hours. There are two major peak show about the same intensity at molecular weight of 17171.3 and 17404.6 Da, indicate that the 30% of CaM gained 2 dansyl groups and 33% of CaM gained 3 dansyl groups during the dansylation process. 10% of

CaM remained unlabeled form, 17% of CaM gained 4 dansyl groups, and 10% of CaM gained more than 4 dansyl groups. **Figure 4.8 C** shows the mass spectra of dansylated CaM from condition of dansylation at 700 W for 5 min. A major peak shows molecular weight of 16715.1 Da indicate 79% of CaM remain unlabeled. 24% of CaM gain one dansyl group during the dansylation process shows 16943 Da. Only 7% of CaM gains multiple dansyl groups during the dansylation. The mass spectrum suggests that all three methods can dansylate CaM. However, dansylation at 75°C for 45 min. give highest percentage of single dansylation among those three conditions.

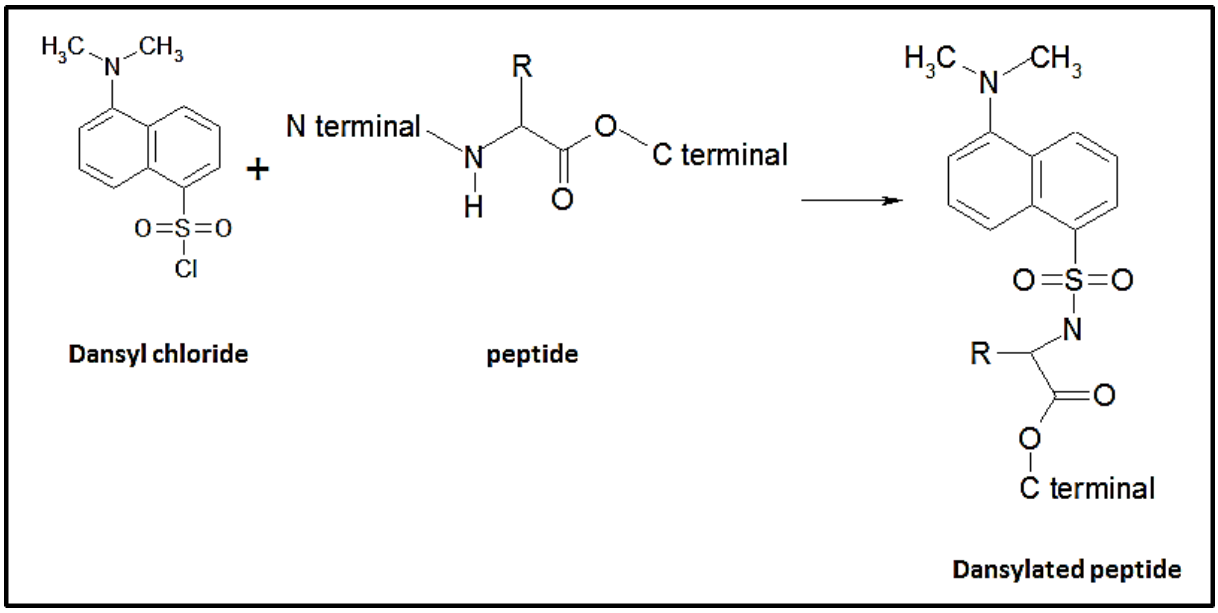

Figure 4.6. Reaction of danylation of a peptide

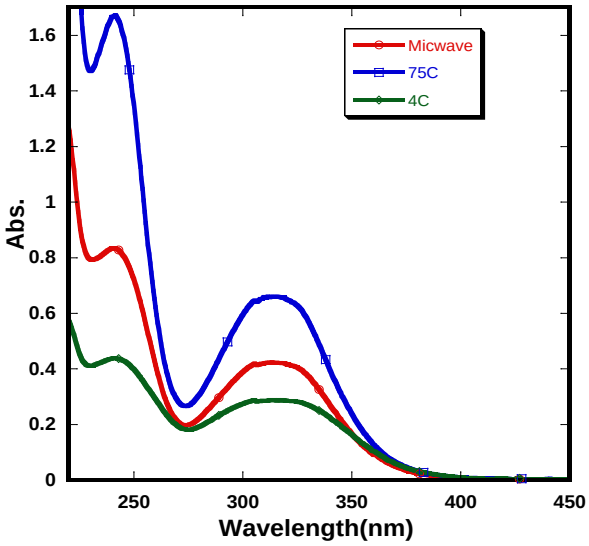

Figure 4.7. UV spectrum of Danylated wt-CaM at different conditions.
300 µM Danysl Chloride was dissolved in acetonitrile and it was added to 100 µM wt-CaM in 10 mM Mops, 100 mM KCl, 3 mM EGTA, 1 mM CaCl2, pH=7.0). (Red: reaction heat in a water bath for 5 min in a microwave at 700 W; Blue: reaction was heated for 45 min at 75°C; Green: reaction react at 4°C for 2 hours.)

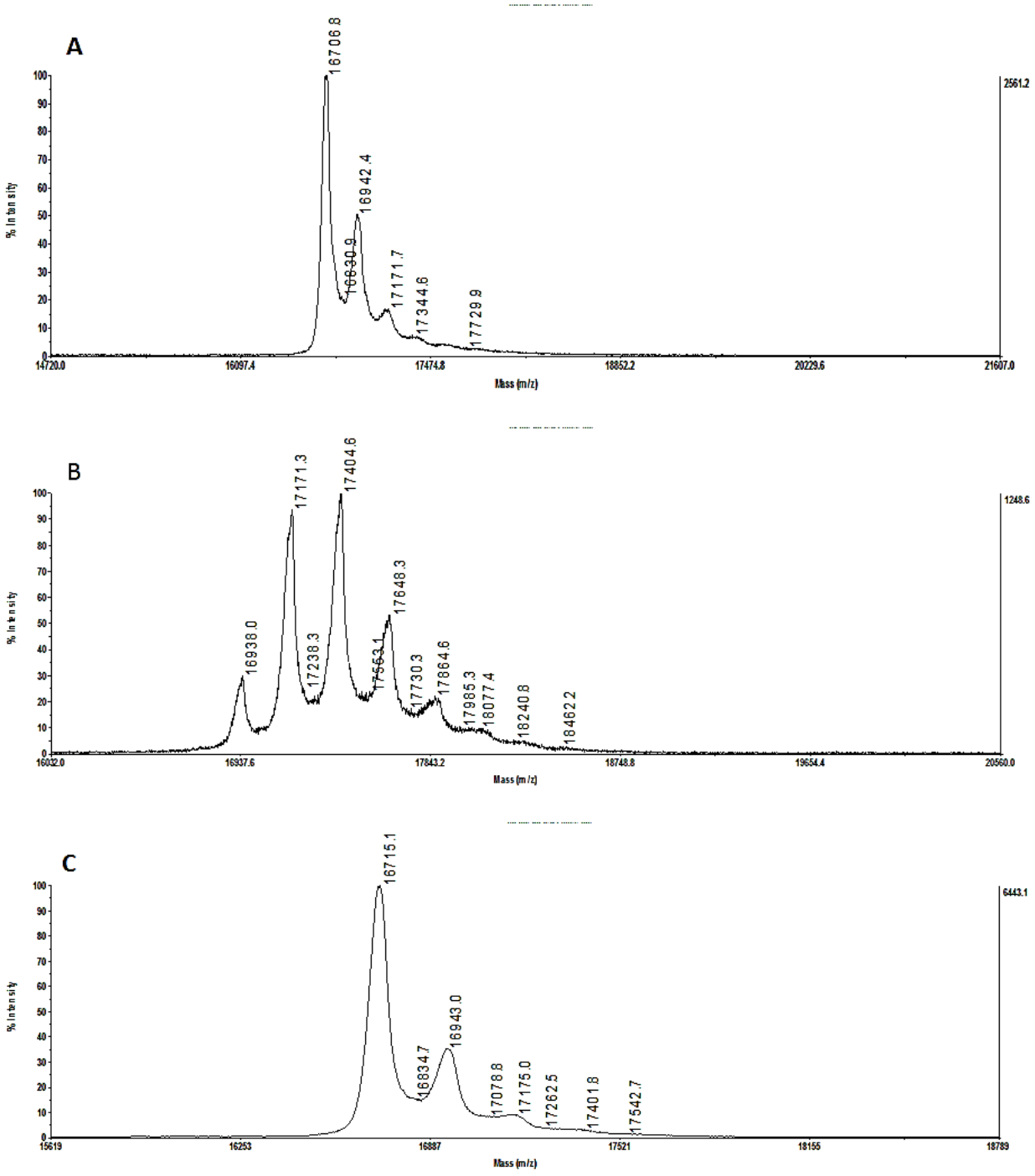

Figure 4.8. Mass spectrum of Dansylated CaM.
A) Dansylation at 75°C for 45 min; B) Dansylation at 4°C for 2 hours; C) Dansylation at 700 W in microwave for 5 min.

4.3. Conclusion

The ^{15}N isotopic labeled wt-CaM was expressed in the SV medium environment that has been established by generating and purifying as soluble protein. The actual yield for a liter of expressed cell culture is around 42 mg. The theoretical yield of ^{15}N isotopic labeled wt-CaM has decrease 40% compare to the theoretical yield of wt-CaM that express from the LB medium system. It required 7-8 hours for optical density of bacteria to reach to 0.6-0.8 at 600 nm in the SV medium environment, but it only required 2-3 hours for optical density of bacteria to reach to 0.6-0.8 at 600 nm in the LB SV medium environment. Therefore, the decreasing of theoretical yield is due to the limited nutrient resources in the SV expression environment.

M9 medium is used to improve expression environment for the isotopic labeled protein with higher theoretical yield. 2g and 5g of regular glucose were tested to compare the theoretical yield of the wt-CaM. 2g and 5g of glucose give 56 and 62 mg/L as theoretical yield, which indicated no big significant yield different between using 2g and 5g glucose in the M9 medium expression system. Thus, 2g of ^{13}C glucose is chosen to use in the M9 system to improve the theoretical yield in a lower cost. ^{15}N and ^{13}C isotopic labeled (double labeled) wt-CaM was expressed in the M9 medium environment and purifying as soluble protein. The theoretical yield for a liter of expressed cell culture has risen impressively to ~70 mg (shows in **Table 4.2**), which is very close to the theoretical yield of wt-CaM expressed in the LB medium environment due to the improvement of the nutrient resources in the M9 medium.

^{2}H, ^{15}N, and ^{13}C isotopic labeled (triplet labeled) wt-CaM is expressed in the deuterium environment as soluble protein. The theoretical yield for the triplet labeled wt-CaM is 40 mg/L (shows in **Table 4.2**), which is 50% lower than the theoretical yield of wt-CaM that expressed in

LB medium environment. The deuterium water does have certain toxicity towards the growth of bacteria; therefore, it required 24 hours for optical density of bacteria to reach 0.6 at 600 nm. By using the mineral rich M9 medium, the isotopic labeled wt-CaM has been improved. However, the triplet labeled wt-CaM can be improving by more modification.

Three conditions (dansylation at 75°C for 45 min, dansylation at 4°C for 2 hours, and ansylation at 700 W in microwave for 5 min.) are chosen to test the fast and efficient time for single dansylation of CaM. All three conditions can dansylated CaM. Although carrying out the dansylation at 75°C for 45 min. can give highest single dansylation at shorter time among the three condition.

In summary, M9 medium do give much more nutrient for the bacteria growth compare to the SV medium. The yield of the isotopic labeled protein is significantly higher in the M9 than the SV medium. 2g of glucose can substitute the 5g of glucose in the M9 medium since there is no significant different of their yield. The deuterium labeled wt-CaM is successful; the lower yield is due to the toxicity of the deuterium environment to the bacteria growth. Three dansylation methods can danylated wt-CaM, and the danylated CaM can be used to study the protein protein interaction in chapter 6.

5. RyR 1 mini domain

5.1. Introduction

Ryanodine receptor type 1 (RyR1) with a tetramer structure is one of the major CaM binding protein in sarcoplasmic reticulum (SR) membranes isolated from skeletal muscle. At low Ca^{2+} concentration (nano-molar), CaM opens the RyR1 channel; however, CaM becomes RyR1 channel inhibitor at higher Ca^{2+} concentration (micro-molar). The switch from a channel activator to a channel inhibitor is due to Ca^{2+} binding to CaM as Ca^{2+} insensitive mutants of CaM activator to a channel inhibitor suggests that the RyR1 activation profile might be manipulated by tuning the CaM Ca^{2+} affinity. Rodney *et al.* and Fruen *et al.* purposed that Ca^{2+} binding to C domain CaM switch CaM to an activator of RyR1 channel.[58 59] On the other, Boschel *et al.* compared the Ca^{2+} dependent of skeletal muscle SR [^{3}H] ryanodine binding with Ca^{2+} induced signal change of fluorescently labeled CaM (on either the N or C domain of CaM) by binding to a putative RyR1 CaM binding peptide. They found that amount of Ca^{2+} concentration cause the conformational change of C domain of CaM is the same concentration range as the Ca^{2+} activation of SR vesicle ryanodine binding, the Ca^{2+} concentration rage cause conformational changes in the N domain of CaM is the same Ca^{2+} rage for the inhibition of SR vesicle ryanodine binding. Therefore, conclude Ca^{2+} bind to C domain CaM causes activation of RyR1 but N domain is inhibitor of RyR1 channel.[60] In our lab previous study, we used CaM variants that are designed to enhance the Ca^{2+} binding affinity of each individual EF hand of CaM to track the Ca^{2+} activation profile of RyR1. Our data result support the hypothesis of Ca^{2+} binding to C domain of CaM inhibits the RyR1 channel.

Today, there are three CaM binding region of RyR1 have been reported. Hamilton and co-workers had reported RyR1 region 3614-3643 and 1975-1999 are the potential CaM binding

regions base on the peptide studies.[61 23 62] Region 3614-3643 of RyR1 have been proved to be one of the true CaM binding region, and it displays a high affinity for both apo and Ca^{2+} form of CaM. Later on, region 4064-4210 is found and it contain two putative EF hands that could compete CaM to bind RyR1 region 3614-3643.[63] Susan L. Hamilton group have showed that CaM contact with region 3614-3643 in both high and low Ca^{2+} conditions with C domain of Ca^{2+} form CaM binds tightly to the N terminal of peptide 3614-3643 and Ca^{2+} binding to C domain is critical for channel inhibition. A 2.0 Å crystal structure of Ca^{2+} form of CaM bind to peptide 3614-3643 reveals an antiparallel interaction between CaM and the peptide. The complex shows CaM interact with target with 1-17 spacing with C and N domain of CaM contact the N terminal and C terminal of the peptide through hydrophobic interaction.[64] (More detail NMR data is described in Dr. Jie Jiang's dissertation)

Even though CaM regulate RyR1 trough Ca^{2+} dependent activation is well established, the precise mechanism of which CaM regulate RyR1 remain unknown due to several major stumbling block. First, since both CaM and Ca^{2+} regulate RyR1, it is hard to distinguish the effect between the RyR1 channel regulate directly through Ca^{2+} and RyR1 channel regulated indirectly through Ca^{2+} mediated via CaM. Second, because the massive size and the location of this membrane protein, the structure of the atomic level of this protein not know. Thus, the interaction of CaM and it binding region is hard to study through a direct approach. At last, CaM modulate Ca^{2+} activation of RyR1, however, in vivo, the primary mechanism by which RyR1 is activated vis an allosteric coupling to the L-type Ca^{2+} channel in the transverse-tubule membrane, with Ca^{2+}-activation possibly playing a secondary role. CaM modulation of this allosteric activation of RyR1 has not yet been demonstrated due to the difficulty of simultaneously

manipulating concentration and type of CaM in the skeletal muscle triad and controlling the membrane potential of the transverse-tubule membrane.

5.2. Our knowledge through previous studies and our proposed model of study

Based on the previous NMR studies, Ca^{2+} CaM interact with peptide 3614-3643 through one to one ratio. Significant chemical shifts were observed in both domain suggest both domain of CaM interact with peptide, which indicated the conformational changes occurs in the whole CaM protein during the interaction with peptides $RyR1_{3614-3643}$. Apo form of CaM interacts with peptide 3614-3643 (43% of hydrophobicity) also through one to one ratio. On the other hand, both apo and Ca2+ form of CaM interact with RyR1 peptide 1975-1999 (40% of hydrophobicity) with ratio one to one. However, only C domain of apo-CaM shows significant chemical shift during the interaction with peptides. The chemical shift change of Ca^{2+}-CaM interacts with peptide 1975-1999 also shows both domains of and flexible region of CaM interact with peptide. Therefore, it is also possible for the whole CaM interact with peptide 1975-1999.

As **chapter 5.1** mentioned, there are three major challenges for direct study the interaction of CaM with entire RyR1. Moreover, massive membrane protein, RyR1 might loss its native function in the pure form. Therefore, an indirect approach which combines the structural studies of CaM with RyR1 synthesized peptides. **Figure 5.3** shows two hypotheses in our working model. At the low Ca^{2+}, the C domain of CaM can bind to region 2 of RyR1 (3613-3643), shows in model A. However, if the distant between region 1 (1975-1999) and region 2 are very close, while C domain of CaM can bind to region 2 and N domain of CaM can bind to region 1 of RyR1 (Shows in model B). When the Ca^{2+} concentration increases, both domains of

CaM can bind to both region 1 and 2, shows in bottom of model B. Or, C domain of CaM binds to region 2 of RyR1 more tightly, and N domain of CaM binds to region 1 of RyR1 more tightly. Within mind that region 3 of RyR1 (4114-4142) contains two putative EF hands, which can compete CaM to bind region 2 of RyR1 at low Ca^{2+} concentration. Alternatively, an interaction between site 2 and site 3 (4064-4210) maybe required for channel opening and disrupting the interaction may close the channel.[65] Thus, Ca^{2+} induced shift in CaM binding to 3614-3643 may disrupted the interaction of site 2 with site 3. To testify the two model, our RyR1 mini domain is designed by combine site 1 (1975-1999) and site 2 (3614-3643) with a flexible linker to study the interaction with CaM.

In this chapter RyR1 mini domain is first designed as GST tagged protein. The RyR1 mini domain is expressed and purified as GST fusion protein. RyR1 mini domain is redesigned as His tag fusion protein to improve the quantity yield of the RyR1 mini domain.

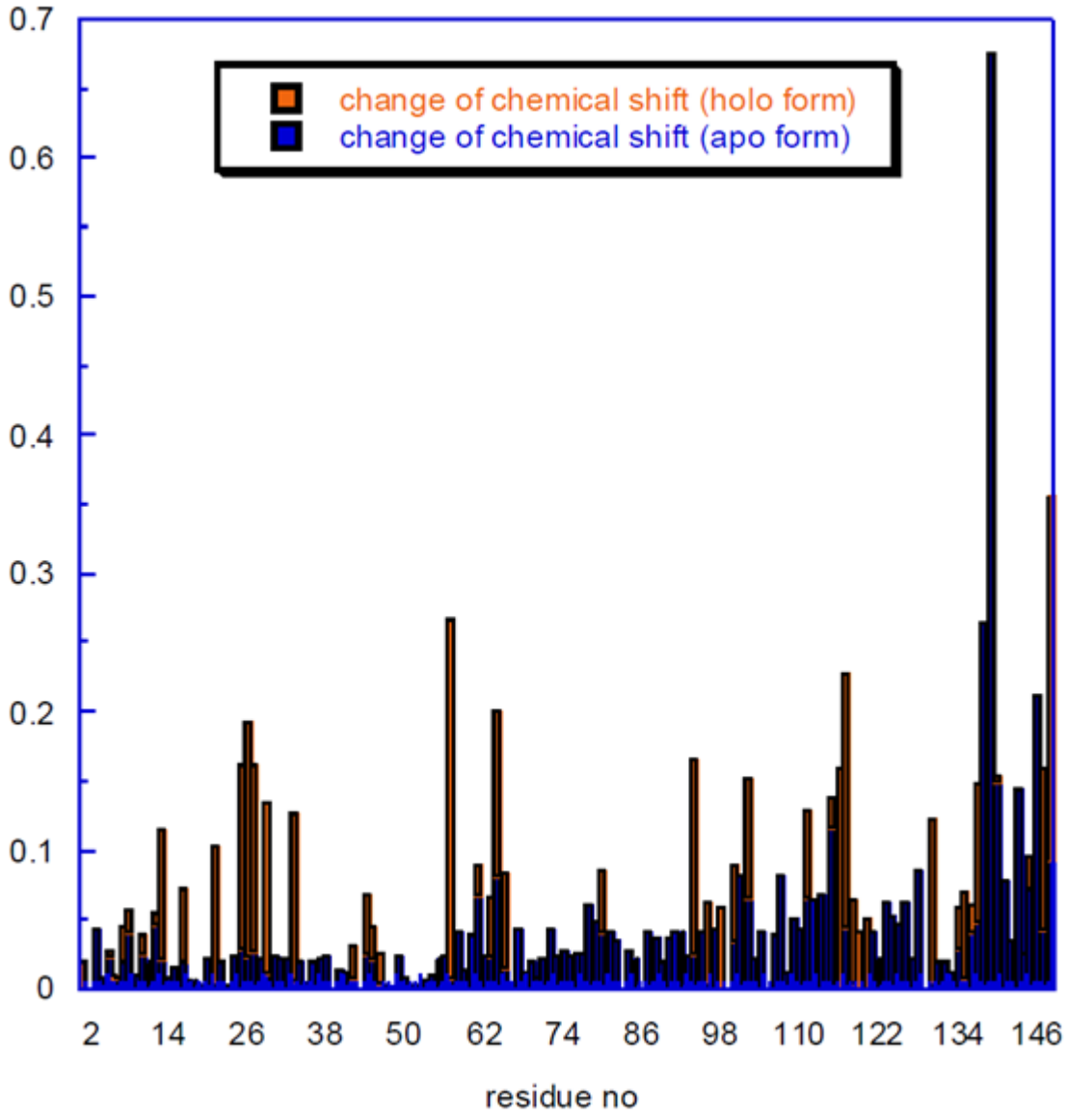

Figure 5.1. Chemical shifts comparison of CaM-RyR1$_{3614-3643}$ complex on 600 MHz in present of Ca^{2+} and EGTA.
Chemical shift changes of HSQC signal from selected residues of the ^{15}N-Ca^{2+}-CaM-RyR1$_{3614-3643}$ complex (orange) and ^{15}N-EGTA-CaM-RyR1$_{3614-3643}$ complex (blue). This Figure is adopt from Jie Jiang's dissertation

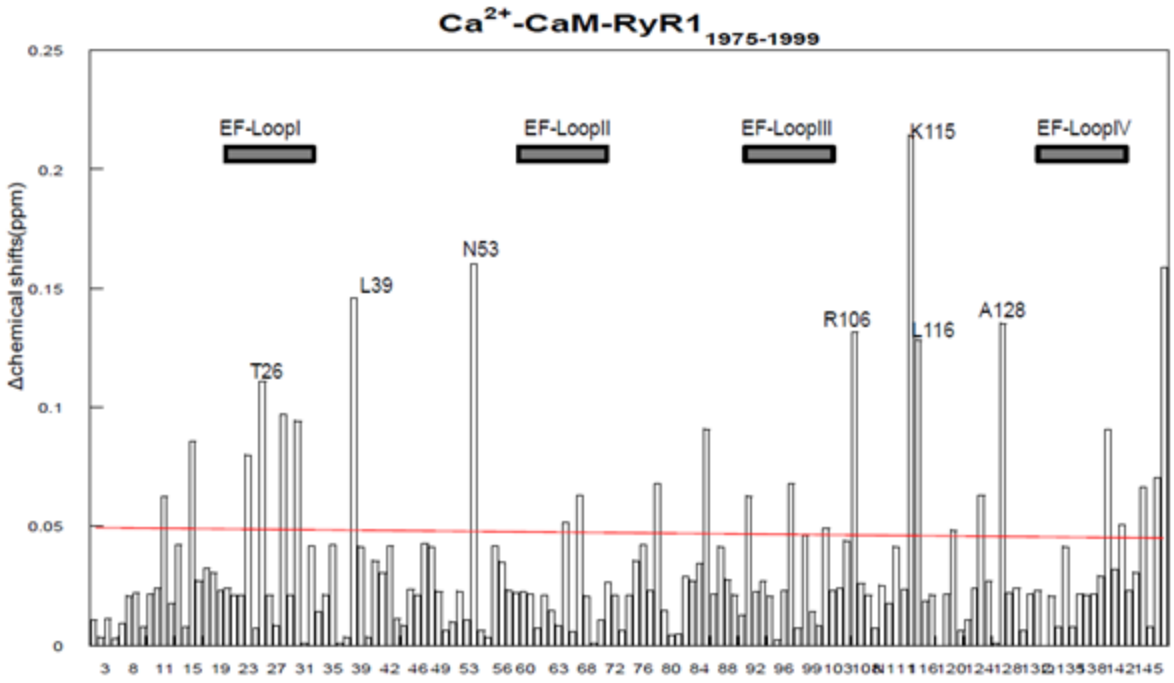

Figure 5.2. Chemical shifts CaM-RyR1$_{1975-1999}$ complexes collected on 600 MHz. Residues with significant chemical shift changes bigger than 0.05 were labeled. This Figure is adopt from Jie Jiang's dissertation.

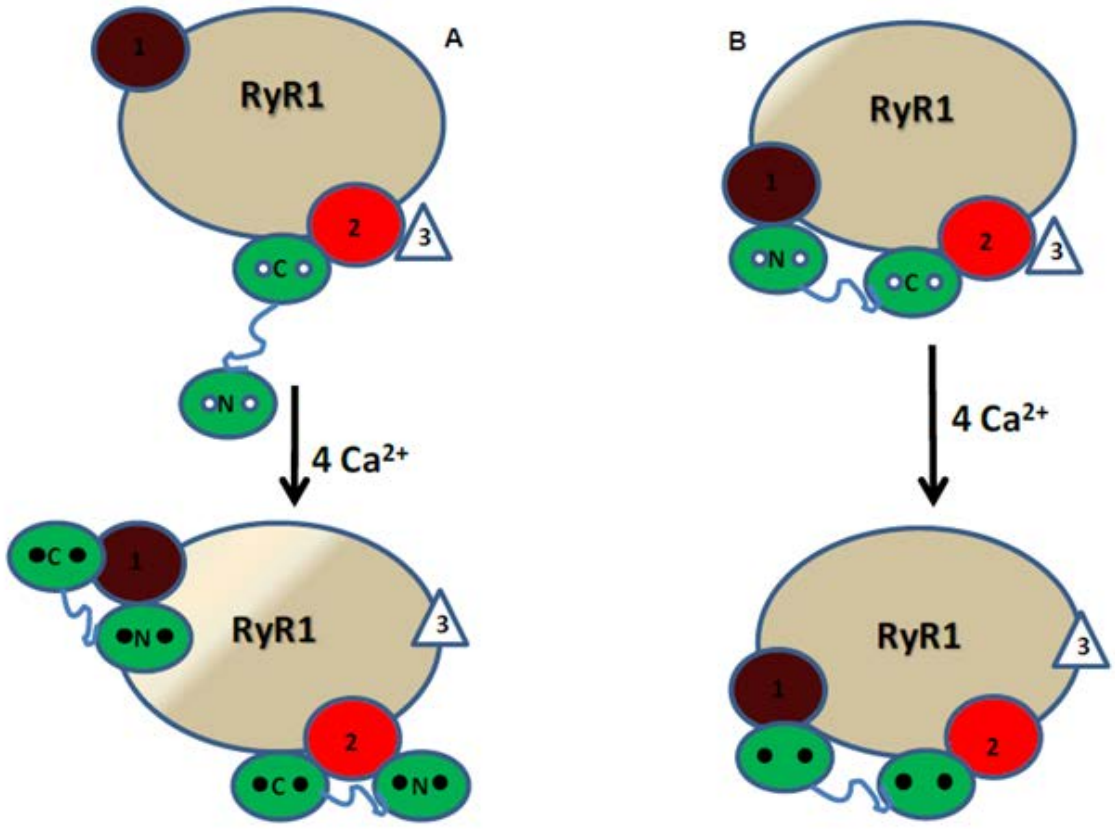

Figure 5.3. Our designed working models of CaM regulation on RyR1 in three possible binding region.
Symbols labeled 1, 2, and 3 represent three sites 1975-1999, 3614-3643, and 4114-4142 on RyR1. Green symbol is CaM molecule. White dots on CaM represent apo form of CaM, black dots on CaM represent Ca^{2+} ion.

5.3. Expression and Purification of GST tagged RyR1 mini domain

Expression of RyR1 mini domain was performed with GST tag vector pGEX-2T at 37 °C 4 hours in LB medium with *E. coli* cell strain BL21(DE3) after additional of IPTG. The GST tag (26 kDa) is to help the folding and the production of the RyR1 mini domain (7.2 kDa). **Figure 5.4 A** shows the bacteria growth rate of the GST-tagged RyR1 mini domain with cell strain BL21(DE3). The growth rate indeed shows an exponential curve, and the growth rate slow down after the addition of IPTG. The SDS-PAGE shows that before induction, basal expression of other protein was low as is expected of BL21(DE3) cell strain. After the addition of IPTG, the engineered protein was produced as optical density increased with correct molecular weight (33.2 kDa), demonstrating a successful expression outcome. (**Figure 5.4 B**) The protein is purified by using the glutathione sepharose resins; the soluble GST tagged protein will binds to the resins. However, most of the protein remains in the debris after cell lysis. (**Figure 5.4 C**) The refolding method was used to recover the expressed protein as using in the SDS-PAGE. Majority of the protein was recovered from the inclusion body. (**Figure 5.5 A**) However, most of the protein cannot bind onto the resins; this might because the protein did not folded well so that it cannot bind to the resins. (**Figure 5.5 B**)

Different cell strains are used for expression of GST tagged RyR1 mini domain as soluble form. Cell strains, BL21(DE3)pLysS, Tunner, and Rosetta are used to express RyR1 mini domain at lower temperature (30 °C) in LB medium after additional of IPTG. SDS-PAGE shows the expression condition of GST RyR1 mini domain as shows in **Figure 5.6 A**, **B**, and **C**. However, SDS-PAGE shows protein is still expressed as inclusion body in the debris after cell lysis. (**Figure 5.4 D**)

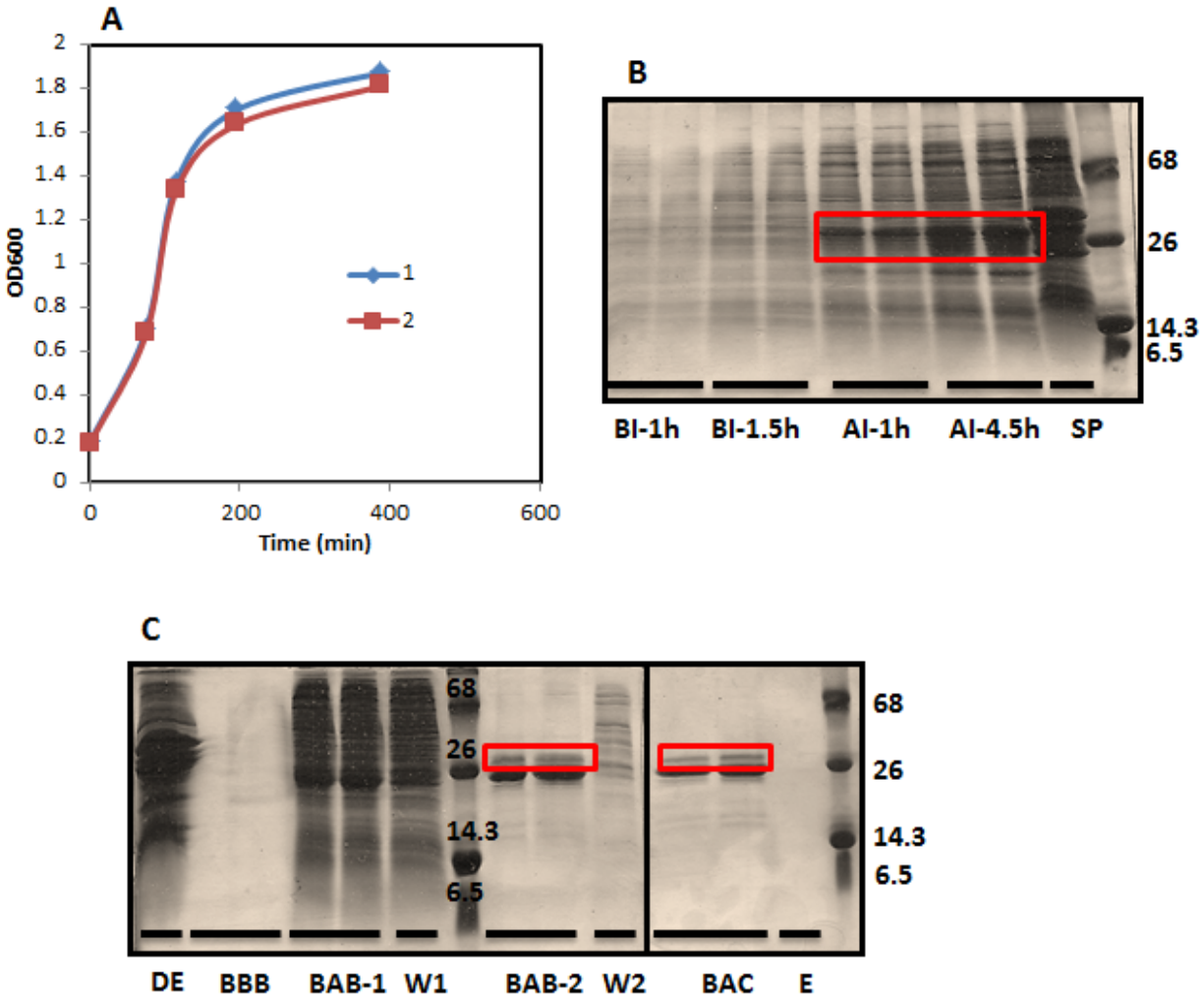

Figure 5.4. 15% SDS-PAGE of RyR1 mini domain expression and purification.
A. Growth rate of RyR1 mini domain; B. Expression of RyR1 mini domain; C. purification of RyR1 mini domain (BI: before induction; AI: after induction; S: supernatant; P: pellet; BBB: beads before binding; BAB-1: beads after binding before wash with PBS; W1: waste after binding before wash with PBS; BAB-2: beads after binding after wash with PBS; W2: waste after binding after wash with PBS; BAC: beads after cleavage; E: elution.)
The molecular weight of the GST tagged RyR1 mini domain is 33.2 kDa. Beads are the glutathione sepharose resins.

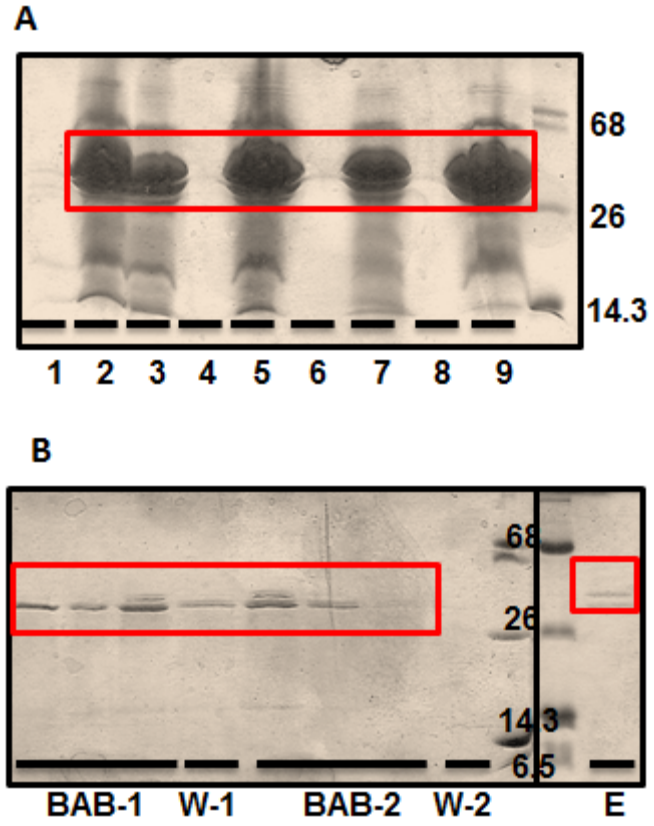

Figure 5.5. SDS-PAGE of GST tagged RyR1 mini domain during the refolding process. 1: supernatant after sonication; 2: pellet after sonication; 3: pellet after 2nd wash with 2% Triton-x-100; 4: supernatant after 2nd wash with 2% Tirton-x-100; 5: pellet after 3th wash with 2% Tirton-x-100; 7: pellet after 4th wash with 2% Triton-x-100; 8: supernatant after 4th wash with 2% Triton-x-100; 9: supernatant after refold with 4 M Urea; BAB-1: beads after binding before wash with PBS; W1: waste after binding before wash with PBS; BAB-2: beads after binding after wash with PBS; W2: waste after binding after wash with PBS; E: elution.

The molecular weight of the GST tagged RyR1 mini domain is 33.2 kDa. Beads are the glutathione sepharose resins.

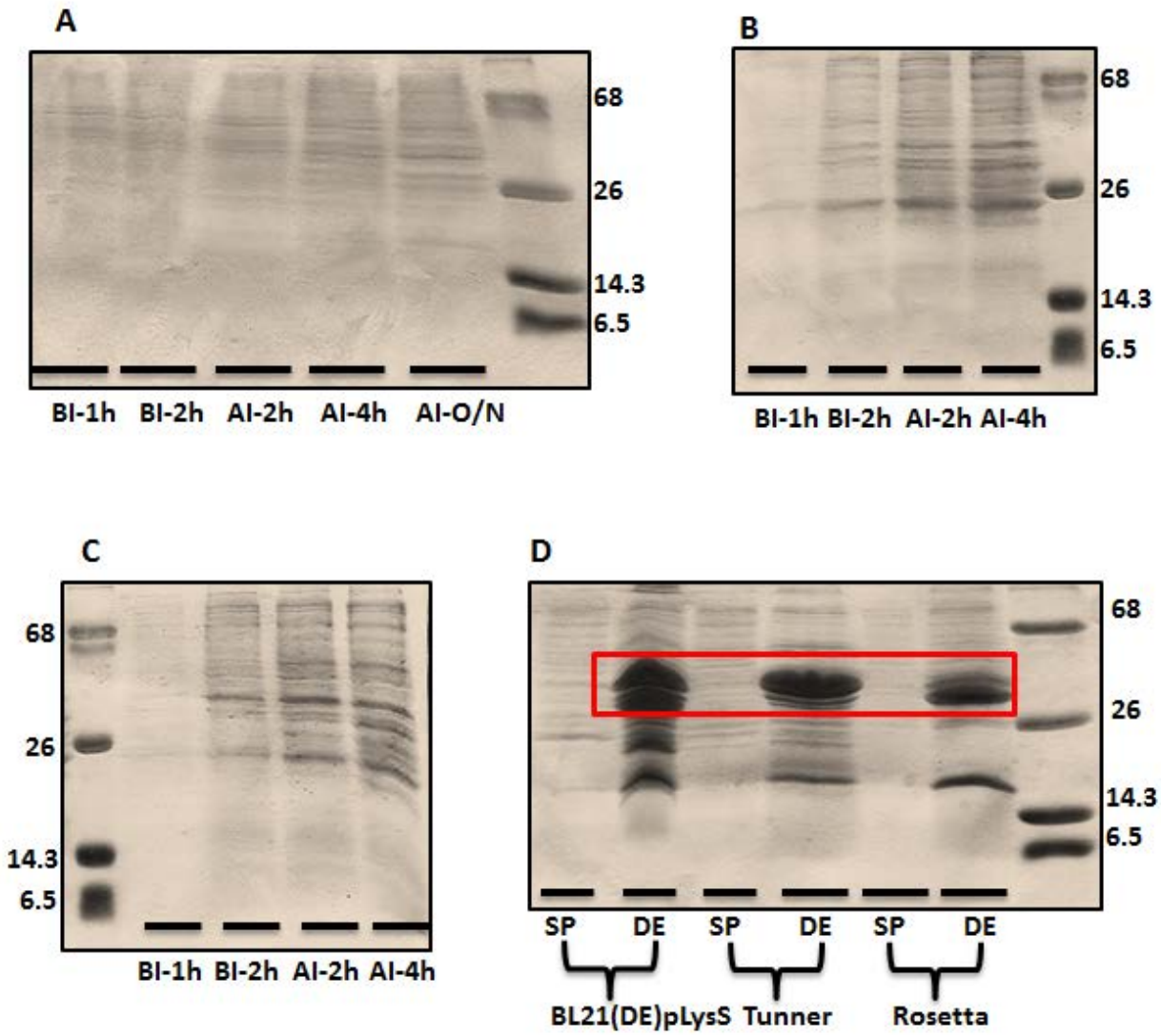

Figure 5.6. 15% SDS-PAGE of RyR1 mini domain expression by using different cell strains.

A) Rosetta; B) BL21(DE3)pLysS and Tunner; C) cell lysis of protein in three cell strains. (BI: before induction, AI: after induction, SP: supernatant after cell lysis, DE: debris after cell lysis)

The molecular weight of the GST tagged RyR1 mini domain is 33.2 kDa.

5.3. Expression and purification of His-tagged RyR1 mini domain

The RyR1 mini domain is reconstructed as His-tag protein to improve the product of the protein. His-tagged protein does not require maintaining the secondary or tertiary structure to binds on the his-tagged column; thus, if the his-tagged RyR1 mini domain expressed as inclusion body, refolding method can be used to recover the protein. The DNA sequence of RyR1 mini domain is inserted into the reconstructed vector that was gift from Dr. Ramona J. B. Urbauer in UGA. This reconstructed vector combined both pET-32a and pET-15b. Two different mediums (LB and M9) are used to compare the expression level of his-tagged RyR1 mini domain. The expression of RyR1 mini domain was performed with His-tagged vector at 28 °C after the addition of IPTG overnight with E. coli strain BL21(DE3). **Figure 5.7** shows the expression condition of his-tagged RyR1 in M9 (**Figure 5.7 A**) and LB (**Figure 5.7 B**) medium on SDS-PAGE. The predicted molecular weight of his-tagged RyR1 mini domain is 24.5 kDa. It is clear that protein expression level in the M9 medium is much higher than the protein expression in the LB medium.

Overnight expression at a low temperature was designed to express protein was soluble form without the formation of inclusion body. However, most of the protein expressed as inclusion body that remain in the cell pellet after cell lysis. The inclusion bodies are insoluble aggregates of misfolded protein that lacking biological activity. The high buoyant density of inclusion bodies facilitate their separation from soluble E. coli proteins and cell debris by differential centrifugation. Conventional methods for refolding of insoluble recombinant proteins include slow dialysis or dilution into a buffer of near neutral pH. Affinity tagging of the recombinant protein and the addition of several consecutive histidine residues open the possibility of efficient purification and refolding in a single chromatographic step. Since binding

of the histidine tract to immobilized divalent metal ion can occur in the presence of chaotropic agent, such as urea or guanidine hydrochloride at high concentration. His-tagged inclusion body protein can be solubilized by chaotropic extraction and directly bound to an affinity matrix. Removal of contaminating proteins and refolding by exchange to non-denaturing buffer conditions can then be performed before elution of the protein from the column. The protein eluted from the FPLC by using on column refolding method shows a clean single band at the predicted molecular way, which indicate the protein is relatively pure. (**Figure 5.8**)

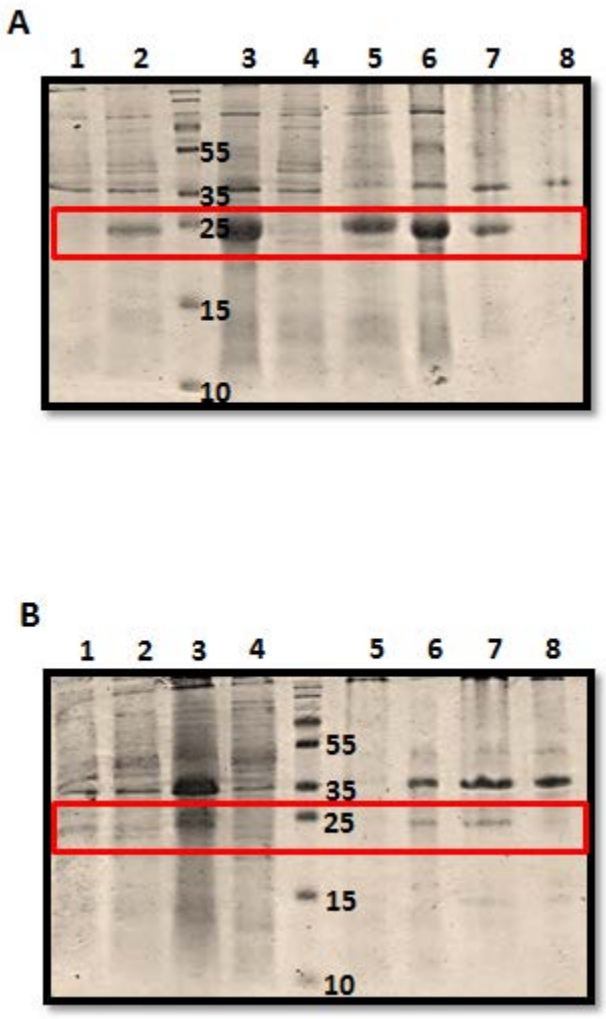

Figure 5.7. Comparsion of His-tagged RyR1 mini domain in M9 and LB medium.
A. SDS-PAGE of expression and purification of His-tagged RYR1 mini domain in M9 medium; B. SDS-PAGE of expression and purification of His-tagged RyR1 mini domain in LB mediu. (1. Before induction;2. After induction 3. Debris after lysis 4. Supernatnat after lysis; 5. Supernatant after wash with 2 M Urea and 2% Triton; 6. Debris after wash with 2 M Urea and 2% Triton; 7. Supernatant after wash with 6 M guanidine; 8. Debris after wash with 6 M guanidine.)

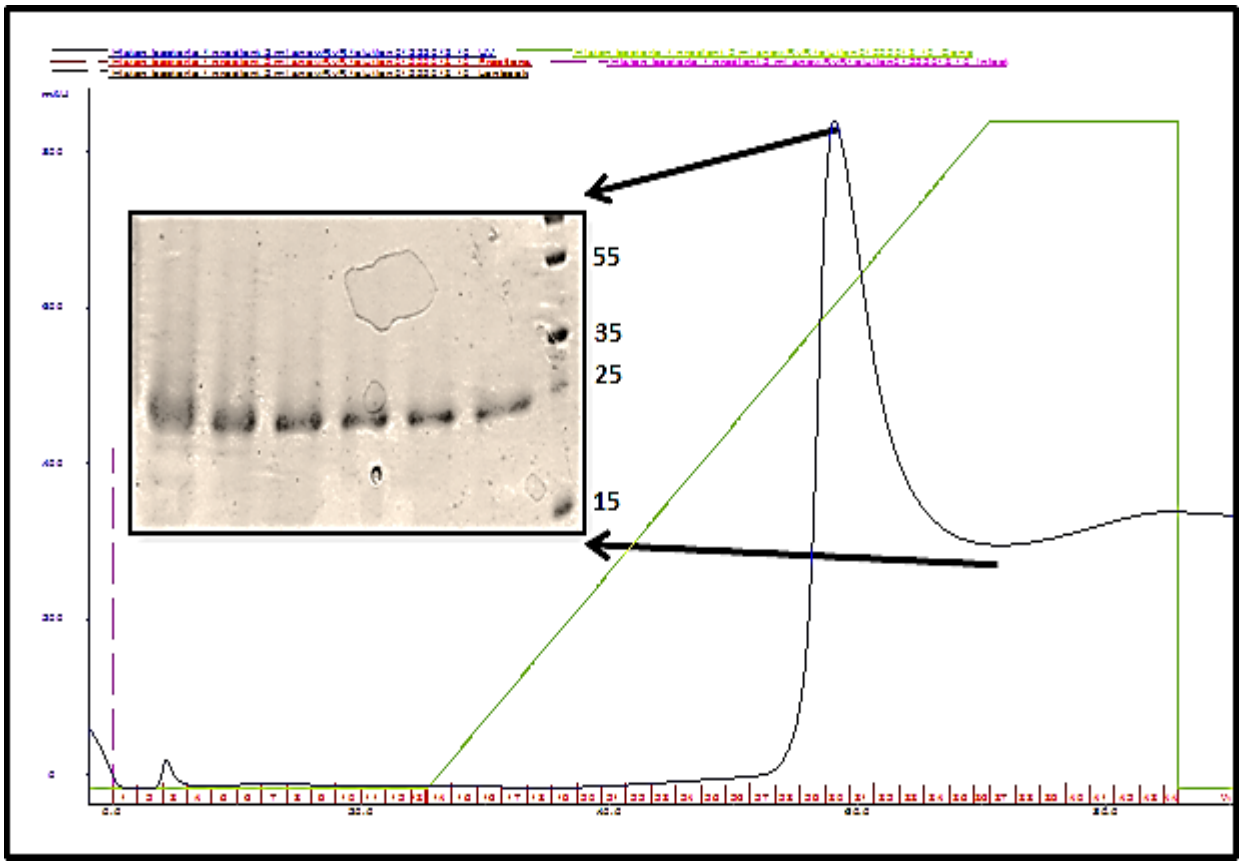

Figure 5.8. Elution spectra of His-tagged RyR1 mini domain before cleavage.

5.4. Conclusion and future work

The RyR1 mini domain with GST tagged expressed as inclusion body in vector pGEX-2T. Refolding method is designed to totally denature the protein, then refolding the protein back by graduatelly decrease the concentration of urea. However by using the refolding method, majority of the protein remain in the inclusion body, and remain protein cannot bind to the affinity column during the purification process. This might due to the relatively big size of GST tag protein (26 kDa), 34 kDa of GST tagged RyR1 mini domain is hardly to refolded back to the native form. Different cell strains, BL21(DE3)pLysS, Tunner, and Rosetta are used to try to express the GST tagged RyR1 mini domain as soluble protein. Unfortunately, majority of the protein is misfolded as including body.

The reconstructed his-tagged RyR1 mini domain is expressed with cell strain BL21(DE3). The his-tagged RyR1 mini domain is also expressed as inclusion body. Since the his-tagged protein does not need to secondary or tertiary structure to bind the his-tag column; thus, on column refolding his-tagged protein and the purification process can be performed in one step. There are two different medium (LB and M9) are used to expressed the his-tagged RyR1 mini domain. There is more protein expressed in M9 medium than LB medium. Majority of the protein did recovered by using on column refolding method, and the protein is relative pure. However, the protein starts to precipitate immediately during the dialysis process. Changing pH is trying to dissolve the protein, but the protein still remains in the insoluble form. The precipitation might due to the highly hydrophobicity of the RyR1 mini domain and preferring aggregation to dispersion in water. On column digestion will be perform to cut the desire peptide form the tag.

6. Gap junction

6.1 Introduction

Gap junction is intercellular protein channel that span on the lipid bilayers of the cell member which allows intercellular communication of adjacent cell by allows the direct exchange of ions and some molecules that is less than 1 kDa. A complete gap junction is formed by hemichannels (connexon) from adjacent cell docking together. One hemichannel is formed by hexamer of connexin subunits in the lipid bilayer. The transmembrane protein, connexin family share a common topology that contain four α helical transmembrane domains, two extracellular loops, a cytoplasmic loop, and N and C termini that local on the cytoplasmic membrane face. There are 3 highly conserved cysteine residues on each extracellular loop that form disulfide bonds which stabilized the loops during the docking process.[66,67,68](**Figure 1.7**) Two different nomenclature are in use for connexin (Cx) family protein, one is naming Cx according to species form and their theoretical molecular mass, and another naming is dividing Cx to different subgroups with respect to their extent of sequence identity and length of the cytoplasmic loop.[26] As channel close, two adjacent cells uncouple from each other electrically and metabolically. Uncoupling of two docking cell is one way that normal health cells protect itself from the unhealthy cells. To understand the role of gating agent is the primary goal before we focus on the regulation of gap junction channel. The uncoupling process is sensitivity to a low pH through a Ca^{2+} concentration increase in the intracellular; also, CaM was also suggest to be one of the gating particle of the channel.

The role of CaM in the chemical gating was first suggested by the ability of calmodulin antagonist (trifluorperazine) to prevent CO_2 inducted uncoupling of Xenopus embryonic cells.[69] This suggestion was supported by the observation of CaM blockers (calmidazolkum and W7)

prevented uncoupling in various cell types.[70],[71] Peracchia *et al.* have further showed that CaM involved in chemical gating by directly interact with Cx32.[72] To date, there are at least 20 connexin gene in the human genome have been identified, and Cx43 is the most ubiquitous connexin.[73] Our previous study have predicted three CaM binding region (CaM binding region I, II, and III) at intracellular region. (**Figure 6.1**) Region II (residue 136-158) showed the highest prediction score than region I and III. The peptide mode also showed region II bind to Ca^{2+} form CaM with 1:1 stoichiometry. Our NMR data also classified the binding mode of this region with CaM to be 1-5-10 hydrophobic residue motif.[28] Xu *et al.* have hypothesize that Ca^{2+} form of CaM bind to region II (residue 136-158) which induces a gating response that close the Cx43 gap junction.[74] There are two gating mechanism that have been proposed. One is the "cork" model showing in **Figure 6.2 A**. which the Ca^{2+} form CaM may act cork or induce a conformational change in the central loop domain that stop the opening of the connexin. Another model is "iris" model that base on the Unwin and Ennis' hypothesis which suggest that Ca^{2+} form of CaM induced conformational change of the connexin, which make a less than 10° tilting of the connexin subunits that narrow the pore of channel.[75] (**Figure 6.2 B**)

To understand how the entire intracellular loop of Cx43 interact with CaM, and whether the transmembrane domain next to the intracellular loop play any role during the CaM binding process, the designed Cx43 fragments are expressed and purified as His tag inclusion body. In this chapter, the achievement of the initial expression and purification work is reported. The interaction study of CaM with Cx4388-164 is also discussed in this chapter.

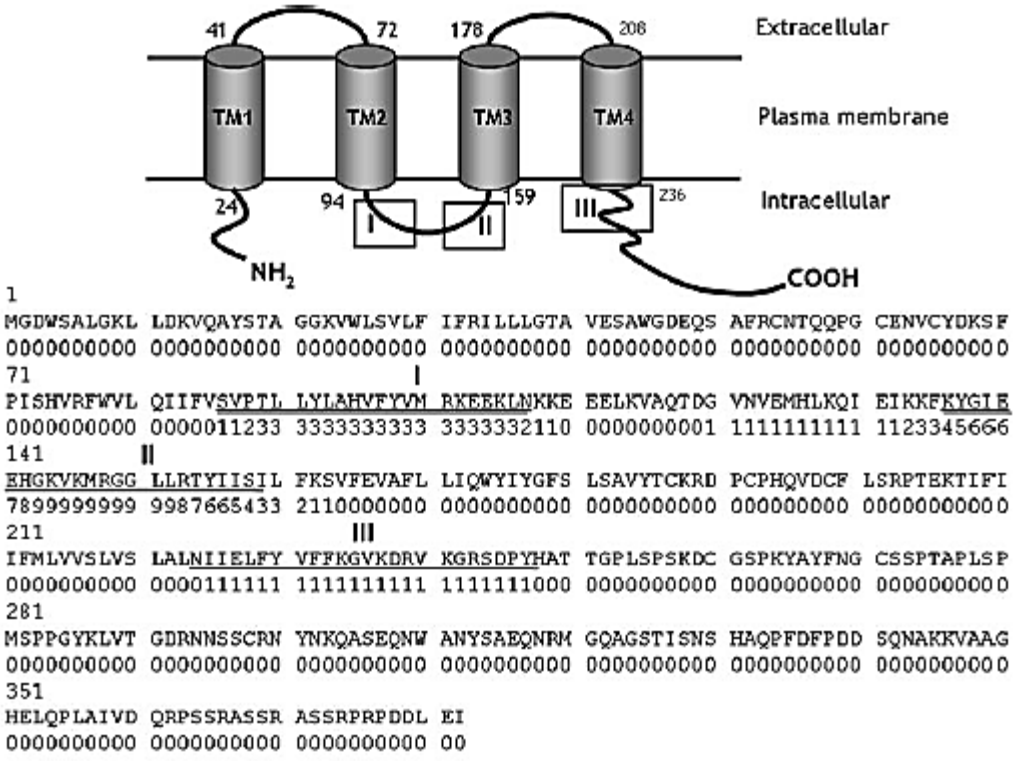

Figure 6.1. Structure of Connexin 43 and primary sequence with highlight of CaM binding sites. Box I, II, and III are the putative CaM binding sites. This is figure is adopt from Zhou *et al.*[28]

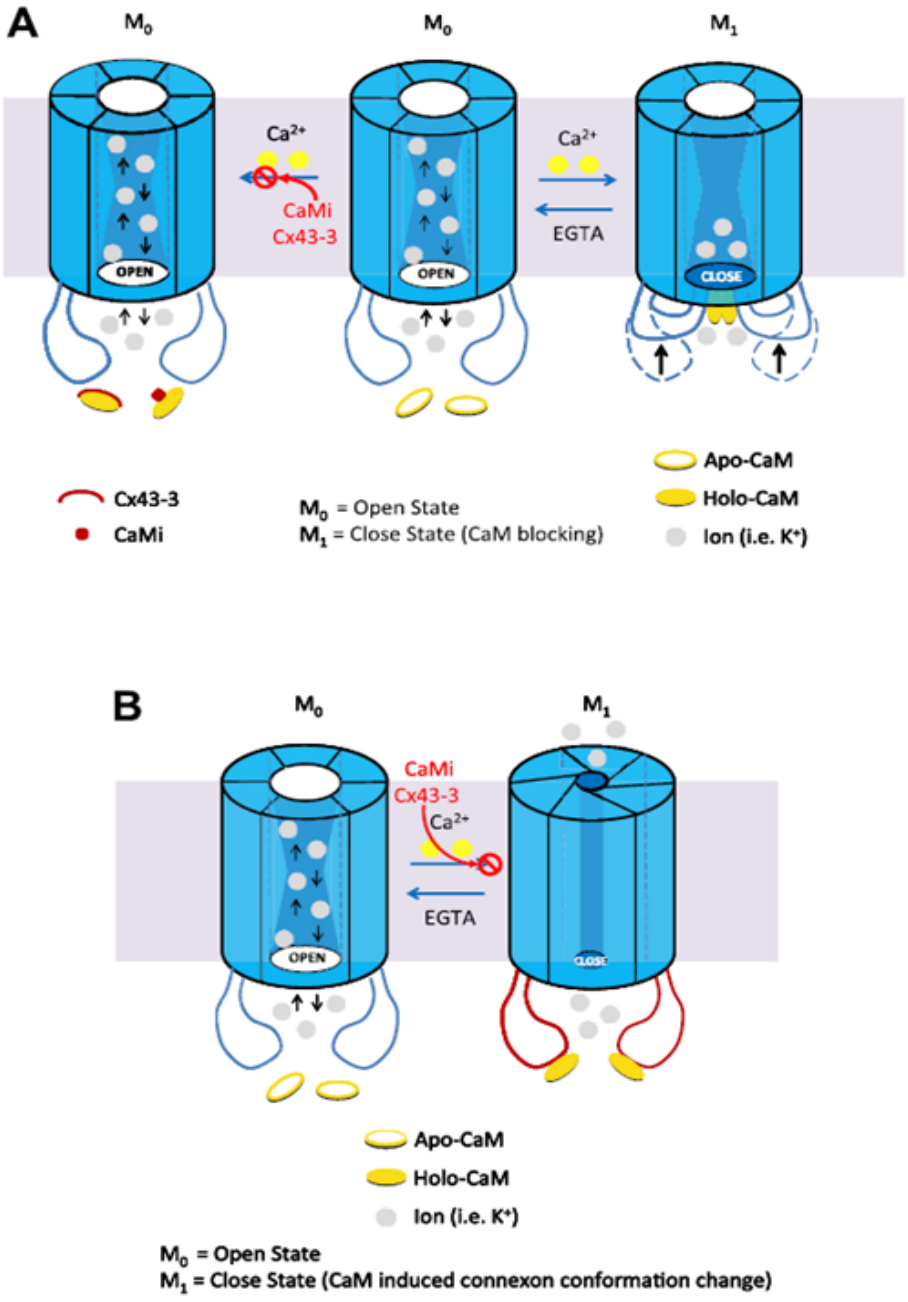

Figure 6.2. Mechanism of CaM regulate gap junction. A. The 'cork' model; B. CaM induced connexon conformation change model. This figure is adopt from Xu *et al.*[74]

6.2. Result

6.2.1 Design of Cx family peptide to test the interaction with CaM

Two predicted CaM binding region of Cx43 are located at the same intracellular loop with region II has higher CaM binding score than region I. Since the location of the two CaM binding regions are very close and all in the same intracellular loop, we designed a peptide (peptide I shows in **Figure 6.3**) that cover the entire intracellular loop of Cx43 (residue 99-154) to study the interaction of the entire intracellular loop with CaM. We also think that the part of the transmembrane domain served as an anchor that stabilized the entire intracellular loop during the binding process. Thereby, another peptide (peptide II shown in **Figure 6.3**) include the entire intracellular loop and part of the transmembrane domain of Cx43 (residue 88-164) was also design to study the difference with peptide I.

Our desired peptide is inserted into the reconstructed vector that was gift from Dr. Ramona J. B. Urbauer at the UGA. The protein expressed form this vector is a his-tagged (**Figure 6.4 Blue**) fusion protein. There is enterokinase cleavage site (**Figure 6.4 Red**) and our desired peptide is inserted right after this cleavage site. By doing this way, we can get a very clean peptide without any tag after the cleavage. The advantage about this method is that we can uniformly label our peptide and get a very clean peptide to study the binding mode by using the NMR spectroscopy.

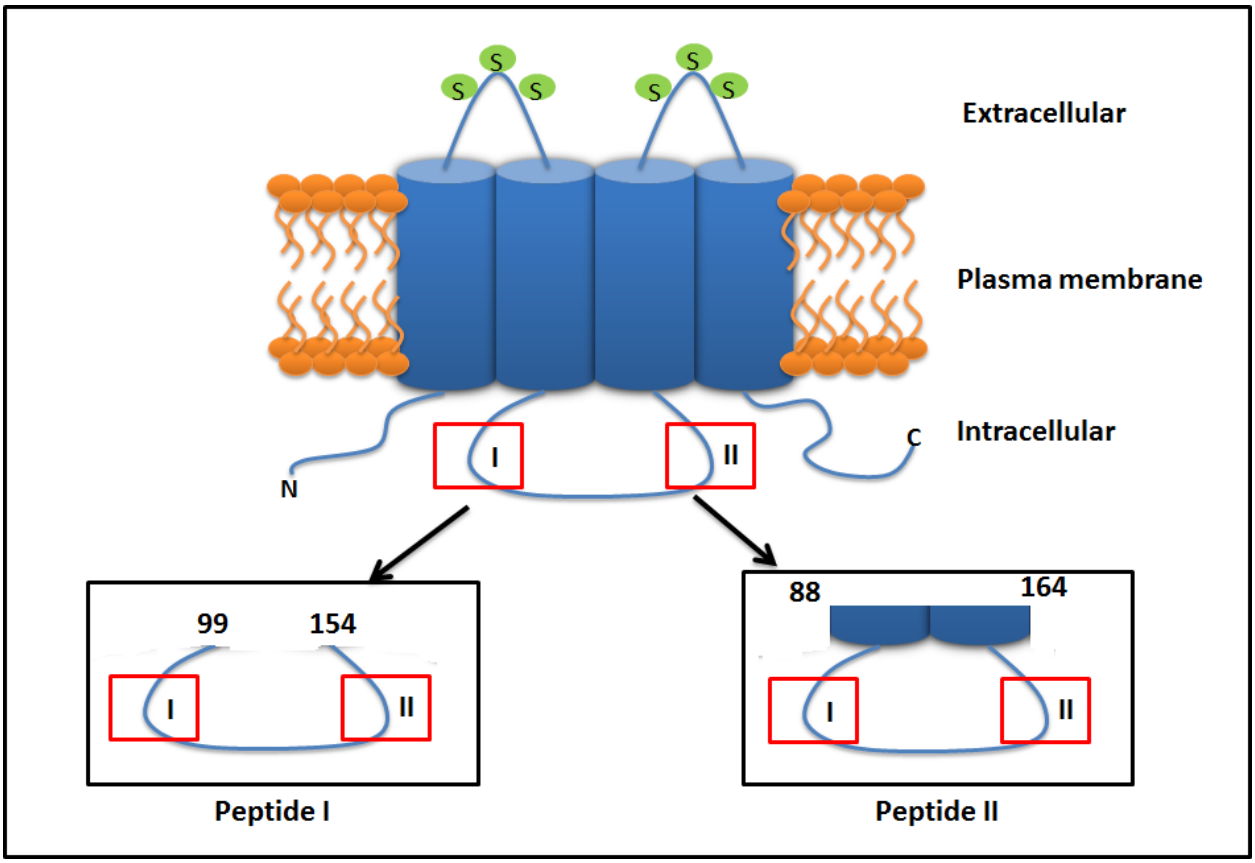

Figure 6.3. Schema of the designed peptides of Cx43.

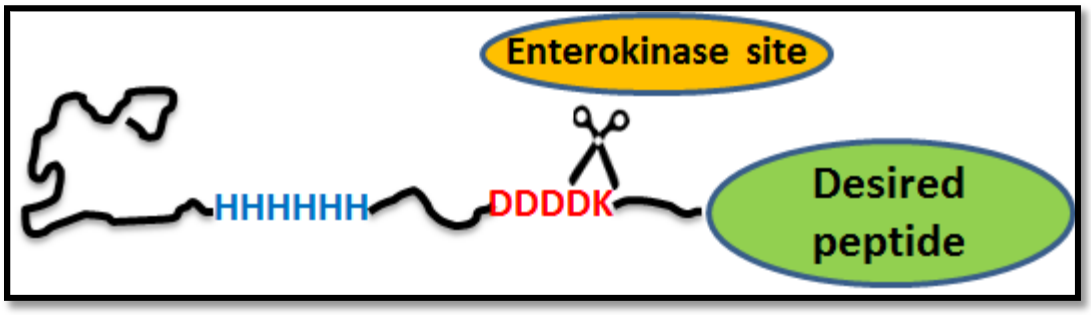

Figure 6.4. Schema of reconstructed peptide was fusion body. Blue highlight is the his-tag, red highlight is the enterokinase cleave site.

Table 4. Sequence of Cx family peptides and their molecular weight.

CaM binding peptides	Sequence	Molecular weight before cleave (kDa)	Hydrophobicity (%)
rCx43$_{88\text{-}164}$	SVPTLLYLAHVFYVMRKEEKLNKKEEELKVAQTDGVNVEMHLKQIEIKKFKYGIEEHGKVKMRGGLLRTYIISILFKS	26.71	40
rCx43$_{99\text{-}154}$	MRKEEKLNKKEEELKVAQTDGVNVEMHLKQIEIKKFKYGIEEHGKVKMRGGLLRT	24.04	31
mCx26$_{99\text{-}144}$	HEKKRKFMKGEIKNEFKDIEEIKTQKVRIEGSLWWTYTTSIFFRV	23.28	33
mCx26$_{207\text{-}226}$	ITELCYLFVRYCSGKSKRPV	19.91	35

6.2.2. Small scale expression and purification of reconstructed peptide

The small scale expression was used to test the expression condition of the recombined protein. A positive control and recombined $Cx26_{207-226}$ was expressed with his-tag vector at 37°C in M9 medium with BL21(DE3). 100 μM IPTG was added for the induction once the optical density reach to 0.6-0.8, the protein was then expressed at 28°C low temperature for overnight. The bacterial cell growth is exponential to the point of induction and the cell growth show down at 600 nm. (**Figure 6.5 A**) The expecting molecular weight of positive control and $Cx26_{207-226}$ as His-tag protein are 20 and 19.91 kDa. **Figure 6.5 B-C** shows the expression level of positive control and $Cx26_{207-226}$. The SDS-PAGE shows that before induction, the expression of our desired protein did not show and other protein expression bands got thicker along with time. However, after induction there is a clear band that is not there after the induction. (Highlight in red box at **Figure 6.5 B-C**) The SDS-PAGE shows evidence that the conditions used for expression were optimal.

After cell lysis, most the protein of both positive control and $Cx26_{207-226}$ remain in the debris. (**Figure 6.6 A&B**) The supernatant after cell lysis was used to bind on the nickel charge beads and processed purification. The SDS-PAGE shows the concentrated elution of both the positive control and $Cx26_{207-226}$ at correct molecular weight. (**Figure 6.6 C**) This proved that this method can be used but need further modification.

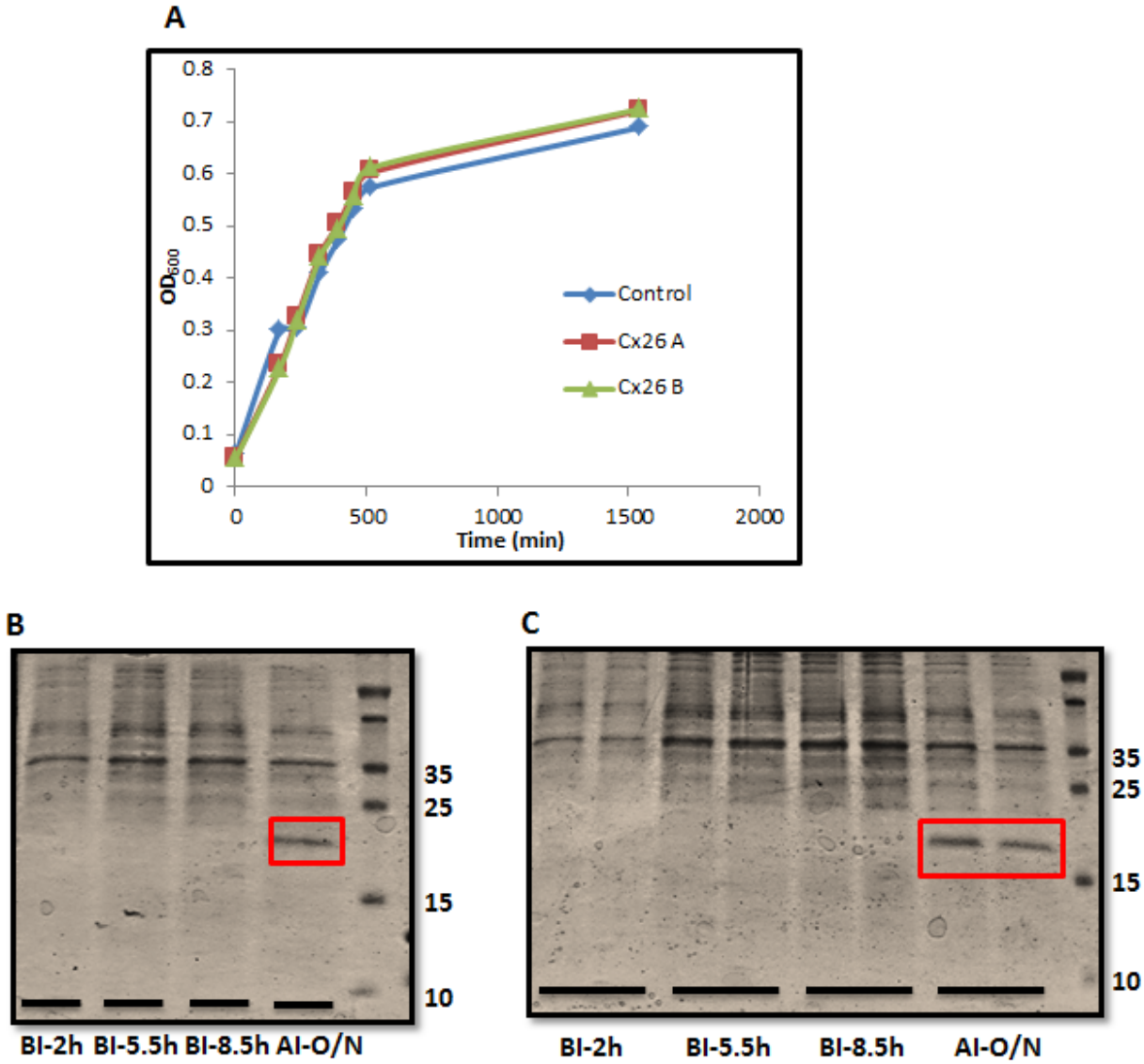

Figure 6.5. Expression of small scale protein.
A)Growth curve of positive control and $Cx26_{207-226}$; B) SDS-PAGE of expression of positive control; C) SDS-PAGE of expression of $CX26_{207-226}$ (Red box highlight is the positive control and $Cx26_{207-226}$; BI-before induction; AI-after induction)

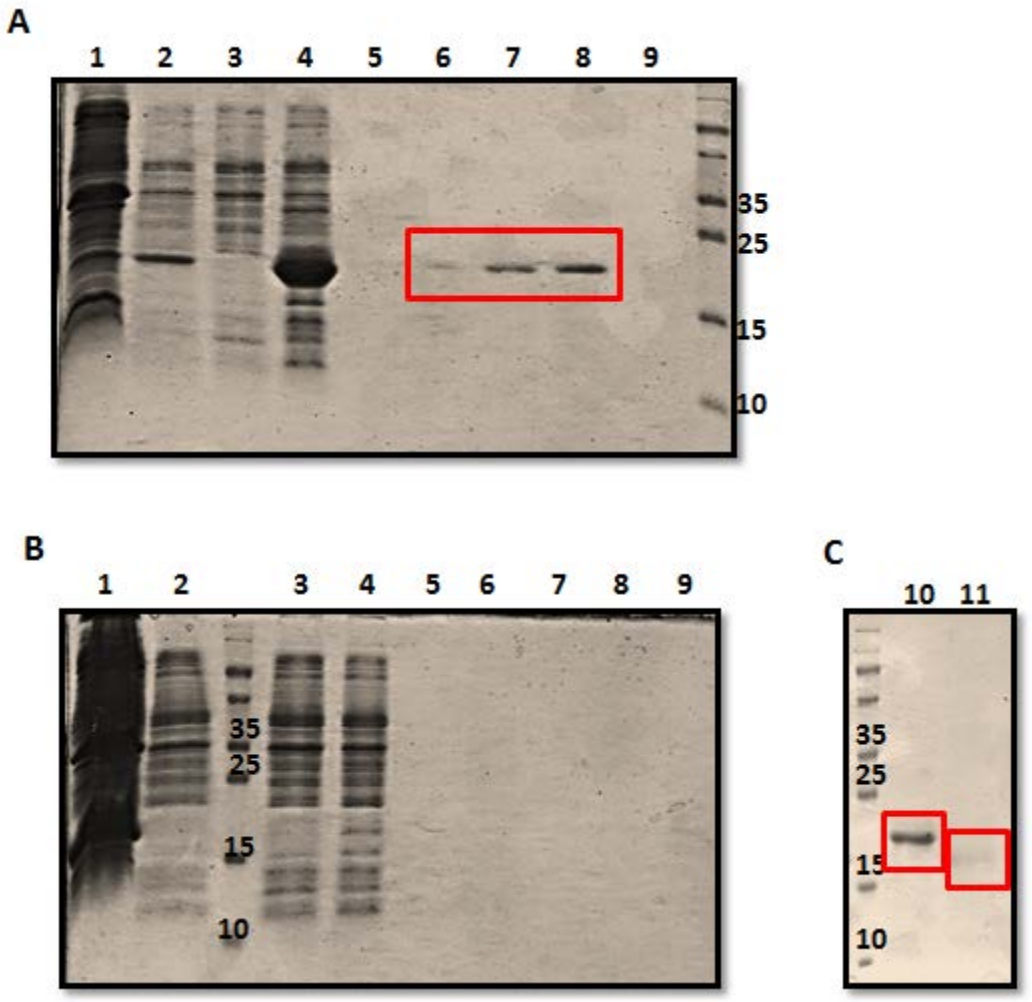

Figure 6.6. Purification of small scale of recombined protein.
A) SDS-PAGE of purification of positive control; B) SDS-PAGE of purification of $Cx26_{207-226}$ (1. Debris after cell lysis; 2. Supernatant after cell lysis; 3. Binding waste; 4. Beads after binding; 5. Elution after wash with 10 mM Imidazole; 6. Elution after wash with 20 mM Imdazole; 7. Elution after wassh with 40 mM Imidazole; 8. Elution after wash with 120 mM Imidazole; 9. Beads after 250 mM Imidazole); C) SDS-PAGE of concentrated elution (10. Positive control; 11. $Cx26_{207-226}$)

6.2.3. Modified protein expression and protein purification by using refolding method

Large scale of $Cx26_{207-226}$ was expressed in low temperature 28°C to avoid formation of inclusion body. The SDS-PAGE shows that before induction, the expression of other protein increase with time. After the addition of IPTG, the engineered protein was produced. (**Figure 6.7**) The low temperature expression did improve the solubility of the protein; however, majority of the protein still remain in the cell pellet. (**Figure 6.8**) The elution protein that comes out of the HPLC system shows multiple bands on the SDS-PAGE, which indicate the many impurity of the protein.

The purification of supernatant from the cell lysis did not come out the FPLC system successful as expected. The refolding method is used to recover the protein from the debris. The binding of histidine to immobilized divalent metal ions can occur in the present of high concentration of chaotropic agent, such as urea or guanidine. Therefore, his-tagged inclusion body can be solubilized by high concentration of guanidine and directly bound to the affinity matrix. Refolding his-tagged protein, removing other unwanted protein, followed by eluting of his-tagged protein can be perform on column by one signal step. [76] **Figure 6.9** shows the SDS-PAGE of on column refolding of $Cx26_{207-226}$ in small scale by using the gravity nickel charged column. The protein after refolded from urea and guanidine is much clean compare to the non-refolding method at **Figure 6.9** it shows one single band around 20 kDa that is about the predicted molecular weight of $Cx26_{207-226}$. This indicates that the refolding method is more suitable method to purify this type of protein.

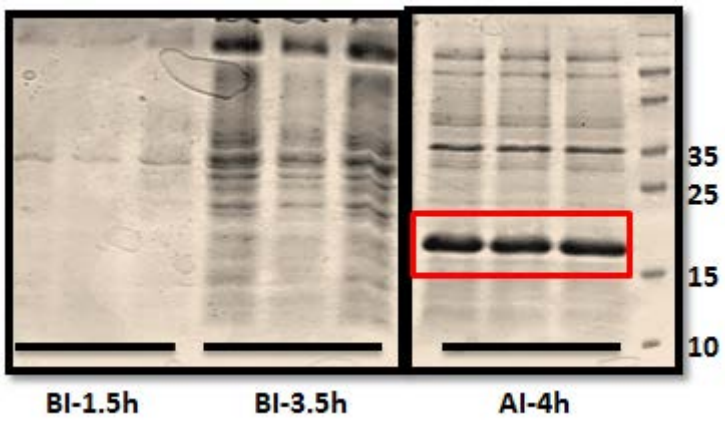

Figure 6.7. SDS-PAGE of large scale expression of $Cx26_{207-226}$. (BI-Before induction; AI-After induction)

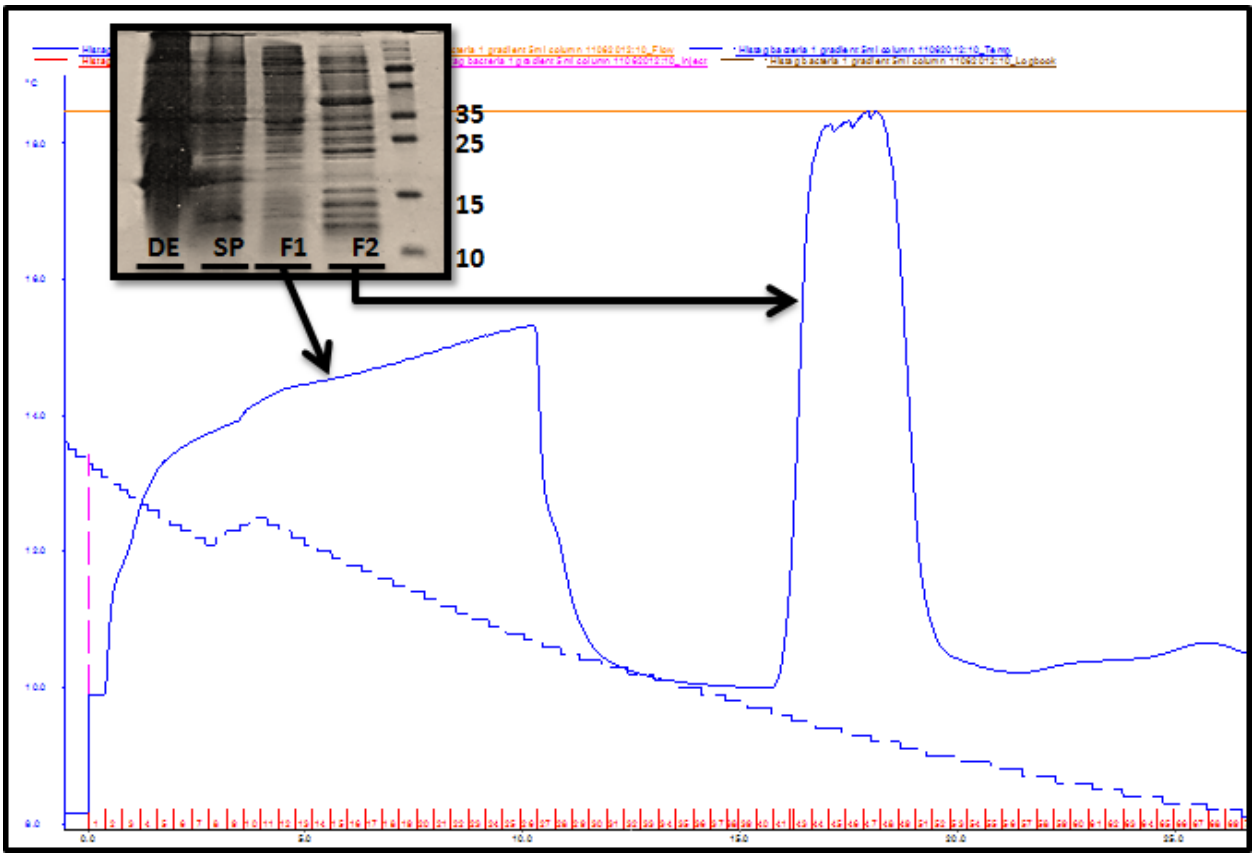

Figure 6.8. FPLC spectra of purification of $Cx26_{207-226}$ and SDS-PAGE accordingly.

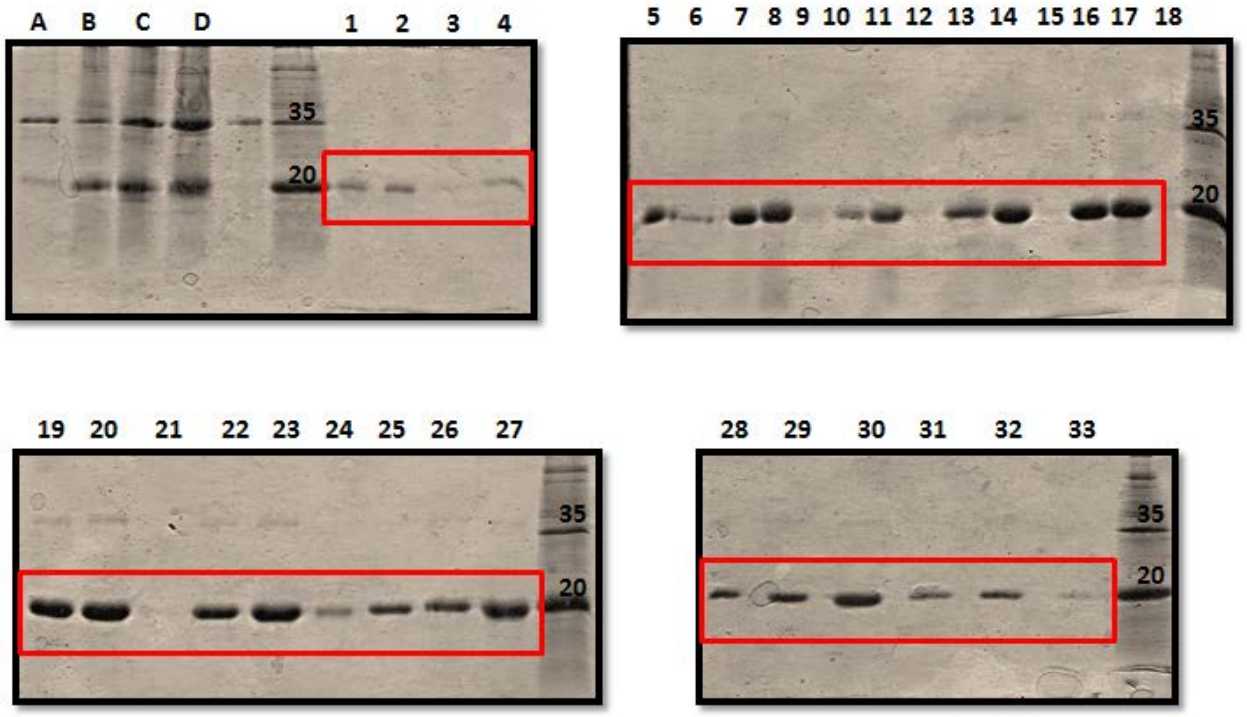

Figure 6.9. Recover $Cx26_{207-226}$ by using refolding method by using the gravity nickel charged column.

A) Supernatant after 1st time Urea wash; B) Supernatant after 2nd time urea wash; C) Debris after 2nd time urea wash; D) Supernatant after 6 M Guanidine wash; F) Debris after wash with 6 M Guanidine; 1&2) Beads after binding; 3) Binding waste; 4&5) Bead after wash with 6M urea; 6) Elution after wash with 6 M Urea; 7&8) Bead after wash with 4 M urea; 9) Elution after wash with 4 M urea; 10&11) Bead after wash with 2 M urea; 12) Elution after wash with 2 M urea; 13&14) Bead after wash with 0 M urea; 15) Elution after wash with 0 M urea; 16&17) Bead after wash with 20 mM imidazole; 18) Elution after wash with 20 mM imidazole; 19&20) Bead after wash with 40 mM imidazole; 21) Elution after wash with 40 mM imidazole; 22&23) Bead after wash with 80 mM imidazole; 14) Elution after wash with 80 mM imidazole; 25&26) Bead after wash with 160 mM imidazole; 27) Elution after wash with 160 mM imidazole; 28&29) Bead after wash with 320 mM imidazole; 30) Elution after wash with 320 mM imidazole; 31&32) Bead after wash with 500 mM imidazole; 33) Elution after wash with 500 mM Imidazole.

6.2.4. Expression and purification of Cx43 peptides by using refolding method

$Cx43_{88-164}$ and $Cx43_{99-154}$ was also expressed with his-tagged vector in low temperature 28°C in M9 medium with BL21(DE3) cell strain. SDS-PAGE shows that majority of the protein remained in the cell pellet as inclusion body after cell lysis for both of the peptides. (**Figure 6.10**) Therefore, both Cx43 peptide can use refolding method to purify. Western blot was used to confirm the formation of the his-tag Cx43 peptides. Western blot is used to detect whether the protein on the SDS-PAGE with correct molecular weight is truly our his-tagged peptides or not. Protein from electrophoresed gel is transferred to nitrocellulose membrane, and any non-specific binding is block by 5% BSA. Anti-polyHistindine is primary antibodies that general from mouse is applying to the nitrocellulose membrane, and only bind to the his-tagged protein. A secondary antibodies that is also general from mouse is apply to the nitrocellulose membrane, and only bind to the first antibodies specifically. Finally, a substrate that will luminesce when exposed to the reporter on the secondary antibody and is detected by photographic film. These, only his-tagged protein can be detected from the digital image of the western blot. Both **Figure 6.11** and **Figure 6.14** show the comparison of SDS-PAGE and Western blot of expression condition of $Cx43_{88-164}$ and $Cx43_{99-154}$. The Western blot Western blot shows a single band around 25 kDa only at the after induction column for both $Cx43_{88-164}$ and $Cx43_{99-154}$, this also confirmed that the band show around 25 kDa on the SDS-PAGE after the induction are the his-tagged Cx43 peptides.

Figure 6.12 and **Figure 6.14** show the FPLC spectrum of $Cx43_{88-164}$ and $Cx43_{99-154}$ by using the on column refolding method. Both spectra show that as the concentration of the imidazole increase, there is a sharp peak show up accordingly. SDS-PAGE and western blot are also used to confirm the elution fragment for fragment 29-34 on the FPLC spectra (**Figure 6.12 A and B**) of $Cx43_{88-164}$, and fragment 29-33 on the FPLC spectrum of $Cx43_{99-154}$. (**Figure 6.14 A**

and B Both SDS-PAGE and Western Blot show band around 25 kDa for elution fragment 29-34 on the FPLC spectra of $Cx43_{88-164}$ indicate that the elution fragment are relatively pure. Both SDS-PAGE and Western Blot show bands around 25 kDa for elution 29-33 on the FPLC spectra of $Cx43_{99-154}$ (**Figure 6.14**) indicate that the elution fragments are the His-tagged $Cx43_{99-154}$. However, there are a second band right below 25 kDa indicate some degree of degradation of $Cx43_{99-154}$. **Figure 6.12 C** and **Figure 6.14 C** are the UV spectra of elution of $Cx43_{88-164}$ and $Cx43_{99-154}$ from the HPLC system, both UV spectra show a sharp peak around 280 nm indicate the tyrosine residues in those peptides.

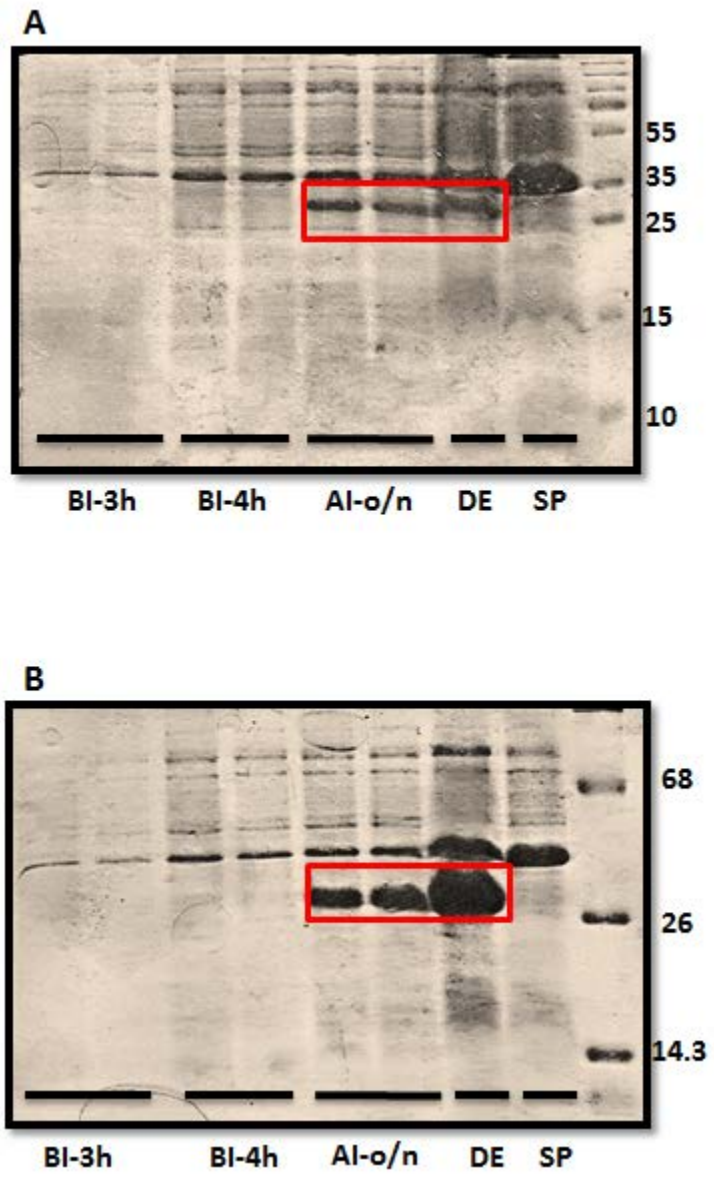

Figure 6.10. SDS-PAGE of Cx43 peptides.
A) $Cx43_{99-154}$; B) $Cx43_{88-164}$. (BI: before induction, AI: after induction, o/n: over night, DE: Debris after cell lysis, SP: supernatant after cell lysis)

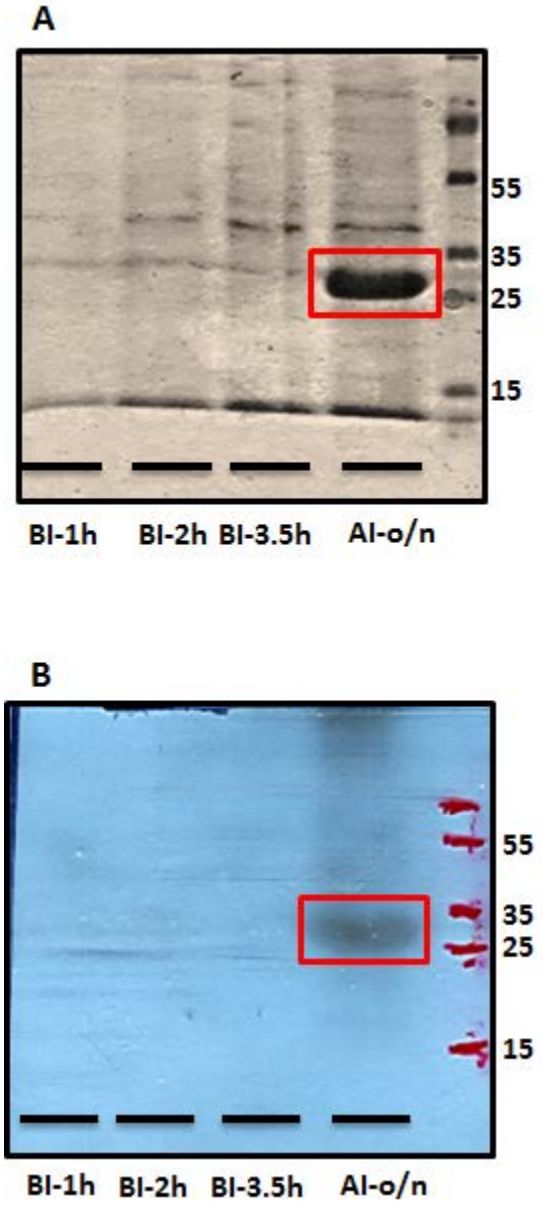

Figure 6.11. Expression of $Cx43_{88-164}$.
A) SDS-PAGE of expression of $CX43_{88-164}$, B) Western blot of expression of $Cx43_{88-164}$. (BI-before induction; AI-after induction; o/n-overnight)

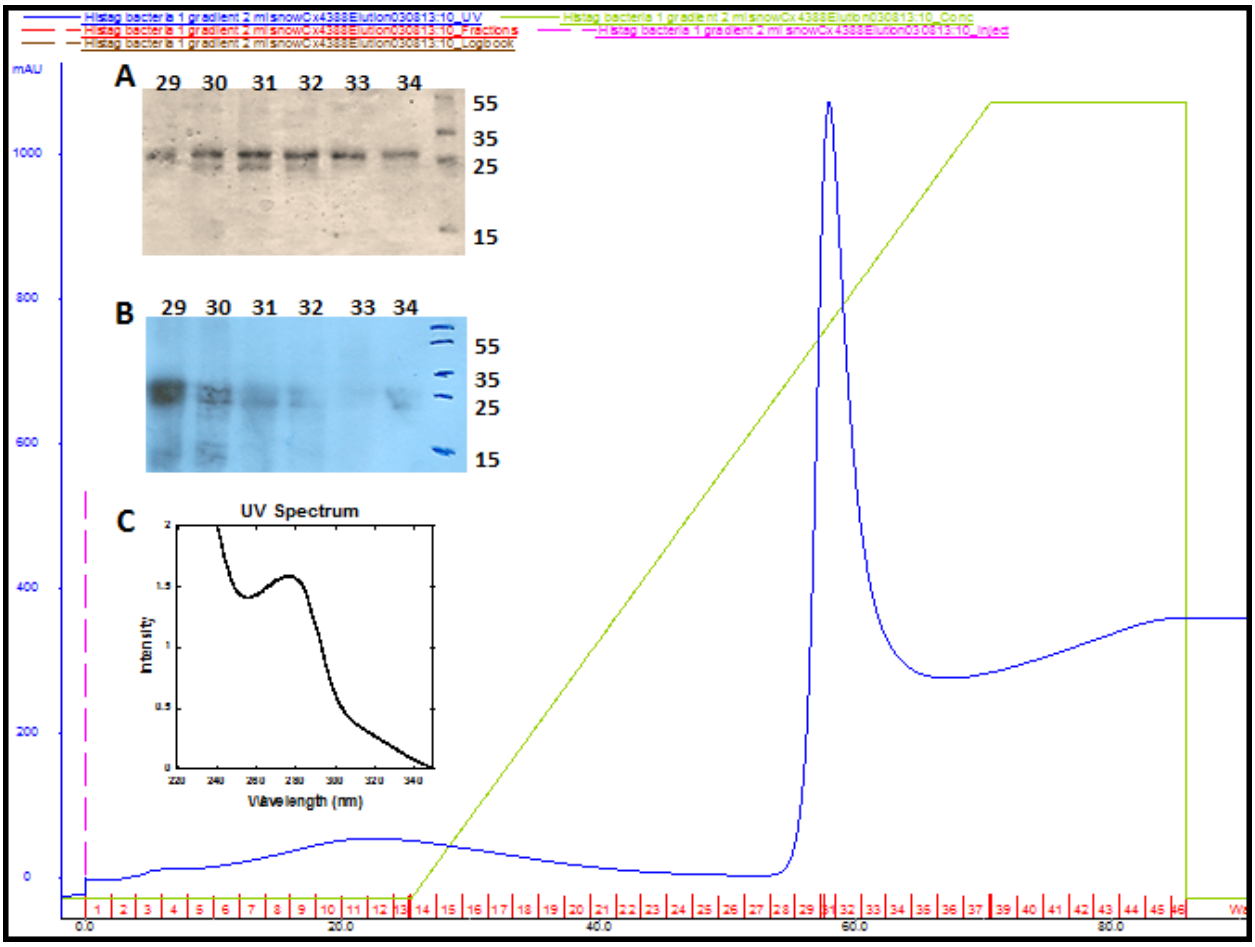

Figure 6.12. FPLC spectra of $Cx43_{88\text{-}164}$ with SDS-PAGE and western blot. A) SDS-PAGE; B) western blot. (The number on the top of each gel are the elution fragment number of $Cx43_{88\text{-}164}$.) C) UV spectrum of the elution.

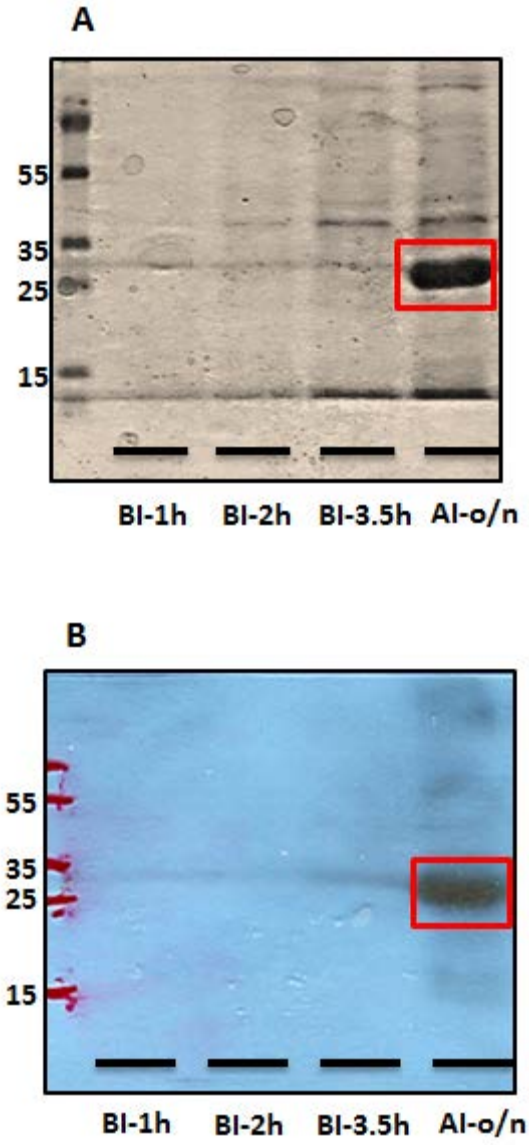

FIgure 6.13. Expression gel of $Cx43_{99\text{-}154}$.
A) SDS-PAGE; B) Western blot. (BI-before induction; AI-after induction; o/n-overnight)

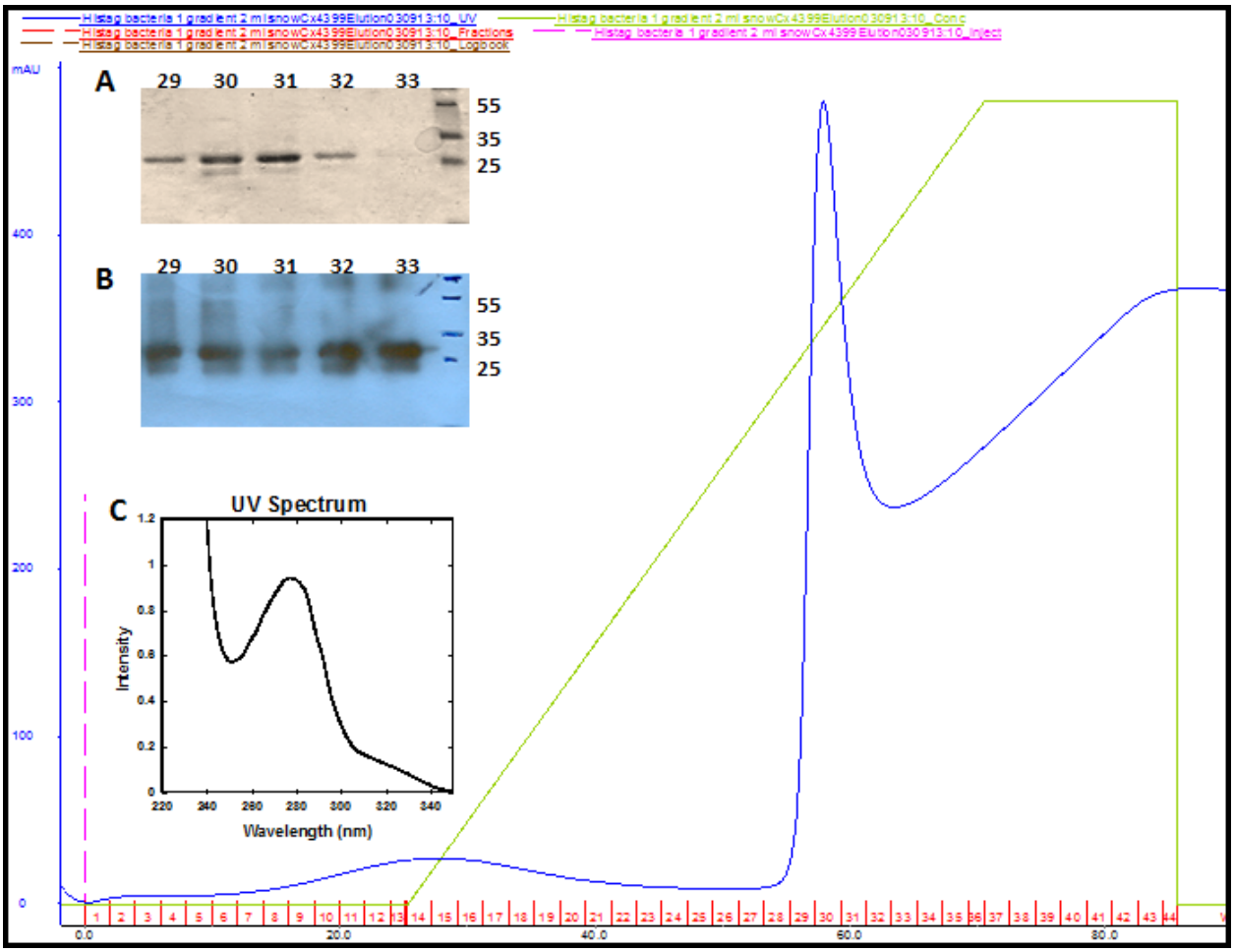

Figure 6.14. FPLC spectra of elution of $Cx43_{99\text{-}154}$ and gels.
A) SDS-PAGE; B) Western blot. (The number on top of each gel are the elution fragment number of $Cx43_{99\text{-}154}$) C) UV spectrum of elution.

6.2.5. Study interaction of Dansyl-CaM with $Cx43_{88-164}$ peptide

Dansyl labeled CaM (Dy-CaM) is used to study the interaction of CaM and His-tagged $Cx43_{88-164}$. Dy-CaM is used because there are other aromatic residue present in the $Cx43_{88-164}$ and CaM. To avoid any interfering of emission wavelength from other aromatic residue, 335 nm is the wavelength that used to excite the dansyl chloride to monitor any conformational change of CaM by interacts with peptide. The CaM binding prediction the his-tagged part of the protein cannot interact with CaM. A negative control (same his-tagged protein without desired peptides) with predicted CaM binding score zero is used to make sure that the his-tagged part of the protein cannot interaction with Dy-CaM, so that any fluorescence intensity change is due to the interaction of Cx43 peptide with Dy-CaM. The fluorescence intensity increase as the concentration of the peptide increase along with a blue shift of the intensity indicate that the interaction of CaM and peptide occur (**Figure 6.15**). There is no interaction show of the negative control with dy-CaM as it predicted. **Figure 6.15** shows the binding curve of the dy-CaM interact with $Cx43_{88-164}$ and the intensity change comparison of $Cx43_{88-164}$ with negative control. After increase the concentration of $Cx43_{88-164}$, there is ~50% intensity increase. (**Figure 6.15 B red bar**) On the other hand, there is no intensity different between the before addition of negative control and after addition of negative control. (**Figure 6.15 B black bar**) Thereby, there is true binding of $Cx43_{88-164}$ with CaM and its binding affinity is 0.107 μM. The binding affinity of this peptides shows 10 time higher binding affinity toward CaM than the region II (K_d ~ 1 μM) of the cytoplasmic loop shows in **Figure 6.1**.

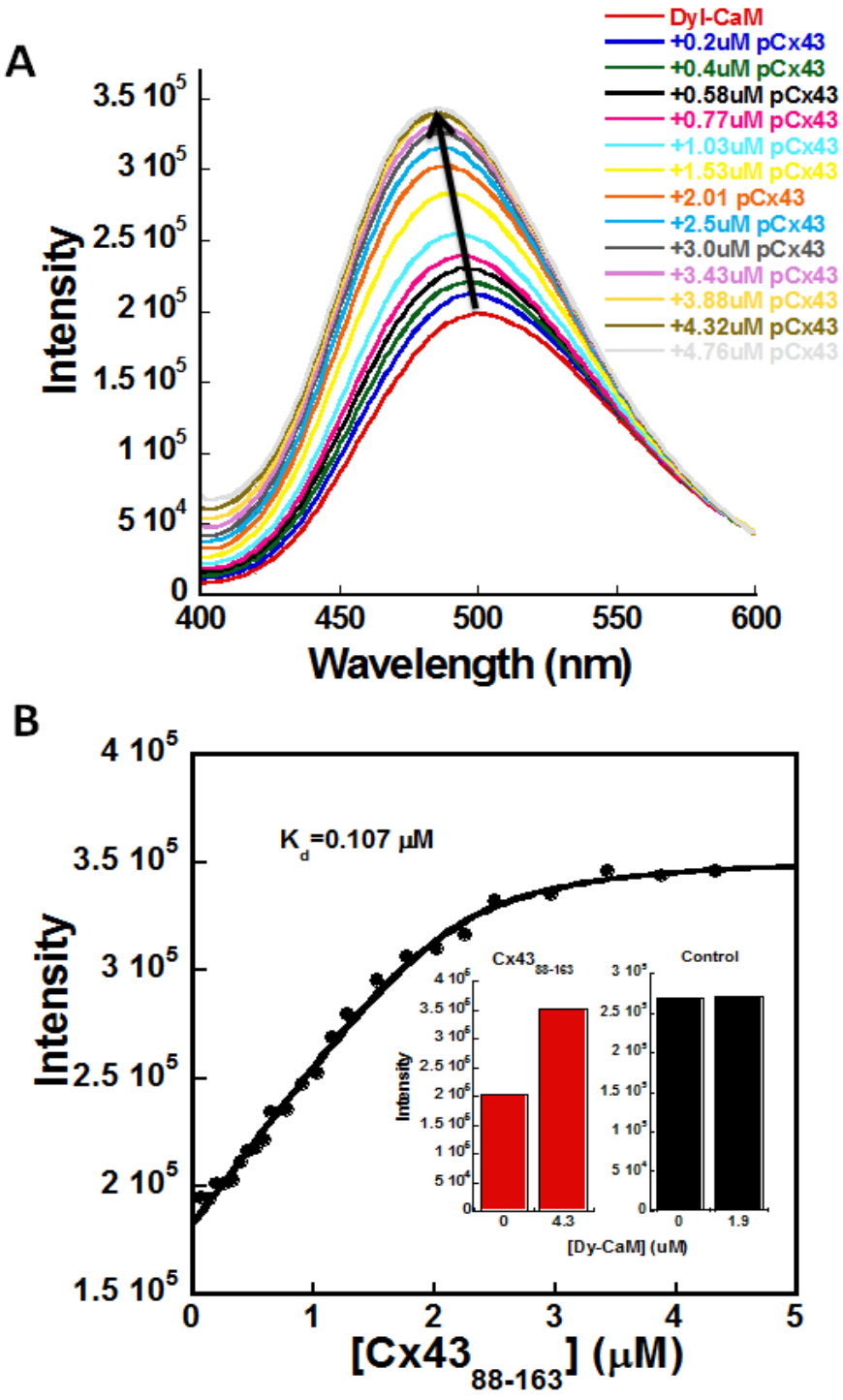

Figure 6.15. Study the interaction of Dy-CaM with $Cx43_{88-164}$.
A) The intensity change of Dy-CaM by increase the concentration of $Cx43_{88-164}$. B) Curve of Dy-CaM interact with $Cx43_{88-164}$. (Red bar is the intensity comparison of before and after of addition of $Cx43_{88-164}$; Black bar is the intensity comparison of before and after of addition of negative control)

6.3. Conclusion and future work

$Cx26_{206-227}$, $Cx43_{99-154}$, and $Cx43_{88-164}$ are expressed well as his-tagged protein. However, most of the protein remains in the inclusion body. The SDS-PAGE and Western Blot conform that the his-tagged Cx peptide is truly expressed. By using the same refolding protocol that is described in Chapter 6.3, the inclusion body was able to refolded and purify at signal step on the FPLC system. All three peptide start precipitate during the elution process before the enzyme digestion. Decrease pH of $Cx43_{88-164}$ to 4.1 is able solubilized some the peptide, but both $Cx26_{206-227}$ and $Cx43_{99-154}$ remain in the insoluble form. The insoluble prosperity of the peptides might due membrane protein fragment that contain high percentage of hydrophobic residues.

The titration of Dy-CaM with designed Cx peptides was performed to study the interaction between CaM with designed Cx peptides. The his-tagged $Cx43_{88-164}$ shows the true binding with Dy-CaM by monitoring the blue shift with increase the fluorescence intensity. The higher binding affinity of his-tagged $Cx43_{88-164}$ indicates that this peptide fragment can binds CaM tighter than region II on the cytoplasmic loop.

Since the his-tag of the protein might interfering the Dy-CaM signal during the titration, the on column digestion will be performing to cut the desired Cx peptides form the tag. In this way, the precipitate might be avoided and the interaction study of the Dy-CaM and Cx peptide can be monitored without the interfering. Protein redesigned might also carry out in the future to avoid the precipitation of the protein and the complication of the protocol.

7. Significance of this work

CaM is one of the most important intracellular Ca^{2+} signaling proteins because the variety of proteins that it regulates. It contains 4 Ca^{2+} binding sites with two on each domain with the flexible central linker connects the two domains. CaM undergoes a conformational change after the binding with Ca^{2+}, and adapt to a dumbbell shape that expose more hydrophobic patch of the protein. CaM have been the hot topic for many researchers because its two domain can binds to Ca^{2+} independently, the flexibility of the central linker, the percentage of the Met contain, and its hydrophobic. Thus, we know lots about this unique protein but also know so little about it at same time. We designed isolated C domain of CaM, N domain of CaM, CaM with 5 residues that are deleted from the central linker, so that we gain more detail of the specific role of each domain and the central linker interact with other target proteins.

In this project, The wt-CaM and three mutant CaM were able to expressed well and generate large quantities of protein for structural study, and was confirmed their well folded structural. Metal bindings and PDE assay also confirm the wt-CaM contain the correct metal binding affinity and able to active enzyme.

The modified expression condition of isotopic labeled CaM was able improve the quantities yield of ^{15}N labeled wt-CaM and ^{15}N and ^{13}C labeled wt-CaM. Moreover, the bacteria were able to adopt the toxic deuterium environment and produce relatively high yield of ^{2}H, ^{15}N and ^{13}C labeled wt-CaM. The isotopic labeled CaM allows us to study the interaction of CaM with massive target protein by using NMR. The modified expression condition of isotopic labeled CaM method can be used to express isotopic labeled CaM variants, such as isolated C-CaM, isolated N-CaM and del-CaM (future).

The RyR1 mini domain was expressed and purified with GST tag as inclusion body. The RyR1 mini domain then was redesigned into different vector to improve the production of the protein yield during the purification process. Preliminary studies how that future work is needed to further develop to improve this approach.

Multiple CaM binding sites have been predicted and locate on the location of the cytoplasmic loop of Cx43 and Cx26. In our project, we want to understand how the entire cytoplasmic loop interacts with CaM, we also hypothesized that the residues in the cytoplasmic member might help the process of CaM binding and regulation. Therefore, we designed several Cx peptides to test our theory. The designed peptides are express and purified with his-tag as inclusion body. The co-column refolding method was able to produce relatively high protein with high purity. However, future work is needed to further develop to improve the solubility of the protein. These studies in this thesis have contributed to the growing field of further understand CaM and several candidates of CaM binding target peptides.

Reference:

1. Berridge, M. J.; Bootman, M. D.; Lipp, P., Calcium--a life and death signal. *Nature* 1998, *395* (6703), 645-8.

2. Williams, R. J. P., The evolution of calcium biochemistry. *Biochim Biophys Acta.* 2006, *1763* (11), 1139-49.

3. Levine, B.; Levine, The mobility of calcium-trigger proteins and its function. *Ciba Foundation symposium* 1983, *93* (Mobility Funct. Proteins Nucleic Acids), 72.

4. Niki, I.; Yokokura, H.; Sudo, T.; Kato, M.; Hidaka, H., Ca^{2+} signaling and intracellular Ca^{2+} binding proteins. *J. Biochem.* 1996, *120* (4), 685-98.

5. Schroder, B.; Schlumbohm, C.; Kaune, R.; Breves, G., Role of calbindlin-D9k in buffering cytosolic free Ca2+ ions in pig duodenal enterocytes. *J Physciol.* 1996, *492* (3), 715-22.

6. Gifford, J. L.; Walsh, M. P.; JVogel, H., Structures and metal-ion-binding properties of the Ca^{2+}-binding helix–loop–helix EF-hand motifs. *Biochem. J.* 2007, *405* (2), 199-221.

7. Gifford, J. L.; Walsh, M. P.; Vogel, H. J., Structures and metal-ion-binding protperites of the Ca^{2+}-binding helix-loop-helix EF-hand motifs. *Biochem. J.* 2007, *405*, 199-211.

8. WY, C., Cyclic nucleotide phosphodiesterase. *Adv Biochem Psychopharmacol.* 1970, *3*, 51-65.

9. Kim, M. C.; Chung, W. S.; Yun, D. J.; Cho, M. J., Calcium and calmodulin-mediated regulation of gene expression in plants. *Mol Plant* 2009, *2* (1), 12-21.

10. Ikura, M.; Ames, J. B., Genetic polymorphism and protien conformational plasticity in the calmodulin superfamily: two ways to promote multifunctionality. *Proc . Natl Acad. Sci U. S. A.* 2006, *103* (5), 1159-64

11. Klevit, R. E.; Dalgarno, D. C.; LEvine, B. A.; Williams, R. J. P., ^{1}H-NMR studies of calmodulin. The nature of the Ca2+-dependent conformational change. *Eur. J. Biochem.* 1984, *139* (1), 109-14.

12. Ciivici, A.; Ikura, M., Molecular and structural basis of target recognition by calmodulin *Annu Rev Biophys Biomol Struct.* 1995, *24*, 84-116.

13. Starovasnik, M. A.; Davis, T. N.; Klevit, R. E., Similarities and Differences between Yeast and Vertebrate Calmodulin: An Examination of the Calcium-Binding and Structural

Properties of Calmodulin from the Yeast *Saccharomyces cerevisiae*. *Biochemistry* 1993, *32* (13), 3261-70.

14. Luan, Y.; Matsuura, I.; Yazawa, M.; Nakamura, T.; Yagi, K., Yeast calmodulin: structural and functional differences compared with vertebrate calmodulin. *J. Biochem.* 1987, *102* (6), 1531-7.

15. Yoshino, H.; Izumi, Y.; Sakai, K.; Takezawa, H.; Matsuura, I.; Maekawa, H.; Yazawa, M., Solution X-ray Scattering Data Show Structural Differences between Yeast and Vertebrate Calmodulin: Implications for Structure/Function. *Biochemistry* 1996, *35* (7), 2388-93.

16. Petegem, F. V., Ryanodine Receptors: Structure and Function. *J. Biol. Chem.* 2012, *287*, 31624-32.

17. Nakai, J.; Imagawa, T.; Hakamata, Y.; Shigekawa, M.; Takeshima, H.; Numa, S., Primary structure and functional expression from cDNA of the cardiac ryanodine receptor/calcium release channel. *FEBS Lett.* 1990, *271* (1-2), 169-77.

18. Otsu, K.; Willard, H. F.; Khanna, V. K.; Zorzato, F.; Breen, N. M.; MacLennan, D. H., Molecular Cloning of cDNA encoding the Ca2+ release channel (Ryanodine Receptor) of rabbit cardiac muscel sarcoplasmic reticulum. *J Biol Chem.* 1990, *265*, 13472-83.

19. Lanner, J. T.; Georgiou, D. K.; Joshi, A. D.; Hamilton, S. L., Ryanodine Receptors: Structure, Expression, Molecular Details, and Function in Calcium Release *Cold Spring Harb Perspect Biol.* 2010, *2* (11), 003996.

20. Serysheva, I. I.; Ludtke, S. J.; Baker, M. L.; Cong, Y.; Topf, M.; Eramian, D.; Sali, A.; Hamilton, S. L.; Chiu, W., Subnanometer-resolution electron cryomicroscopy-based domain models for the cytoplasmic region of skeletal muscle RyR channel. *Proc . Natl Acad. Sci U. S. A.* 2008, *105* (28), 9610-5.

21. Rodney, G. G.; Moore, C. P.; Williams, B. Y.; Zhang, J.-Z.; Krol, J.; Pedersen, S. E.; Hamilton, S. L., Calcium Binding to Calmodulin Leads to an N-terminal Shift in Its Binding Site on the Ryanodine Receptor. *J. Biol. Chem.* 2001, *267* (3), 2069-74.

22. Zhang, J.; Zhang, J.-Z.; Danila, C. I.; Hamilton, S. L., A Noncontiguous, Intersubunit Binding Site for Calmodulin on the Skeletal Muscle Ca^{2+} Release Channel. *J. Biol. Chem.* 2003, *278* (10), 8348-55.

23. Xiong, L.; Zhang, J.-Z.; He, R.; Hamilton, S. L., A Ca2+-Binding Domain in RyR1 that Interacts with the Calmodulin Binding Site and Modulates Channel Activity. *Biophys J.* 2006, *90* (1), 173-82.

24. Wagenknecht, T.; Samso, M., Three-Dimentional Reconstructuion of Ryanodine Receptor. *Front Biosci.* 2002, *7* (1464-74).

25. Yeager, M.; Nicholson, B. J., Structure of gap junction intercellular channels. *Curr Opin Struct Biol.* 1996, *6* (2), 183-92.

26. Sohl, G.; Willecke, K., Gap junctions and the connexin protein family. *Cardiovasc Res.* 2004, *62* (2), 228-32.

27. Gerido, D. A.; White, T. W., Connexin Disorders of the ear, skin, and lens. *Biochim Biophys Acta.* 2004, *1662* (1-2), 159-70.

28. Zhou, Y.; Yang, W.; Lurtz, M. M.; Ye, Y.; Huang, Y.; Lee, H.-W.; Chen, Y.; Louis, C. F.; Yang, J. J., Identification of the Calmodulin Binding Domain of Connexin 43. *J. Biol. Chem.* 2007, *282* (48), 35005-17.

29. Seamon, K. B.; Kretsinger, R. H., Calcium-modulated protein. *Met. Ions Biol.* 1983, *6*, 1-51.

30. Barbato, G.; Ikura, M.; Kay, L. E.; Pastor, R. w.; Bax, A., Backbone dynamics of calmodulin studied by ^{15}N relaxation using inverse detected two-dimensional NMR spectroscopy: The central helix is flexible. *Biochemistry* 1992, *31*, 5268-78.

31. Waltersson, Y.; Linse, S.; Brodin, P.; Grundstrom, T., Mutational Effects on the Cooperativity of Ca2+ Binding in Calmodulin. *Biochemistry* 1993, *32* (31), 7866-71.

32. Ye, Y.; Shealy, S.; Yang, J. J., A grafting approach to obtain site-specific metal-binding properties of EF-hand proteins. . *Protein Eng.* 2003, *16*, 429-34.

33. Rose, G. D.; Geselowitz, A. R.; Lesser, G. J.; Lee, R. H.; Zehfus, M. H., Hydrophobicity of amino acid resdiues in globular protein. *Science* 1985, *229*, 834-8.

34. Gellman, S. H., On the Role of Methionine Residues in the Sequence-Independent Recognition of Nonpolar Protein Surfaces. *Biochemistry* 1991, *30* (27), 6633-6.

35. Walsh, M.; Stevens, F. C., Chemical modification studies on the Ca^{2+}-dependent protein modulator: The role of methionine residues in the activation of cyclic nucleotide phsophodiesterase. *Biochemistry* 1978, *17*, 3924-30.

36. Gopalakrishna, R.; Anderson, W. B., The effects of chemical modification of calmodulin Ca2+-induced exposure of hydrophbic region. Separation of active and inactive forms of calmodulin. *Biochim Biophys Acta.* 1985, *844*, 265-9.

37. Guerini, D.; Krebs, J.; Carafoli, E., Stimulation of the erythrocyte Ca2+-ATPase and of bovine brain cyclic nucleotide psophodiesterase by chemically modified calmodulin. *Eur. J. Biochem.* 1987, *170*, 35-42.

38. O'Neil, K. T.; Erickson-Viitanen, S.; DeGrado, W. F., Photolabeling of calmodulin with basic, amphiphilic a-helical peptides containing *p*-benzoylphenylalanine. *J Biol Chem.* 1989, *264*, 14571-8.

39. Siivari, K.; III, M. Z. A. G. P.; Vogel, H. J., NMR studies of the methionine methyl groups in calmodulin. *FEBS Lett.* 1995, *366* (2-3), 104-8.

40. Davis, T. N.; Urdea, M. S.; Masiarz, F. R.; Thorner, J., Isolation of yeast calmdoulin gene: calmodulin is an essential protein. *Cell* 1986, *47* (3), 423-31.

41. Ohya, Y.; Uno, I.; IShikawa, T.; YasuhiroAnraku, Purification and biochemical properties of calmodulin from Saccharomyces cerevisiae. *Eur. J. Biochem.* 1987, *168* (1), 13-9.

42. Brockerhoff, S. E.; Edmonds, C. G.; Davis, T. N., Structural analysis of wild-type and mutant yeast calmodulins by limited proteolysis and electrospray ionization mass spectrometry. *Protein sci.* 1992, *1* (4), 504-16.

43. Kawasaki, H.; Kretsinger, R. H., Calcium-binding proteins. 1: EF-hands. *Protein Profile* 1994, *1* (4), 343-517.

44. Martin, S. R.; bayley, P. M., The effects of Ca^{2+} and Cd^{3+} on the secondary and tertiary structure of bocine testis calmodulin. *Biochem. J.* 1986, *238* (2), 485-90.

45. VanScyoc, W. S.; Sorensen, B. R.; Rusinova, E.; Laws, W. R.; Ross, J. B. A.; Shea, M. A., Calcium Binding to Calmodulin Mutants Monitored by Domain-Specific Intrinsic Phenylalanine and Tyrosine Fluorescence. *Biophys J.* 2002, *83* (5), 2767-80.

46. Jiang, J.; Zhou, Y.; Zou, J.; Chen, Y.; Patel, P.; Yang, J. J.; Balog, E. M., Site-specific modification of calmodulin Ca2+ affinity tunes the skeletal muscle ryanodine receptor activation profile. *Biochem. J.* 2010, *432* (1), 89-99.

47. Darnall, D. W.; Birnbaum, E. R., Lanthanide ions activate alpha-amylase. *Biochemistry* 1973, *12* (18), 3489-91.

48. Kuiper, H. A.; Agro, A. F.; Antonini, E.; Brunori, M., The replacement of calcium by terbium as an allosteric effector of hemocyanins. *FEBS Lett.* 1979, *99* (2), 317-20.

49. Furie, B. V.; Mann, K. G.; Furie, B., Substitution of lanthanide ions for calcium ions in the activation of bovine prothrombin by activated factor X. High affinity metal-binding sites of prothrombin and the derivatives of prothrombin activation. *J Biol Chem.* 1976, *251* (11), 3235-41.

50. Wallace, R. W.; Tallant, E. A.; Dockter, M. E.; Cheung, W. Y., Calcium Binding Domains of Calmodulin. Sequence of fill as dtermined with terbium luminescence. *J. Biol. Chem.* 1982, *257* (4), 1845-54.

51. Wang, C.-L. A.; Leavis, P. C.; Gergely, J., Kinetic Studies Show That Ca^{2+} and Tb^{3+} Have different Binding Preferences tward the Four Ca^{2+}-Bining Sites of Calmodulin. *Biochemistry* 1984, *23*, 6410-6415.

52. Kakiuchi, S.; Yamazaki, R., Calcium dependent phosphodiesterase activity and its activating factor (PAF) from brain: Studies on cyclic 3',5'-nucleotide phosphodiesterase (III). *Ciochem. Biophys. Rec. Commun.* 1970, *41*, 1104-10.

53. Kakiuchi, S.; Yamazaki, R.; Teshima, Y.; Uenishi, K., Regulation of nucleotide cyclic 3',5'-monophosphate phosphodiesterase activity from rat brain by a modulator and Ca^{2+}. *Proc. Natl. Acad. Sci. USA* 1973, *70* (3526-30).

54. Foster, M. P.; McElroy, G. A.; Amero, C. D., Solution NMR of Large Molecules and Assemblies. *Biochemistry* 2007, *46* (2), 331-40.

55. Gardner, K. H.; Kay, L. E., The use of ^{2}H, ^{13}C, ^{15}N multidimensional NMR to study the structure and dynamics of proteins. *Annu Rev Biophys Biomol Struct.* 1998, *27*, 357-406.

56. Burgess, W. H.; Jemiolo, D. K.; Kretsinger, R. H., Interaction of Calcium and Calmodulin in the Presence of Sodium Dodecyl Sulfate. *Biochim. Biophys. Acta.* 1980, *623* (2), 257-70.

57. Park, S.-J.; Song, J.-S.; Kim, H.-J., Dansylation of tryptic peptides for increased sequencecoverage in protein identification by matrix-assisted laser desorption/ionization time-of-flight mass spectrometric peptide mass fingerprinting. *Rapid Commun Mass Spectrom.* 2005, *19* (21), 3089-96.

58. Rodney, G. G.; Krol, J.; Williams, b.; Beckingham, K.; Hamilton, S. L., The Carboxy-Terminal Calcium Binding Sites of Calmodulin Control Calmodulin's Switch from an Activator to an Inhibitor of RyR1. *Biochemistry* 2001, *40* (41), 12430-5.

59. Fruen, B. R.; Black, D. J.; Bloomquist, R. A.; Bardy, J. M.; Johnson, J. D.; Louis, C. F.; Balog, E. M., Regulation of RyR1 and RyR2 Ca^{2+} Release Channel Isoforms by Ca^{2+}-Insensitive Mutants of Calmodulin *Biochemistry* 2003, *49* (9), 2740-7.

60. Boschek, C. B.; Jones, T. E.; Squier, T. C.; Bigelow, D. J., Calcium Occumpancy of N-Terminal Sites within Calmodulin Induces Inhibition of the Ryanodine Receptor Calcium Release Channel. *Biochemistry* 2007, *46* (37), 10621-8.

61. Nakashima, K.-i.; Ishida, H.; Ohki, S.-y.; Hikichi, K.; Yazawa, M., Calcium Binding Induces Interaction between the N- and C-Terminal Domains of Yeast Calmodulin and Modulates Its Overall Conformation. *Biochemistry* 1999, *38* (1), 98-104.

62. Zhang, H.; Zhang, J.-Z.; Danila, C. I.; Hamilton, S. L., A Noncontiguous, Intersubunit Binding Site for Calmodulin on the Skeletal Muscel Ca^{2+} Release Channel. *J Biol Chem.* 2002, *278* (10), 8348-55.

63. Xiong, L.-W.; Newman, R. A.; Rodney, G. G.; Thomas, O.; Zhang, J.-Z.; Persechini, A.; Shea, M. A.; Hamilton, S. L., Lobe-dependent Regulation of Ryanodine Receptor Type 1 by Calmodulin. *J Biol Chem.* 2002, *277* (43), 40862-70.

64. Maximciuc, A. A.; Putkey, J. A.; Shamoo, Y.; Mackenzie, K. R., Complex of Calmodulin with a Ryanodine Receptor Target Reveals a Novel, Flexible Binding Mode. *Structure* 2006, *14* (10), 1547-56.

65. Gangopadhyay, J. P.; Ikemoto, N., Interaction of the Lys^{3614}-Asn^{3643} calmodulin-binding domain with the Cys^{4114}-Asn^{4142} region of the type 1 ryanodine receptor is involved in the mechanism of Ca^{2+}/agonist-induced channel activation. *Biochem. J.* 2008, *411* (2), 415-23.

66. Herve, J.-C.; Bourmeyster, M.; Sarrouilhe, D., Diversity in protein–protein interactions of connexins: emerging roles. *Biochim Biophys Acta.* 2004, *1662* (1-2), 22-41.

67. Bukauskas, F. F.; Verselis, V. K., Gap junction channel gating. *Biochim Biophys Acta.* 2004, *1662* (1-2), 42-60.

68. Nakase, T.; Naus, C. C. G., Gap junctions and neurological disorders of the central nervous system. *Biochim Biophys Acta.* 2004, *1662* (1-2), 149-58.

69. Peracchia, C.; Bernardini, G.; Peracchia, L. L., Is calmodulin involved in the regulation of gap junction permeability? *Pfugers Arch.* 1983, *399* (2), 152-4.

70. Peracchia, C., Calmodulin-like proteins and communicating junctions. Electrical uncoupling of crayfish septate axons is inhibited by the calmodulin inhibitor W7 and is not affected by cyclic nucleotides. *Pfugers Arch.* 1987, *408* (4), 379-85.

71. Peracchina, C., Communicating junctions and calmodulin: inhibition of electrical uncoupling in Xenopus embryo by calmidazolium. *J Membr Biol* 1984, *81* (1), 49-58.

72. Peracchia, G.; Sotkis, A.; Wang, X. G.; Peracchia, L. L.; Persechini, A., Calmodulin Directly Gates Gap Junction Channels. *J Biol Chem.* 2000, *275* (34), 26220-4.

73. LS, M.; EC, B.; DA, G., Expression of gap junction protein connexin43 in embryonic chick lens: molecular cloning, ultrastructural localization, and post-translation phsophorylation. *J Membr Biol* 1990, *116* (2), 163-75.

74. Xu, Q.; Kopp, R. F.; Chen, Y.; Yang, J. J.; Roe, M. W.; Veenstra, R. D., Gating of connexin 43 gap junctions by a cytoplsmic loop calmoudlin binding domain. *Am J Physiol Cell Physiol* 2012, *302* (10), 2548-56.

75. PN, U.; PD, E., Two configuration of a channel-forming membrane protein. *Nature* 1984, *307* (5952), 609-13.

76. Colangeli, R.; Heijbel, A.; Willams, A. M.; Manca, C.; Chan, J.; Lyashchenko, K.; Gennaro, M. L., Three-step purification of lipopolysaccharide-free, polyhistidine-tagged recombinant antigens of *Mycobacterium tuberculosis*. *J chromatogr B biomed Sci Appl* 1998, *714* (2), 223-3.

Appendix

Expression isotopic labeled protein by using deuterium environment

Expression:

1. Transformation (Follow the normal protocol)
2. Instead of the LB plate, use ECAM (see Ingredients above) plate to grow colonies by following the regular agar plate making protocol (with 7.5 g bacto agar in 500 ml, pH 7.0).

   NOTE: Glucose concentration can be increased if small or no colony grows.
3. Select one health colony and inoculate into 50mL 100% water based M9 medium, let it grow for overnight to reach the optical density.

   Note: Recommending do this step at late afternoon around 5-6.
4. Centrifuge 10mL of step 3 medium at 3000-4000 rpm for 5-10min at 20°C.

   NOTE: Before centrifuge, check the cell density. Make sure that the medium is cloudy, but no cell clusters. Cell clusters indicate the cell are dead, you cannot process farther experiment. You need to regrow the cell. Before the centrifugation, please keep the cell

in the shaker for cells' good condition. You can decrease the shaker's temperature if the cell density already reached the optical condition.

5. Transfer the centrifuged cell pellet from step 4 into 50mL 70% D_2O based M9 medium and let it grow to optical density (might take 24 hours)

   NOTE: Recommending do this step around afternoon around 3.

6. Centrifuge 10mL of step 5 medium at 3000-4000 rpm for 5-10min at 20°C.

   NOTE: see NOTE under step 4. Also recommending to do this step around afternoon around 3.

7. Save all the waste from step 5&6 into a waste container A

8. Transfer the centrifuged cell pellet from step 6 into 50mL of 100% D_2O based M9 medium and let it grow to optical density (might take more than 24 hours)

   NOTE: This step is recommended to use ^{15}N NH_4Cl and ^{13}C glucose instead of the regulate glucose and NH_4Cl. Also recommended to do this step around afternoon 4.

9. Transfer all the medium into 1L of fresh 950mL of 100% D_2O based M9 medium

   NOTE: Recommended to express two of 500mL instead of one of 1L medium. By doing so, if the cell condition of one flask is not good, you still have the second flask. In addition, we noticed that the cell's condition is better by using 500mL instead of one 1L medium. This step is recommended to do at afternoon around 4-5. It make a longer time for cell to reach the optical density. Let the cell to grow overnight, and come in early the next day to check OD_{600} of the cell. Cell should not reach to 0.8-1.0 by this time. If the cell reach more than 1.0, don't panic, add IPTG anyway.

10. Added IPTG for induction once the OD_{600} reach to 0.8-1.0
11. Let it grow for 5 hours and then collect the cell pellet

Note: Adding isotopic chemical NH_4Cl and Glucose from step 8. For double label protein, skip step 4, 5 and 7.

A suitable method for recycling D_2O

1. Remove visible debris by centrifuging and/or settling and/or filtering.
2. Using a common laboratory distillation apparatus, distill two or three times.
3. Mix and activated charcoal (1 g/100 mL works well) and stir for 20 min.
4. Remove charcoal by filtration. This D_2O is ready for growing cells.

   Note: This method is good to recycle D_2O used previously to grow cells and/or D_2O accumulated over the years from various NMR samples. A good rule of thumb is: distill until visibly clear, then distill one more time. This distillate will still contain trace amounts of volatile organic compounds, which are toxic to biological organisms so will not support life. It can therefore be stored indefinitely in the refrigerator or at room temperature.

   This step should be done immediately before use. Because this D_2O will now support life, it should be stored at refrigeration temperature otherwise mould, alga, and other exotica will grow in it and it will have to be recycled again.

   The most convenient way to determine the percent deuteration of the D_2O recycled is gravimetrically.